Catabolite regulation analysis of *Escherichia coli* and its mutants with the application to co-consumption of multiple sugars

Kyushu Institute of Technology

Department of Bioscience and Bioinformatics

Supervisor: Professor Hiroyuki Kurata

Ruilian Yao

Table of contents

Chapter 1
Introduction

1.1 General background

Due to the energy security and global warming problems caused by increased use of fossil fuels, alternative renewable energy sources have been paid recent attention (Schmidt and Dauenhauer, 2007; Kerr, 2007). In light of such attention, the conversion of various types of biomass to biofuels and biochemicals has been the subject of recent intense research efforts (Fig.1.1) (Huffer et al., 2012; Mazzoli et al., 2012; Kim et al., 2012, Yao and Shimizu, 2013). In particular, lignocellulosic biomass consisting of cellulose, hemicellulose and lignin is currently under intensive study as a sustainable and carbon-neutral energy source (Lynd et al., 2002; Clomburg et al., 2010). In contrast to the readily fermentable, and mainly starch- or sucrose-containing feedstocks in the current biotechnological production processes, lignocellulose biomass requires pretreatment and hydrolysis, which yields complex mixtures of five- and six- carbon sugars prior to, or concurrently with the fermentation (Aristidou and Penttilä, 2000; Zaldivar et al., 2001; Galbe and Zacchi, 2007). In order to achieve maximum product yield and productivity, fast and complete conversion of all sugars derived from lignocellulosic biomass is essential (Saha, 2003). However, during the fermentation of a mixture of sugars, wild-type *E. coli* exhibits a specific hierarchy for their utilization, causing slow and/or incomplete utilization of the mixed sugars. When sugars are consumed sequentially during the fermentation, the non-preferred sugars (such as pentoses) accumulate in the media until the preferred sugar (i.e., glucose) is completely consumed. Due to the high concentration of inhibitory fermentative end products such as lactate or ethanol (Alakomi et al., 2000; Ingram and Vreeland, 1980), the utilization rate of remaining pentose is slower than it is fermented as a sole carbohydrate. Repression of the use of alternate substrate is termed carbon catabolite repression (CCR) (Stülke and Hillen, 1999), making it challenging to design and efficiently control the fermentation processes using lignocellulosic biomass as a feedstock (Kim et al., 2010).

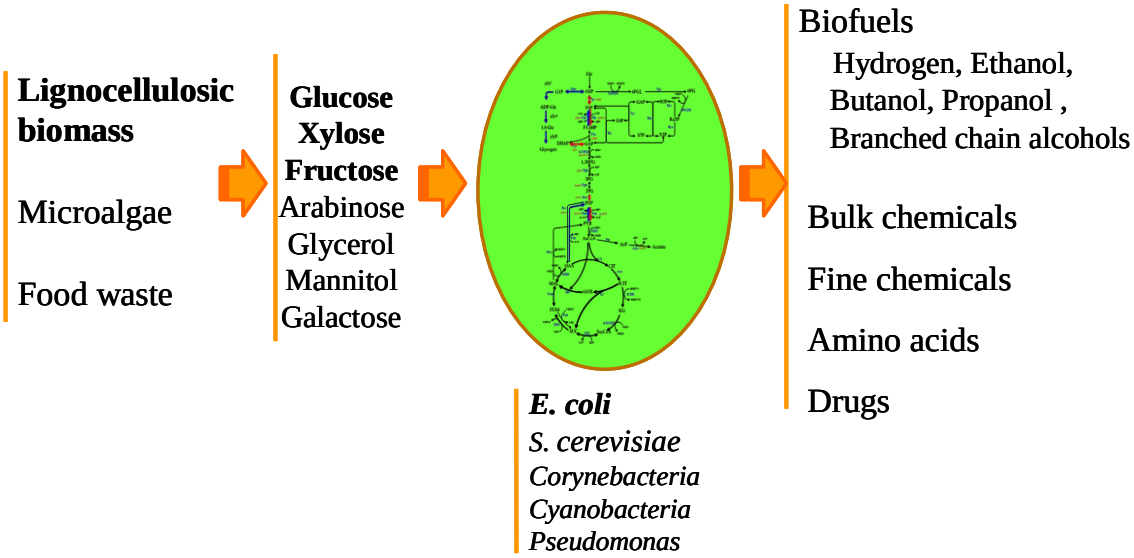

Figure 1.1 Production of biofuels and biochemicals from renewable resources using a variety of microorganisms.

CCR is considered as the most important regulatory mechanism in many bacteria (Blencke et al., 2003; Liu et al., 2005). CCR is defined more broadly as the inhibitory effect of a certain carbon source, usually glucose, in the growth medium on gene expression and/or the activity of enzymes involved in the catabolism of other carbon sources (Deutscher et al., 2006).

The central players in CCR in *E. coli* are transcriptional activator Crp, cyclic AMP (cAMP) receptor protein, the signal metabolite cAMP, adenylate cyclase (Cya), and the phosphorylation system (PTS) (Fig. 1.2), where these systems are involved in both transport and phosphorylation of carbohydrates (Postma et al., 1996; Görke and Stülke, 2008; Bahr et al., 2011). The PTS in *E. coli* consists of two common cytoplasmic proteins, EI (enzyme I) encoded by *ptsI* and HPr (histidine-phosphorylatable protein) encoded by *ptsH*, as well as carbohydrate-specific EII (enzyme II) complexes. The glucose-specific PTS in *E. coli* consists of the cytoplasmic protein $EIIA^{Glc}$ encoded by *crr* and the membrane-bound protein $EIICB^{Glc}$ encoded by *ptsG*, which transports and concomitantly phosphorylates glucose (Gosset, 2005). The phosphoryl groups are

transferred from phosphoenolpyruvate (PEP) by successive phosphorelay reactions in turn by EI, HPr, EIIA^{Glc}, and EIICB^{Glc} to glucose. When glucose is present in the medium, unphosphorylated form of EIIA^{Glc} is dominant, inhibiting of uptake of a number of non-PTS carbon sources by the so-called 'inducer exclusion' (Hogema et al., 1999; Deutscher, 2008). Upon glucose depletion, phosphorylated EIIA^{Glc} (EIIA^{Glc}-P) level increases. EIIA^{Glc}-P binding is localized to the C-termnal region of Cya, stimulating Cya activity, and leads to an increase in the intracellular cAMP level. Then cAMP combines with Crp forming cAMP-Crp complex, and activates the promoters of many catabolic genes and operons related to xylose, lactose, melibiose, glycerol, etc. (Kremling et al., 2004; Park et al., 2006). Furthermore, cAMP-Crp complex plays an important role in regulating genes encoding TCA cycle (Vogel et al., 1987; Cunningham et al., 1997), gluconeogenesis (Goldie, 1984) and other cellular processes (Johansson et al., 2000; Jackson et al., 2002; Mao et al., 2007).

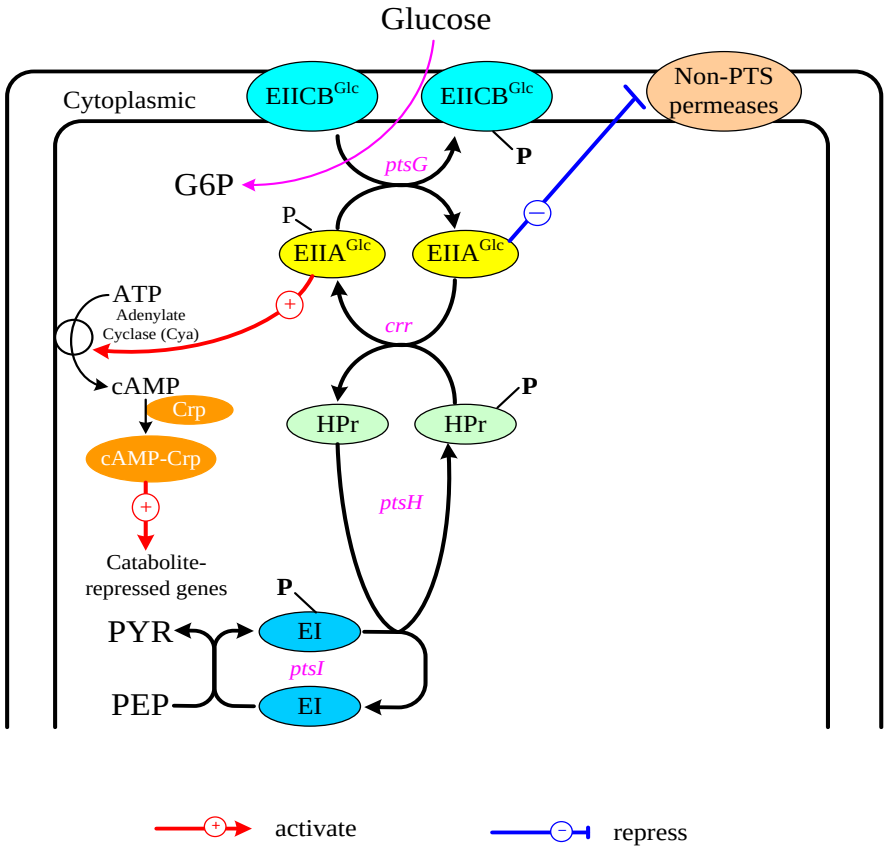

Figure 1.2 Carbon catabolite repression mechanisms in *E. coli*.

As stated above, Crp is an essential global regulator involved in the central metabolism. In addition to Crp, a number of global regulators control the central metabolic pathways (Appendix B) depending on the culture conditions (Shimizu, 2009). These regulators are involved in catabolite repression (Crp, Cya, Cra) (Nanchen et al., 2008; Saier and Ramseier, 1996; Saier et al., 1996), regulation of carbohydrate utilization (Mlc) (Plumbridge, 2002), glyoxylate bypass regulation (IclR, FadR) (Yamamoto and Ishihama, 2003; Gui et al., 1996), regulation under oxygen limitation (ArcA/B, Fnr) (Liu et al.,2004; Kang et al., 2005), oxidative stress regulation (SoxR/S) (Pomposiello and Demple 2001; Liochev et al., 1999), stress responsive regulator (RpoS) (Jung et al., 2005), ferric uptake regulator (Fur) (Zhang et al., 2005), nitrogen regulation (RpoN) (Jiang and Ninfa, 2007), osmotic regulation (OmpR) (de la Cruz et al., 2007), etc. Among them, Cra also mediates CCR. In addition, Mlc is considered to monitor glucose supply (Plumbridge, 2002). These two global regulators Cra and Mlc have important metabolic functions (Fig. 1.3).

Cra (catabolite repressor/activator), initially characterized as the fructose repressor (FruR), controls the carbon flow in *E. coli* (Moat et al., 2002; Saier and Ramseier, 1996). Its control mechanism is cAMP-independent (Dessein et al., 1978; Guidi-Rotani et al., 1980), where Cra represses the expressions of such genes as *ptsHI*, *pfkA*, *pykF*, *zwf*, *edd*, *eda*, *acnB*, while it activates *fbp*, *ppsA*, *pckA*, *aceA*, *icdA*, and *acnA* (Saier et al., 1996; Perrenoud and Sauer, 2005; Nachen et al., 2008) (Appendix B). The set of such genes implies that Cra activates the gluconeogenic pathway genes and represses the glycolytic pathway genes.

The global regulator Mlc represses the PTS transporters for glucose and mannose encoded by *ptsG*, *ptsHI*, *crr* and *manXYZ* operon (Kimata et al., 1998; Plumbridge, 2002). In contrast to Mlc, cAMP-Crp activates *ptsG* gene expression (de Reuse and Danchin, 1988). As a consequence, these two antagonistic regulatory mechanisms guarantee a precise adjustment of *ptsG* expression levels under various conditions (Bettenbrock et al., 2006). As explained previously, PTS activity in the presence of

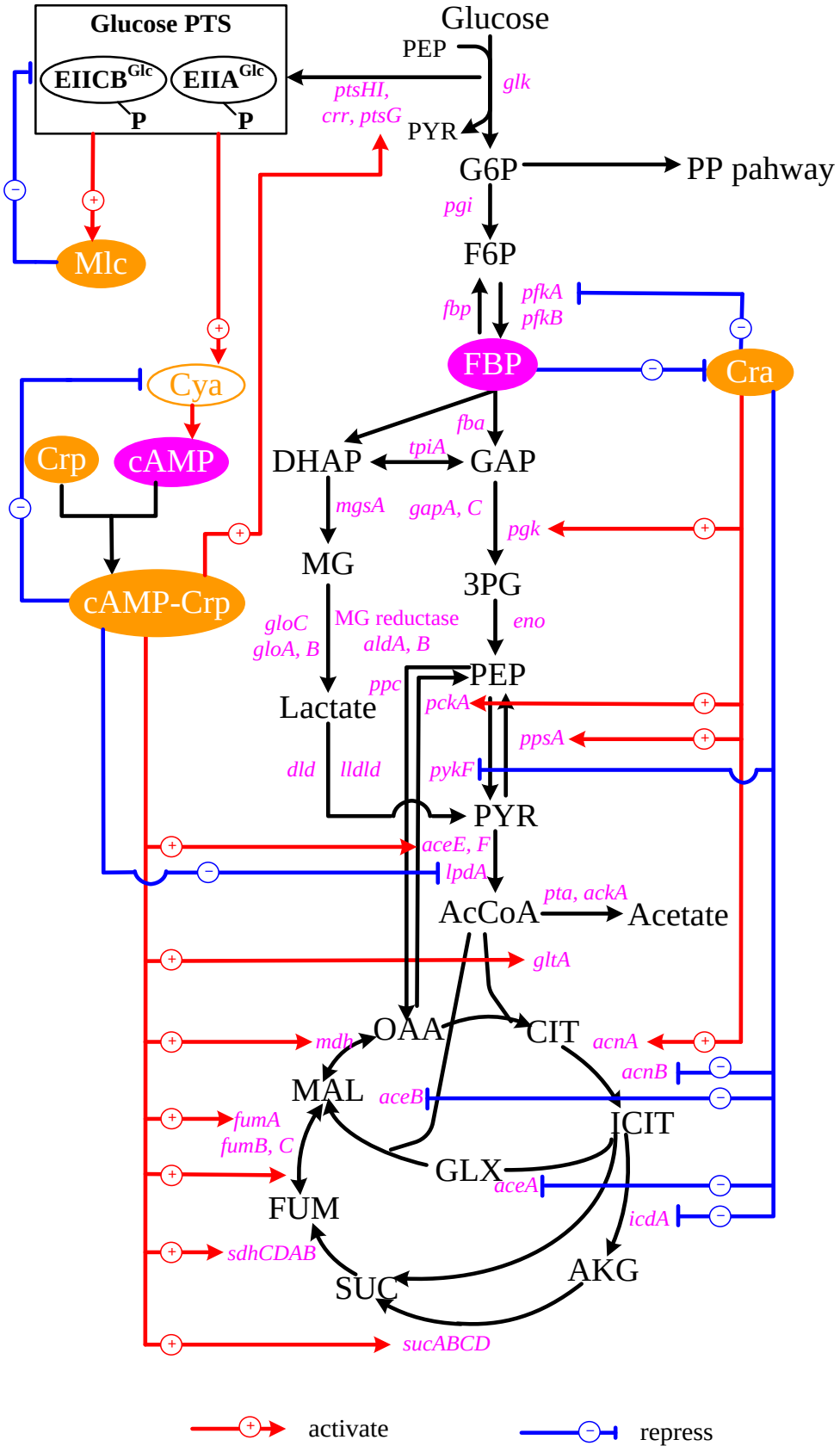

Figure 1.3 The regulation of main metabolic pathway genes mediated by global regulators Crp, Cra, and Mlc.

glucose leads to $EIIA^{Glc}$ and $EIICB^{Glc}$ being predominantly unphosphorylated. In this situation, Mlc binds to $EIICB^{Glc}$, and thus it does not bind to the operator region of *pts* genes. In the absence of glucose, Mlc binds to the promoters of *pts* genes and prevents their transcriptions (Tanaka et al., 2000).

The global regulators Crp and Cra mediated CCR together with the modulations of metabolic pathway genes, making the bacteria able to select a rapidly metabolizable carbon source in order to improve the growth rate. Then this results in survival as compared to other competing organisms in nature (Shimizu, 2013). However, this selective and sequential utilization of mixed carbon sources caused by CCR is a prevailing obstacle in industry (Bothast et al., 1999). Thus, extensive engineering efforts to construct genetically altered *E. coli* strains capable of co-consumption of multiple sugars are essential for the large scale production of biofuels and biochemicals from lignocellulosic biomass.

One metabolic engineering strategy for co-consumption of multiple sugars is the inactivation of the PTS genes (Hernández-Montalvo et al., 2001; Nichols et al., 2001; Dien et al., 2002), since CCR is caused by phosphorylation/dephosphorylation of cAMP-Crp in PTS. An ethanologenic *E. coli* strain with a glucose phosphotransferase (*ptsG*) mutation abolished CCR and allowed simultaneous fermentation of the mixtures of glucose, arabinose, and xylose to ethanol (yielding 87-94% of theoretical) (Nichols et al., 2001). In addition, another *E. coli ptsG* mutant strain FBR19 showed a yield of 0.77 (g lactic acid/g added sugars) by fermenting 100 g/l of equal mixtures of glucose and xylose (Dien et al., 2002). However, the glucose uptake rate as well as the cell growth was decreased due to the impairment of the main glucose transport. Note that glucose can also be transported by the alternative transporters such as MglCAB and GalP, followed by phosphorylation by glucokinase (Glk) from ATP. This problem can be overcome by the activation of GalP and Glk (Flores et al., 2007; Lu et al, 2012).

Another approach is the deletion of a general inhibitor of sugar metabolism, methylglyoxal synthase gene, *mgsA* (Yomano et al., 2009). Although *mgsA* was not generally considered as a part of the CCR system, it regulated the availability of PEP for the entry for glucose (Tötemeyer et al., 1998). This indirectly affected $EIIA^{Glc}$-P level and CCR. The *mgsA* deletion mutant of ethanogenic *E. coli* (strain LY168) enhanced co-metabolism of glucose and xylose, and accelerated the fermentation rates of 5-sugar mixture (mannose, glucose, arabinose, xylose, and galactose) to ethanol.

These approaches suggest that metabolic phenotype can be improved through local genetic modifications. However, these phenotypes are often suboptimal and unsatisfactory due to the effects to the distant effects of genetic modifications and unknown regulatory interactions (Shimizu, 2009). Therefore, it is strongly desirable to take into account the overall metabolic regulation mechanism based on global regulators and their effects on the related metabolic pathway genes for the efficient fermentation of lignocellulosic biomass.

1.2 Organization of the dissertation

The primary objective of this research is to understand the mechanism of catabolite regulation based on global regulators and their related metabolic pathway genes through different carbon source levels and several gene mutations. In particular, it is quite important to clarify the mechanism of sequential utilization of multiple sugars. Furthermore, it is also important to consider the problem of co-consumption of multiple sugars obtained from lignocellulosic biomass from the application point of view.

The present thesis is organized in six separate chapters. Chapter 2 introduces

materials and methods. Chapter 3 discusses the effect of the dilution rate on the catabolite regulation in the continuous culture of *E. coli*. The Chapter 4 describes the effects of several gene mutations on the catabolite regulation of *E. coli*. The study in Chapter 5 was designed based on the results of Chapters 3 and 4, where this chapter involves the application aspect, using the *E. coli* mutants such as Δ*cra*, *crp*$^{+}$ and Δ*pgi* strains for the simultaneous consumption of multiple sugars. Finally, Chapter 6 summarizes the results, their implications on the *E. coli* metabolic regulations and discusses the perspectives based on the present study.

Chapter 2
Materials and methods

2.1 Strains, media composition, and culture conditions

The strains used were *E. coli* BW25113 (F^- λ^- rph^{-1} $\Delta araBAD_{AH33}$ $lacI^q$ $\Delta lacZ_{WJ16}$ $rrnB_{T14}$ $\Delta rhaBAD_{LD78}$ *hsdR514*) and its single gene knockout mutants lacking *crp* (JW5702), *mlc* (JW1586), *pgi* (JW3985), *mgsA* (JW5129) and *cra* (JW0078), where those were obtained from Keio collection (Baba et al., 2006). The *crp* enhanced (crp^+) strain was constructed based on the method of Pósfai et al. (1999) by introducing the mutation responsible for Crp phenotype which lies in the hinge region between the cAMP- and DNA-binding domains. The amino acid substitutions from Gly to Ser at 122 position altered the allosteric nature of Crp, which corresponds to *crp**2 in Aiba et al. (1985). The Δ*cra.pflA* mutant was also constructed by one-step inactivation method (Datsenko and Wanner, 2001). All the strains were first precultured in the Luria-Bertani medium. In the experiments as described in Chapters 3 and 4, the second preculture and the main culture were carried out using M9 minimal medium containing 5 g/l of glucose for batch culture and 4 g/l for the continuous culture including ^{13}C-labeling experiment together with the following components (per liter): 6.81 g Na_2HPO_4, 2.99 g KH_2PO_4, 0.58 g NaCl and 5.94 g $(NH_4)_2SO_4$. In the experiments as described in Chapter 5, the carbon source was a mixture of glucose, fructose, and xylose each contained 5 g/l, or some of the combinations among them for the batch and continuous culture. The following components were filter sterilized and then added (per liter) with 1 ml of 1 M $MgSO_4 \cdot 7H_2O$, 1 ml of 0.1 mM $CaCl_2 \cdot 2H_2O$, 1 ml of 1 mg/L thiamine HCl and 10 ml of trace element solution containing (per liter): 0.55 g $CaCl_2 \cdot 2H_2O$, 1.67 g $FeCl_3 \cdot 6H_2O$, 0.1 g $MnCl_2 \cdot 4H_2O$, 0.17 g $ZnCl_2 \cdot 2H_2O$, 0.043 g $CuCl_2 \cdot 2H_2O$, 0.06 g $CoCl_2 \cdot 2H_2O$, and 0.06 g $Na_2M_OO_4 \cdot 2H_2O$.

The batch and continuous cultures were conducted in a 2-l fermentor (BMJ02-PI, Able Co., Tokyo, Japan) with a working volume of 1 l. The pH was controlled at 7.0±0.1 using 2 N HCl or 2 N NaOH, and the temperature was set at 37°C. In the

experiments as described in Chapters 3 and 4, the air flow rate was 1 vvm (air volume/working volume/min), and the agitation speed was 400 rpm to maintain the dissolved oxygen concentration to be at 35%-40% (v/v) of air saturation. In the experiments as described in Chapter 5, anaerobic (microaerobic) cultures were initiated after 2 hours of aerobic cultivation by stopping air supply and slowing down the agitation speed to around 100 rpm. The CO_2 and O_2 concentrations were monitored using an off-gas analyzer (DEX-2562, Able Co., Tokyo, Japan). In the experiments as described in Chapters 3 and 4, the dilution rates in the continuous culture were 0.2, 0.4, 0.6 and 0.7 h^{-1} for the wild type, and 0.2 h^{-1} for the mutants. In Chapter 5, the dilution rate in the continuous culture was 0.1 h^{-1}. The triplicate samples were collected at the steady state which was confirmed by the constant cell density and CO_2 concentration in the off-gas. It generally took 3-4 residence times to achieve the steady state.

2.2 Analytical method

Bacterial growth was monitored by measuring the optical density of the culture broth at 600 nm (OD_{600}) using a spectrophotometer (Ubet-30, Jasco, Japan). After the fermentation, *E. coli* cells from 200 ml of culture were harvested by centrifugation and dried. After confirming that the weight of the dried material was constant, the dry cell weight per liter of culture was calculated from the measured weight. It was then converted to dry cell weight (DCW) based on the OD_{600}-DCW relationship (1 $OD_{600} \approx 0.3$ g/l). Glucose, fructose, xylose, lactate, acetate, formate, ethanol and xylitol concentrations in the medium were measured using commercially available kits (Wako Co., Osaka, Japan for glucose, fructose and xylose; Roche, Molecular Biochemical, Mannheim, Germany for others).

2.3 RNA preparation, design of PCR primers

Total RNA was isolated from *E. coli* cells by Qiagen RNeasy Mini Kit (QIAGEN K.K., Tokyo, Japan) according to the manufacture's recommendation. The quantity and purity of RNA were determined by the optical density measurements at 260 and 280 nm and by 1% formaldehyde agarose gel electrophoresis. The primer sequences for respective genes used in this study were reported elsewhere (Kabir and Shimizu, 2003). Criteria for the design of the gene-specific primer pairs were followed according to *Molecular Cloning: A laboratory Mannual* (Sambrook and Russel, 2001). The primers used in this study were synthesized at Hokkaido System Science Co. (Sapporo, Japan). In all cases, the primer-supplied company confirmed the purity and absolute specificity of the primers.

2.4 cDNA synthesis and PCR amplification

RT-PCR reactions were carried out in a Takara PCR Thermal Cycler (Takara TP240, Japan) using Qiagen One-step RT-PCR Kit (QIAGEN K.K., Tokyo, Japan). The reaction mixture was incubated for 30 min at 50°C for reverse transcription (cDNA synthesis) followed by 15 min incubation at 95°C for initial PCR activation. Then, the process was subjected to 30 cycles of amplification which consisted of a denaturing step (94°C for 1 min), an annealing step (approximately 5°C below melting temperature of primers for 1 min) and an extension step (72°C for 1 min), and finally the reaction mixture was incubated for 10 min at 72°C for final extension. To check for nucleic acid contamination, one negative control was run in every round of RT-PCR. This control lacks the template RNA in order to detect possible contamination of the reaction components. 5 ml of amplified products were run on a 1% agarose gel. Gels were stained with 1 μg/ml of ethidium bromide, photographed

using a Digital Image Stocker (DS-30, FAS III, Toyobo, Osaka, Japan) under UV light and analyzed using Gel-Pro Analyzer 3.1 software (Toyobo, Osaka, Japan)). Although the PCR products obtained for all the genes showed the predicted sizes on agarose gel, the identity of amplified fragments of some genes was demonstrated by DNA sequencing. In order to determine the optimal amount of input RNA, the two-fold diluted template RNA was amplified in RT-PCR assays under identical reaction conditions to construct a standard curve for each gene product. When the optimal amount of input RNA was determined for each gene product, RT-PCR was carried out under identical reaction conditions to detect differential transcript levels of genes. The gene *dnaA*, which encodes DnaA, a replication initiation factor in *E. coli* and is not subjected to variable expression, i.e. abundant expression at relatively constant rate in most cells, was used as an internal control for the RT-PCR determinations. To calculate the standard deviation, RT-PCR was independently performed three times for each gene under identical reaction condition. To ensure that the observed changes were statistically significant, the measurements were made in triplicate, and the Student's *t*-test was applied.

2.5 ^{13}C-labeling experiments, sample preparation and GC-MS analysis

The labeling experiments were started after the steady state was confirmed. The unlabeled (naturally labeled) feeding medium was replaced by an identical medium containing 3.2 g/l of unlabeled glucose, 0.4 g/l [U-^{13}C] glucose, and 0.4 g/l [1-^{13}C] glucose. Biomass samples were taken after another two residence times, where 200 mL of culture broth was taken for the measurement of biomass and extracellular metabolite concentrations, and the remaining 800 ml of the culture broth was processed for gas chromatography–mass spectrometry (GC-MS) analysis. The

biomass sample was kept on ice for 2–3 min, and the sample was centrifuged at 6,000 rpm at 2°C for 15 min (Zhao and Shimizu, 2003). The cell pellets were washed three times with 20 mM Tris–HCl at pH 7.6 and suspended in 10 mL of 6 M HCl. The mixture was then hydrolyzed at 105°C for 15 h in a sealed glass tube. During acid hydrolysis, tryptophan and cysteine were oxidized, and glutamine and asparagine were deaminated. The hydrolysate was evaporated to dryness. The dried material was dissolved in Milli-Q water and filtered through a 0.22-μm pore-size filter and evaporated to dryness. About 1.5 ml acetonitrile was added in the dried hydrolyte and incubated at room temperature overnight. After the color of liquid was turned to slight yellow, it was filtrated through 0.22-μm pore-size filter. The filtrate was then derivatized by N-(tert-butyldimethylsilyl)-N-methyl-trifluoroacetamide (Aldrich, USA) at 110°C for 30 min and was transferred to GC-MS sample tube for analysis (Zhao and Shimizu, 2003). GC-MS analysis was carried out using Auto-System XL GC (PerkinElmer Co., USA) equipped with a DB-5MS column (30 m × 0.25 mm × 0.25 mm, Agilent Co., USA) which was directly connected to a TurboMass Gold mass spectrometer (PerkinElmer Co., USA). The program Turbomass Gold (PerkinElmer Co., USA) was used for peak assignment and MS data processing (Zhao et al., 2004).

2.6 Metabolic flux analysis for ^{13}C-labeling experiments

The stoichiometric reaction model of the main metabolic pathway including glycolysis, penptose phosphate (PP) pathway, TCA cycle, anaplerotic pathway, and glyoxylate pathway was constructed for ^{13}C-MFA in Chapter 3 (Appendix C). The main idea is to perform isotopomer balance on carbon atoms in order to track the fate of the labeled carbon atoms from the substrate (Szyperski, 1995). Isotopomer balance enables us to determine the isotopomer distributions of the intracellular metabolites in the central metabolic network. Since the isotopomer distributions of

amino acids can be inferred from the isotopomer distributions of their corresponding precursors, the GC-MS signals for the amino acids can then be simulated. A set of flux distributions is then determined by minimizing the differences between the experimental and simulated data. For the estimation of GC-MS signals using isotopomer balance, three types of corrections were made to take into account the effects of natural abundance, non-steady state condition, and skewing effect. First, the isotopomer distributions of the input substrate were corrected for natural abundance in the unlabeled glucose and impurity in the labeled glucose. Second, the isotopic steady-state condition is normally not attained at the time of harvesting biomass. Thus, the simulated data have to be corrected based on the actual harvesting time by assuming first-order washout dynamics (Dauner et al., 2001). Finally, the simulated GC-MS data were corrected for the natural isotope abundance of O, N, H, Si, S, and C atoms in the derivatizing agent using the correction matrices (Van Winden et al., 2002).

The fluxes were obtained by minimization of the deviation between experimental GC-MS data and the estimated values, using the iterative scheme in the minimization procedure. A set of intracellular fluxes (including net fluxes and exchange fluxes) that gives the minimum deviation could be taken as the best fit. The stage optimization was made by both local search and with global search such as genetic algorithm (Zhao and Shimizu, 2003).The optimizing function was defined as

$$\min \quad J = \sum_{i=1}^{N} \left(\frac{MDV_i^{measured} - MDV_i^{simulated}}{\delta_i} \right)^2 + \sum_{j=1}^{M} \left(\frac{r_j^{measured} - r_j^{simulated}}{\delta_j} \right)^2 \qquad (2.1)$$

where $MDV_i^{measured}$ is the mass distribution of the *i*th measured substance, $MDV_i^{simulated}$ is the simulated mass distribution of the corresponding substance, and N is the number of measured substances, $r_j^{measured}$ is the measured extracellular metabolite or biomass synthesis flux for *j*th reaction, $r_j^{simulated}$ is the simulated

extracellular metabolite or biomass synthesis flux for corresponding reaction, and M the is the number of the reactions for extracellular metabolite or biomass synthesis fluxes, and δ_i and δ_j are the absolute measurement errors. The optimized flux was selected from the results obtained by 100 independent flux estimations using a single mass distribution data set of intracellular metabolites or amino acids, respectively.

2.7 Estimation of the specific ATP production rate and specific NADPH production rate

The ATP production is made by substrate level phosphorylation and oxidative phosphorylation, where the reducing power of NADH and $FADH_2$ can contribute in generating ATP via oxidative phosphorylation. The pathways involved in electron transport and oxidative phosphorylation have variable stoichiometry due to the use of different dehydrogenases and cytochromes. Then the specific ATP production rate as given in Chapter 3 may be estimated by the following equation (refer to Appendix C for the suffix numbers):

$$v_{ATP} = OP_{NADH} + OP_{FADH_2} + v_4 + v_6 + v_8 + v_{20} - v_3 \tag{2.2}$$

where OP_{NADH} and OP_{FADH_2} is the specific ATP production rates via oxidative phosphorylation, and those may be estimated by

$$OP_{NADH} = (v_4 + v_7 + v_{19} + v_{23} + v_{28}) \times (P/O) \tag{2.2a}$$

and

$$OP_{FADH_2} = v_{21} \times (P/O)' \tag{2.2b}$$

where (P/O) and $(P/O)'$ are the P/O ratios for NADH and $FADH_2$, respectively. Here, we set (P/O) to be 2 and $(P/O)'$ to be 1.

The specific NADPH production rate v_{NADPH} may also be estimated by:

$$v_{NADPH} = v_9 + v_{10} + v_{18} + v_{25} - v_{28} \tag{2.3}$$

2.8 Metabolic flux analysis for overdetermined system

In the flux analysis for the case under anaerobic condition as described in Chapter 5, the number of measurements is greater than the number required to determine the system. This, of course, yields an overdetermined system in which redundancies can be exploited to calculate not only the best estimates for the nonmeasured fluxes but also better estimates for the measured fluxes. Let *A* be the stoichiometric coefficient, *r* be the intracellular flux vector, and *q* be the extracellular measured specific substrate consumption rate, and the specific metabolite production rate, etc. Then the mass balance equation becomes as:

$$Ar = q \tag{2.4}$$

Let this equation be expressed as (Tsai and Lee, 1988):

$$\begin{bmatrix} q_m \\ q_c \end{bmatrix} = \begin{bmatrix} A_{11} & A_{12} \\ A_{21} & A_{22} \end{bmatrix} \begin{bmatrix} r_1 \\ r_2 \end{bmatrix} \tag{2.5}$$

Where q_m is the measured specific rate, and q_c is the intracellular specific rate. Suppose A_{22} is the square matrix and non-singular. In general, q_c can be set to zero, and the above equation may be expressed as:

$$q_m = A_{11}r_1 + A_{12}r_2 \tag{2.6a}$$

$$0 = A_{21}r_1 + A_{22}r_2 \tag{2.6b}$$

The following equation can be derived from Eq. (2.6b):

$$r_2 = -A_{22}^{-1} A_{21} r_1 \tag{2.7}$$

Substitution of this into Eq. (2.6a) gives

$$q_m = B r_1 \tag{2.8}$$

where

$$B = A_{11} - A_{12} A_{22}^{-1} A_{21} \tag{2.9}$$

Note that B is not necessarily the square matrix, and thus the least square estimate for r_1 may be obtained from Eq. (2.8) as:

$$\hat{r}_1 = (B^T B)^{-1} B^T q_m \tag{2.10}$$

$$\hat{r}_2 = -A_{22}^{-1} A_{21} \hat{r}_1 \tag{2.11}$$

In the flux calculation, we used above equations.

The simplified central metabolic reactions in *Escherichia coli* are summarized in Appendix D.

2.9 Estimation of the specific ATP production rate (Chapter 5)

In Chapter 5, the specific ATP production rate for the case under anaerobic condition as described in Chapter 5 may be estimated by the following equation:

$$v_{ATP} = -v_3 + v_7 + v_9 - v_{12} - v_{17} - v_{18} + v_{20} + v_{22} \tag{2.12}$$

Chapter 3

The effect of the dilution rate on the catabolite regulation in the continuous culture of *E. coli*

3.1 Introduction

Carbon source is by far important in practice among the culture environments. In particular, carbon source levels affect specific global regulators and their related metabolic pathway genes involved in CCR. In the continuous cultures, the concentration of growth-limiting carbon source can be controlled by the dilution rate (Hoskisson and Hobbs, 2005). Gene transcript data and metabolic flux analysis are essential to detect small changes in response to perturbation caused by the different dilution rate. Gene transcript data can provide important information about cell physiology and has the potential to identify connections between regulatory or metabolic pathways (DeRisi et al., 1997). Another level of information, the metabolic flux analysis, aiming at the quantitative analysis of *in vivo* carbon fluxes in metabolic networks, is considered as a powerful tool for understanding the complex metabolic control mechanism of the whole cell (Wittman, 2007). The most widespread approach is ^{13}C-metabolic flux analysis (^{13}C-MFA) based on GC-MS measurement of labelling pattern of metabolites obtained from the tracer experiments performed (Wiechert, 2001; Shimizu, 2004). It is critical to integrate different levels of information such as fermentation data, gene transcript data and metabolic flux analysis for understanding carbon catabolite regulation mechanism.

In this chapter, the effect of the dilution rate on the catabolite regulation in the continuous cultures of *E. coli* was investigated based on fermentation data, gene transcript data and metabolic flux analysis. The dilution rate was varied from the almost glucose-starved state at 0.2 h^{-1} to the nearly unlimited glucose supply at 0.7 h^{-1}. At first, several fermentations were conducted for wild type *E. coli* at different dilution rates. In addition, the gene expression patterns were analyzed, characterizing how global regulators and their regulated genes change at different carbon source levels. Furthermore, metabolic flux distributions obtained from ^{13}C isotope labeling experiments were compared to get insight into genotype-phenotype relationship (Yao

et al., 2011).

3.2 Results

3.2.1 Fermentation characteristics

Table 3.1 shows the fermentation characteristics of the wild type *E. coli* for the continuous culture at different dilution rates, where it indicates that the specific glucose uptake rate, the specific acetate formation rate, and the specific CO_2 evolution rate (CER) were increased as the dilution rate was increased.

Table 3.1 Effect of the dilution rate on fermentation characteristics of wild type *E. coli*.

Dilution rate (h^{-1})	Biomass conc. (g/l)	Glucose conc. (g/l)	Glucose uptake rate (mmol/g/h)	Acetate formation rate (mmol/g/h)	Biomass yield (g/g)	CER (mmol/g/h)
0.2	1.45±0.06	ND*	3.07±0.13	0	0.37±0.01	9.15
0.4	1.87±0.09	ND*	4.75±0.23	0.01	0.47±0.02	11.61
0.6	2.00±0.09	ND*	6.67±0.30	0.88±0.04	0.50±0.02	13.17
0.7	1.93±0.08	ND*	8.05±0.34	1.33±0.06	0.48±0.02	15.83

ND*: not detectable, where glucose detectable limit was 0.038 g/l.

3.2.2 Gene expression analysis

In order to interpret the fermentation characteristics, the relative mRNA levels were measured at different dilution rates by RT-PCR (Fig. 3.1), where the gene *dnaA* was used as an internal control. As the dilution rate was increased, the transcript levels of *crp*, *cra* as well as *mlc* were decreased accordingly. The decrease in *crp* is also coincident with the decrease in *cyaA* which encodes Cya. In accordance with the

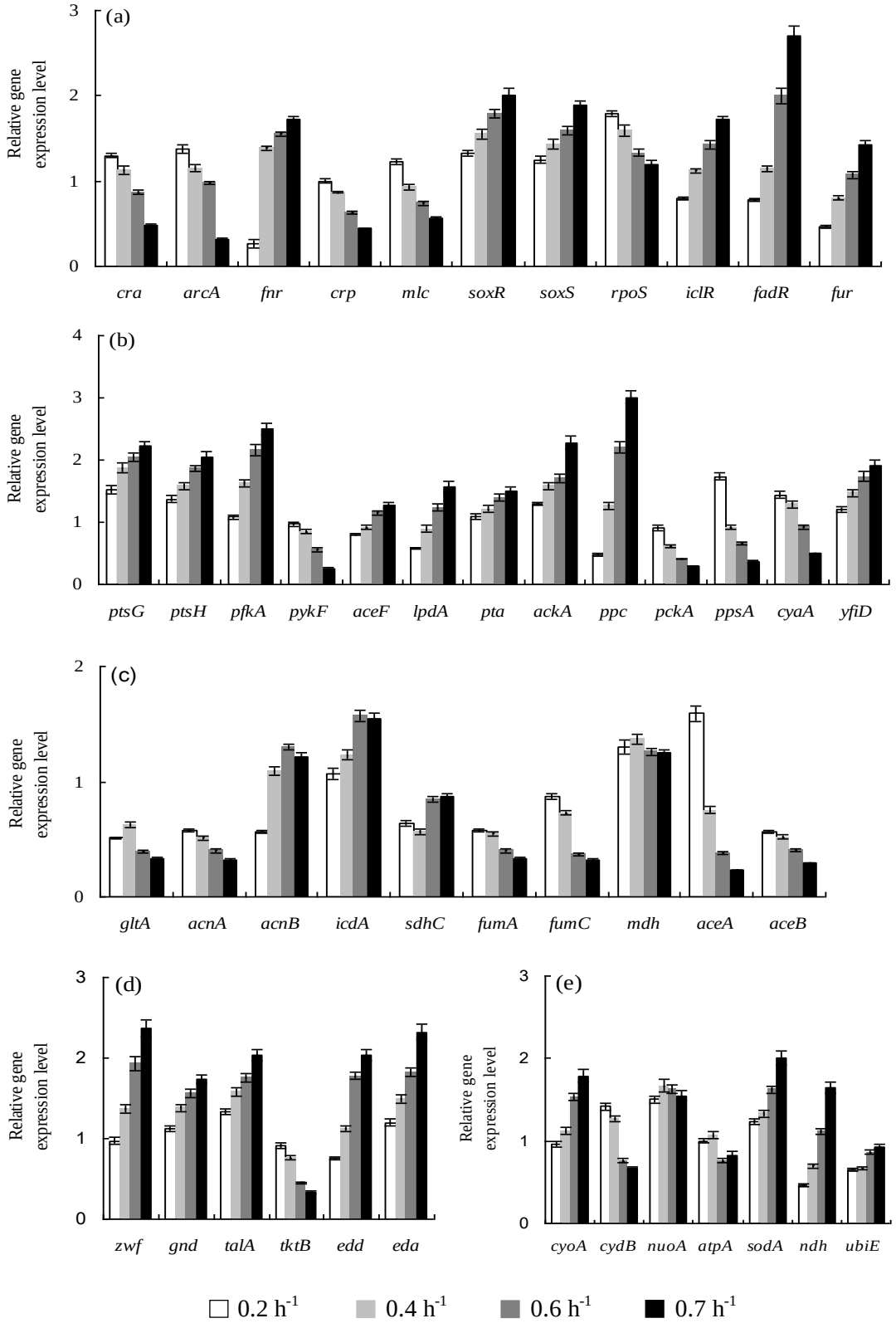

Figure 3.1 The effect of the dilution rate on the gene transcript levels of wild type *E. coli*. (a) Global regulator genes; (b) PTS, glycolysis, anaplerotic pathway, gluconeogenesis, *cyaA* and *yfiD* genes; (c) TCA cycle and glyoxylate pathway genes; (d) PP pathway genes; (e) Respiratory chain genes.

increased specific glucose uptake rate, the transcript levels of *ptsG*, *ptsH*, and *pfkA* were increased as the dilution rate was increased. In accordance with the increased specific acetate formation rate, the transcript levels of *pta* and *ackA* were increased. For the glycolytic genes, the increase in the transcript level of *pfkA* may be due to the decrease in *cra*. For the anaplerotic pathway genes, the transcript level of *ppc* was increased, while *pckA* was decreased as the dilution rate increased. The decrease in *pckA* may be caused by the fact that it is under control of both Crp and Cra. The increase in *yfiD*, whose product is similar to pyruvate-formate lyase, may be due to increase in *fnr* transcript level, though Fnr may be inactive under aerobic condition. TCA cycle genes such as *gltA* (except the case of the dilution rate at 0.4 h^{-1}), *acnA*, *fumA, C* were decreased, while *acnB, icdA* (except the case of the dilution rate at 0.7 h^{-1}) and *lpdA* were increased as the dilution rate increased. The decreased transcript levels of *gltA*, *acnA*, and *fumA* may be due to the decrease in *crp*. The decrease in *acnA* and increase in *acnB* may be caused by decrease in *cra*. The increase in *lpdA* transcript level may be due to decrease in *crp,* where cAMP-Crp represses such gene expression. Moreover, the transcript levels of glyoxylate pathway genes, *aceA* and *aceB* were decreased as the dilution rate was increased, which may be caused by the increased transcript levels of *fadR* and *iclR,* as well as the decreased transcript level of *cra.* For PP and Entner–Doudoroff (ED) pathway genes, the transcript levels of *zwf*, *gnd*, *edd*, and *eda* were increased as the dilution rate increased in accordance with the decrease in *cra*. In accordance with the increase in *soxR/S* transcript levels, *zwf* and *sodA* were increased, whereas *acnA* and *fumC* were decreased. In accordance with the decrease in the transcript level of *arcA*, the transcript level of *cyoA* was increased, while *cydB* was decreased as the dilution rate was increased, where the latter phenomenon also coincided with the decrease in *cra* transcript level (Appendix B). Further observations indicate that in accordance with the decrease in *rpoS* transcript level, *tktB*, *acnA*, *fumC* were decreased, while *fur* was increased as the dilution rate increased in accordance with the increase in *soxR/S*.

3.2.3 Metabolic flux distribution

Fig. 3.2 compares of the metabolic flux distributions of *E. coli* at the dilution rates of 0.2 h^{-1}, 0.4 h^{-1}, 0.6 h^{-1} and 0.7 h^{-1}. For absolute fluxes, the values of PP pathway, anaplerotic pathway and TCA cycle were increased as the dilution rate was increased. For relative fluxes, the decrease in TCA cycle and increase in acetate formation as the dilution rate increased can be observed. The difference in absolute flux and relative flux of TCA cycle will be explained in discussion part. Based on the absolute flux result, the specific ATP production rate and the specific NADPH production rate computed using Eqs. 2.2 and 2.3 as stated in Materials and methods section are plotted with respect to the dilution rate in Fig 3.3, which indicates that these are linearly correlated with the specific growth rate.

3.3 Discussion

Referring to Table 3.1 and Fig 3.1, the overall regulation of the dilution rate on the metabolic regulation of wild type *E. coli* is given in Fig. 3.4. As the dilution rate was increased, the glucose concentration was increased (although not detectable in Table 3.1). The higher concentration of glucose caused decrease in $EIIA^{Glc}$-P. This deactivated Cya (as implied by *cyaA* in Fig. 3.1b), which in turn caused decrease in cAMP concentration, and thus cAMP-Crp or *crp* transcript level was decreased (Fig. 3.1a). Note that cAMP level starts to increase when glucose concentration becomes less than about 0.3 mM (Ferenci, 2001). It has been reported that there is a Crp binding region in the promoter region of *mlc* gene, so that *mlc* transcript level was also decreased (Escalante et al., 2012). The glucose PTS is activated by Crp, but it is also repressed by Mlc. The enhancement of glucose PTS was subject to Mlc under this condition, and caused glucose uptake rate to be increased. Due to higher glucose uptake rate, FBP was accumulated, which repressed *cra* (Fig. 3.1a). For other global regulators, the increase in *iclR* was due to the repression by glyoxylate (Fig. 3.1a),

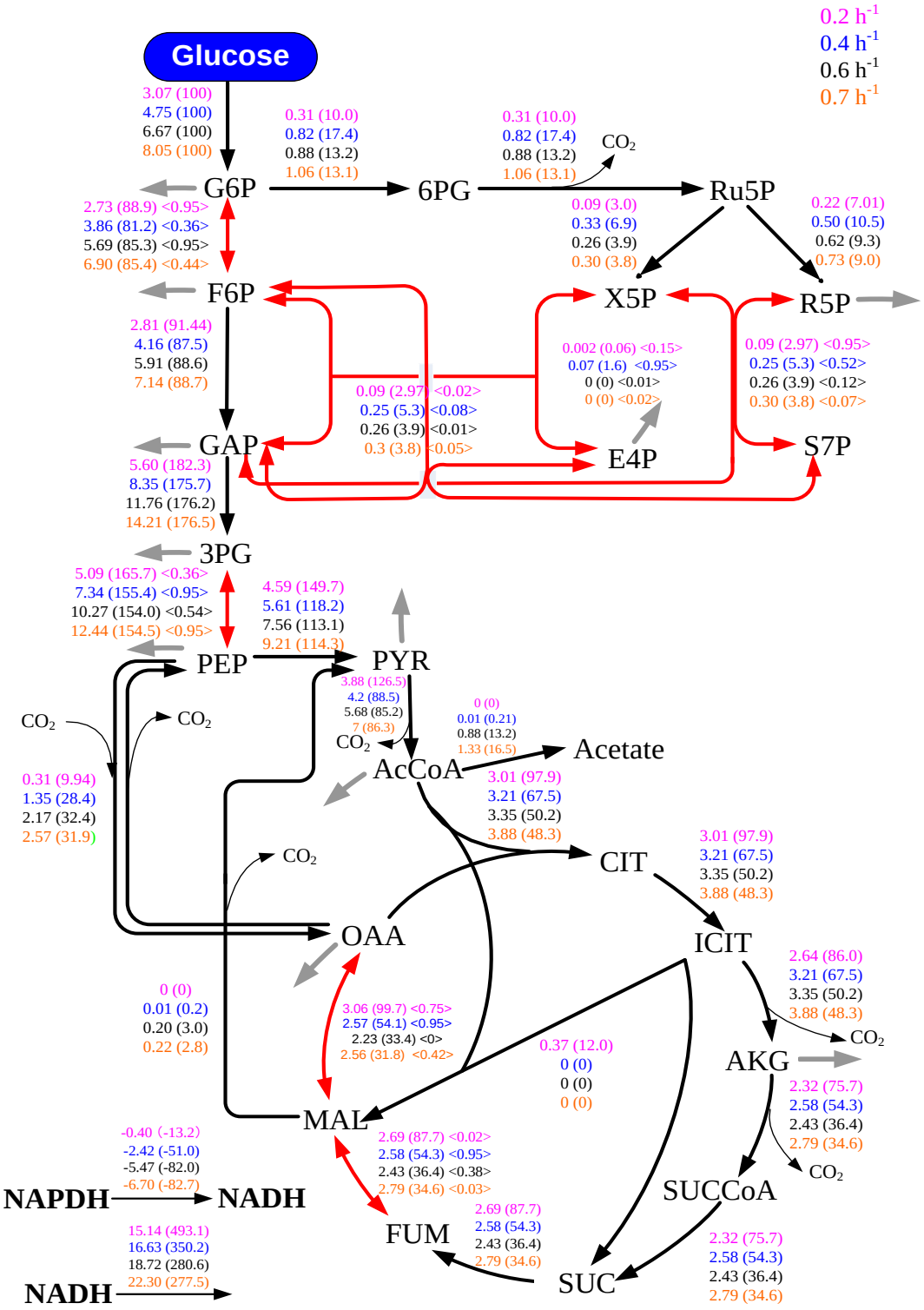

Fig. 3.2 The effect of the dilution rate on the metabolic flux distributions. All fluxes are given as absolute values (mmol/g/h) and as values relative to the specific glucose consumption rate (in parentheses), values in < > indicate exchange coefficients. Arrowheads indicate the direction of the fluxes.

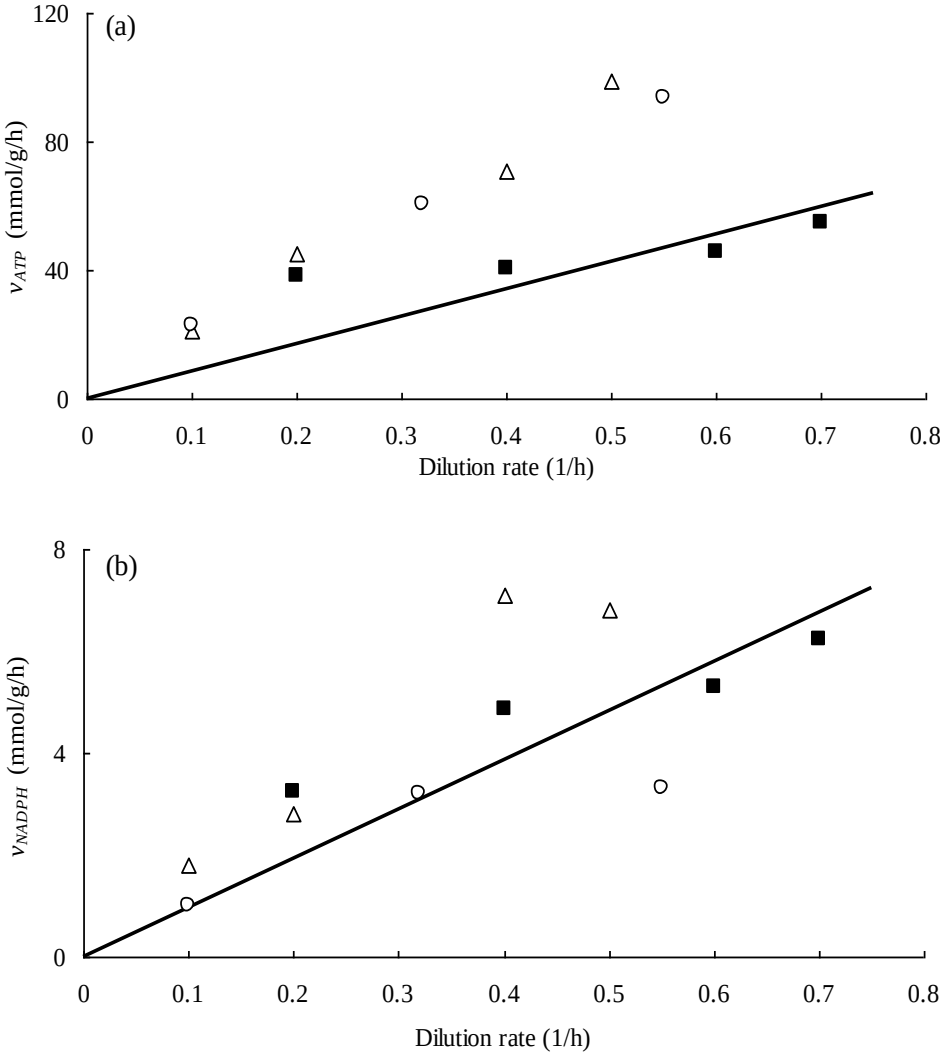

Fig. 3.3 The effect of the dilution rate on the specific ATP production rate (3.3a) and specific NADPH production rate (3.3b). Filled square symbols are from the present study, open triangle symbols are from (Ishii et al., 2007), while open circle symbols from (Yang et al., 2003).

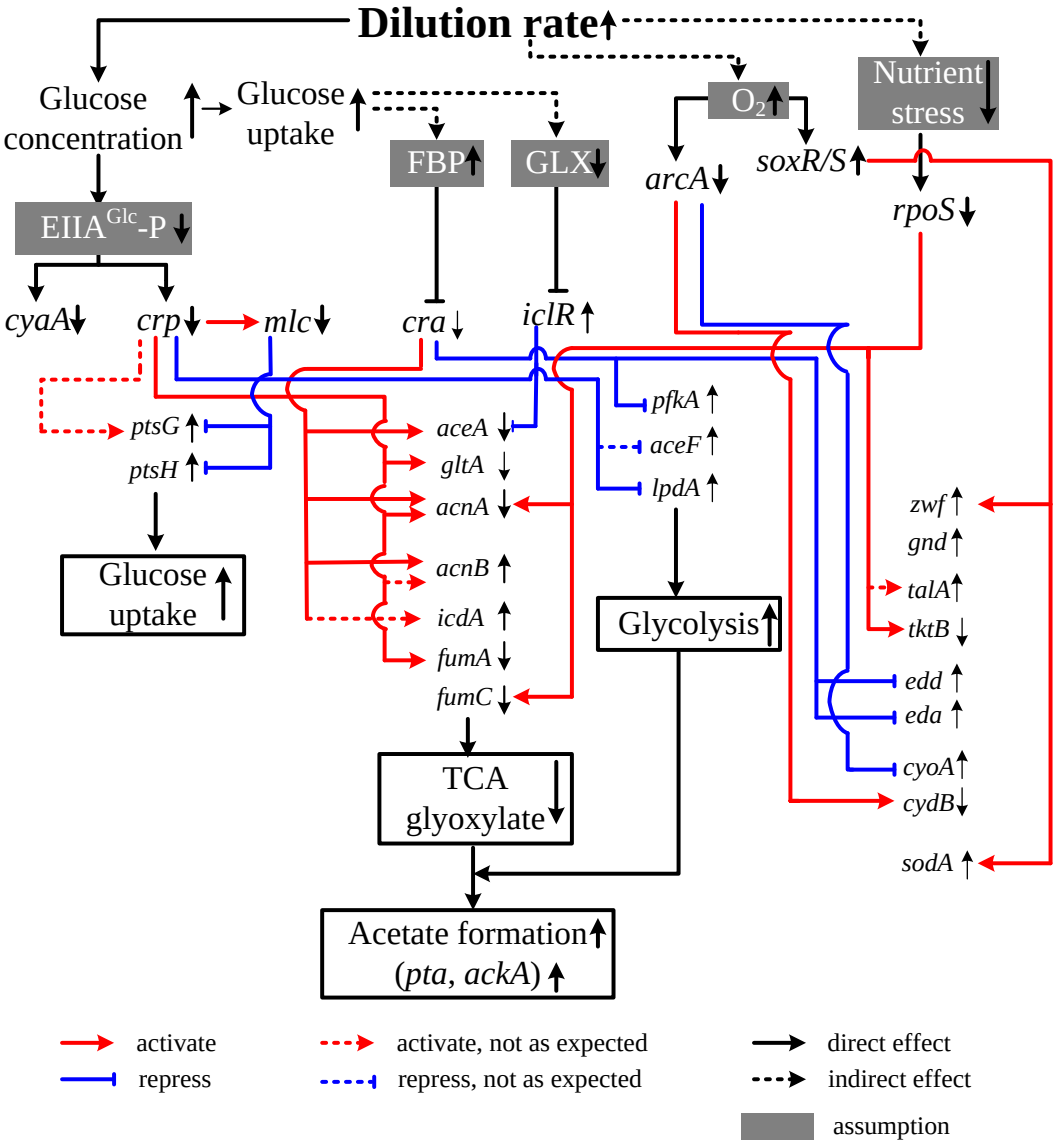

Figure 3.4 The overall regulation of the dilution rate on the metabolic regulation of wild type *E. coli.*

which was coincided with the increase in the glucose uptake rate. The decrease of *arcA* transcript level and increases of *soxR/S* transcript levels may be due to higher dissolved oxygen concentration. The decrease of *rpoS* (Fig. 3.1a) may be explained as less nutrient stress as the dilution rate was increased.

Referring to Table 3.1 and Fig 3.1, the changes in some metabolic pathways may be explained with respect to the changes in global regulators. Under the co-regulation of these global regulators, especially Crp and Cra, TCA cycle and glyoxylate pathway were repressed, and glycolysis was activated as the dilution rate was increased. This caused acetate to be accumulated. These results are also consistent with the relative flux result.

In contrast to the decrease in the relative TCA cycle flux, the absolute flux of TCA cycle was increased, which may be explained as follows (Fig. 3.5): Namely, as the dilution rate was increased, the TCA cycle flux was increased, which was also reflected by the increased CER. The increase in TCA cycle flux caused more production of NADH, which goes to respiratory chain. The increased respiration caused ubiquinone to be increased. It has been reported that ubiquinone acts as a repressor for ArcB phosphorylation (Malpica et al., 2004). Thus, ArcB was less phosphorylated. Unphosphorylated ArcB promoted the dephosphorylation of ArcA-P. Phosphorylated ArcA (ArcA-P) is the active form of ArcA, where ArcA-P represses TCA cycle genes. This forms a feed-back control. In addition, the activated respiratory chain enhanced oxidative stress, which increased SoxR/S level. SoxR/S contributed to upregulation of *sodA* encoding superoxide dismutase. Furthermore, the increased SoxR/S upregulated *zwf* encoding the glucose-6-phosphate dehydrogenase (G6PDH) in the oxidative PP pathway. The flux of oxidative PP pathway was increased, producing more NADPH for more demands of biomass. Moreover, the increase in anaplerotic flux also contributed to the higher cell growth. In the continuous culture, the dilution rate is equal to the specific growth rate. Thus,

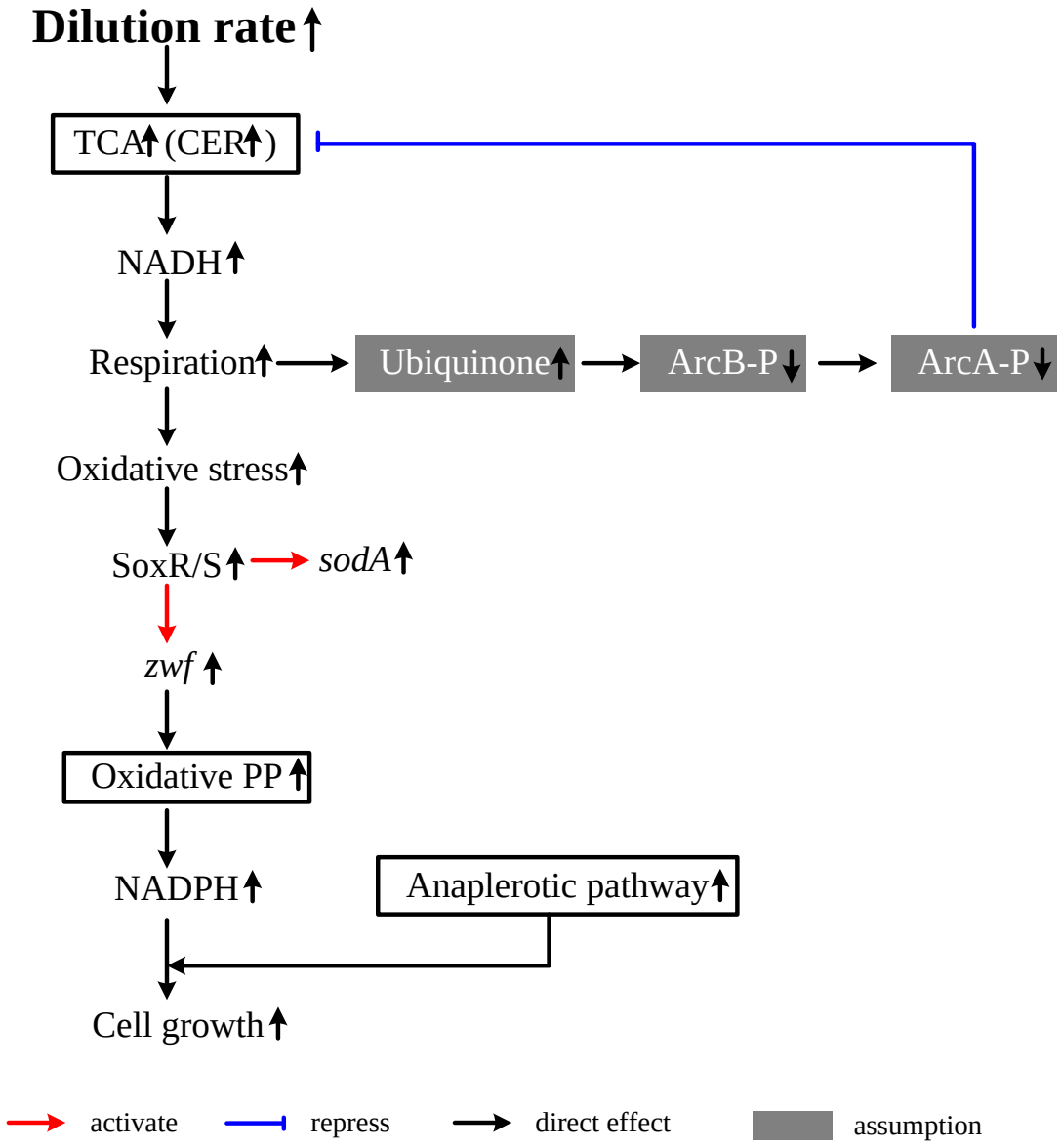

Figure 3.5 The interactions between absolute flux of TCA cycle and the cell growth.

the higher cell growth was consistent with higher dilution rate.

For the cell state, it has been shown that *acnB* is dominant for the exponential growth phase, while *acnA* is dominant at the stationary phase (Rahman et al., 2008; Rahman and Shimizu, 2008). The decrease in *acnA* and increase in *acnB* (except the case of the dilution rate at 0.7 h^{-1}) indicates that the continuous culture at higher dilution rate mimics the cell growth phase in the batch culture, while the continuous culture at lower dilution rate mimics the stationary phase.

3.4 Conclusion

From the glucose limiting state to glucose excess state, *E. coli* can actively respond to the changes by regulating gene expression levels to meet increasing metabolic demands, reflected by the redistribution of fluxes. The fermentation data, gene transcript analysis and ^{13}C-metabolic flux analysis indicate that the glycolysis was activated, while TCA cycle was repressed as the dilution rate was increased. These resulted in acetate overflow.

Chapter 4

The effects of several gene mutations on the catabolite regulation of *E. coli*

4.1 Introduction

In Chapter 3, the effect of the dilution rate on the catabolite regulation of *E. coli* based on global regulators and their metabolic pathway genes was discussed, which demonstrates the essential roles of global regulators, Crp and Mlc. In addition, Crp regulates *mlc* gene (Escalante et al., 2012). Thus, in the present chapter, the effects of *crp* and *mlc* gene knockout and *crp* enhancement (crp^+) on the catabolite regulation of *E. coli* were investigated.

In addition to global regulators, deletions of some metabolic pathway genes such as *mgsA* and *pgi* can also affect catabolite regulation indirectly. Such mutants altered the concentrations of some glycolysis intermediates, and enhance the *crp* level finally. The *mgsA* gene encodes the initial enzyme from dihydroxyacetone phosphate (DHAP) to methylglyoxal (MG). Although it is known to be cytotoxic, MG has been suggested to be a growth regulator, and MG pathway has been indicated to act as a bypass for glycolysis (Hopper and Cooper, 1971; Ackerman et al., 1974). In addition, accumulation of MG can affect intermediates at the level of glyceraldehyde 3-phosphate (GAP) and PEP (Tötemeyer et al., 1998). Furthermore, it has been reported that Δ*mgsA* mutant can improve the co-metabolism of sugars in ethanologenic *E. coli* (Yomano et al., 2009). However, little is known about its global regulation mechanism. In addition, the phosphoglucose isomerase encoded by *pgi* catalyzes the interconversion of glucose-6-phosphate (G6P) to fructose 6-phosphate (F6P), an essential step of the glycolysis and gluconeogenesis. In order to clarify the mechanism of catabolite regulation more clearly, the effects of *mgsA* and *pgi* gene knockout on the catabolite regulation of *E. coli* were investigated in this chapter. In Δ*pgi* mutant, the accumulation of G6P inhibits *ptsG* expression (Morita et al., 2003). This means that the phosphorylation of glucose at $EIICB^{Glc}$ from $EIIA^{Glc}$-P is disrupted, and this causes upregulation of *crp*. The upregulation of *crp* allows the co-consumption of multiple sugars. Much effort has been made in

Δ*pgi* mutant (Kabir and Shimizu, 2003; Toya et al., 2010). Here I conducted the continuous culture of Δ*pgi* mutant using a single carbon source such as glucose. The effect of *pgi* knockout on the simultaneous consumption of multiple sugars will be discussed in Chapter 5.

4.2 Results

4.2.1 Fermentation characteristics

Table 4.1 shows the effects of gene mutations on the fermentation characteristics at the dilution rate of 0.2 h^{-1}. In the case of Δ*crp* mutant, the specific glucose uptake rate was lower and the cell concentration was higher, and the specific acetate formation rate was higher as compared to the wild type. In the case of crp^{+} mutant, the fermentation characteristics were similar to the wild type by considering the statistical significance. In the case of Δ*mlc*, Δ*mgsA* and Δ*pgi* mutants, the specific glucose uptake rates were lower than that of wild type.

Table 4.1 Effects of gene mutations on the fermentation characteristics at the dilution rate of 0.2 h^{-1}.

Strains	Biomass conc. (g/l)	Glucose conc. (g/l)	Glucose uptake rate (mmol/g/h)	Acetate formation rate (mmol/g/h)	Biomass yield (g/g)
BW25113	1.45±0.06	ND*	3.07±0.13	0	0.37±0.01
Δ*crp*	1.57±0.07	ND*	2.83±0.13	0.35±0.02	0.39±0.02
crp^{+}	1.42±0.07	ND*	3.12±0.14	0	0.36±0.02
Δ*mlc*	1.65±0.08	ND*	2.69±0.13	0	0.41±0.02
Δ*mgsA*	1.55±0.07	ND*	2.87±0.14	0.10±0.005	0.39±0.02
Δ*pgi*	1.60±0.08	ND*	2.77±0.14	0	0.40±0.02

ND*: not detectable, where glucose detectable limit was 0.038 g/l.

4.2.2 Gene expression analysis

(a) Δ*crp* mutant and *crp*$^+$ mutant

Figure 4.1 shows the transcript levels of Δ*crp* mutant and *crp*$^+$ mutant as compared to wild type. Global regulator genes *cra* and *mlc* were downregulated ($P<0.01$ for both) in Δ*crp* mutant, and upregulated ($P<0.01$ for both) in *crp*$^+$ mutant. Figure 4.1b shows that *ptsG* and *ptsH* transcript levels changed in a similar fashion as *crp*, which corresponded to the lower glucose uptake rate for Δ*crp* mutant and was similar to the wild type for *crp*$^+$ mutant (Table 4.1). The transcript levels of glycolytic genes *pfkA* and *pykF* were influenced by Cra. In addition, the gluconeogenic genes *pckA* and *ppsA* were also subjects to the control of Cra. TCA cycle genes *gltA, acnA, sdhC, fumA* and *mdh* were all changed in a similar fashion as *crp*, while *acnA* and *icdA* changed in a same fashion as *cra*. The glyoxylate pathway gene *aceA* may be regulated by Cra, which may also be regulated by IclR. For respiratory chain genes, the *cydB* transcript level changed in a similar fashion as *arcA*, while *cyoA* gene changed in a reverse fashion (Appendix B). Furthermore, the *sodA* and *fur* genes changed in a similar fashion as *soxR/S*. The *acnA, tktB* and *fumC* genes changed in a similar fashion as *rpoS* (Appendix B).

(b) Δ*mlc* mutant

Figure 4.2 shows the transcript levels of Δ*mlc* mutant as compared to wild type. The transcript levels of *crp* and *cra* were decreased ($P<0.05$ and $P<0.01$, respectively) as compared to the wild type. Due to *mlc* gene knockout, the transcript levels of *ptsG* and *ptsH* were increased ($P<0.05$ and $P<0.01$, respectively). The transcript levels of glycolytic gene *pfkA* was decreased ($P<0.01$), while *pykF* was increased ($P<0.01$). TCA cycle genes *gltA, acnA, sdhC, fumA* and *mdh* were all downregulated ($P<0.01$ for all genes) due to decrease in *crp* ($P<0.05$). The downregulation of *acnA* and *icdA*

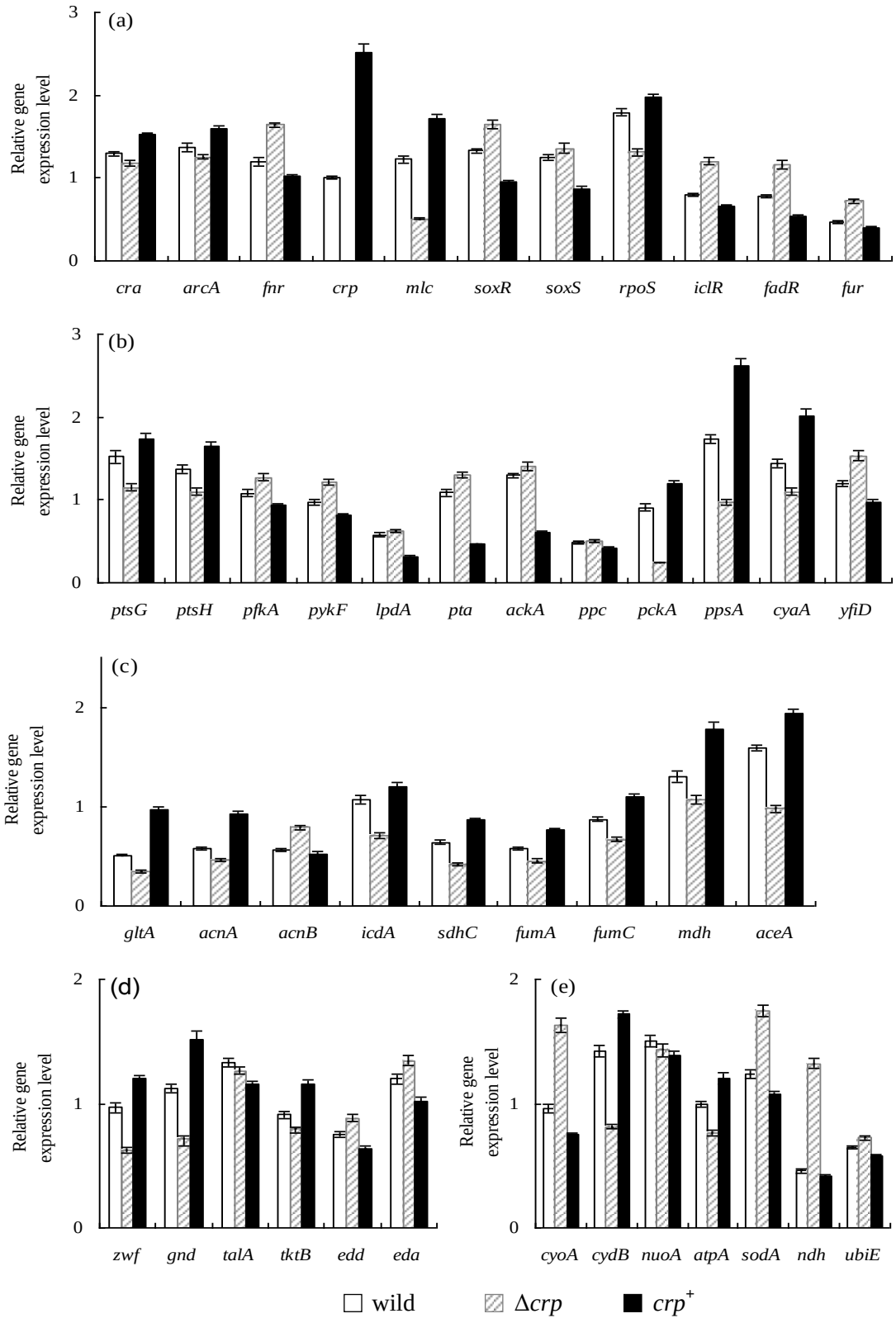

Figure 4.1 Comparison of gene transcript levels among the wild type, Δ*crp* mutant, and *crp*$^+$ mutant. (a) Global regulator genes; (b) PTS, glycolysis, anaplerotic pathway, gluconeogenesis, *cyaA* and *yfiD* genes; (c) TCA cycle and glyoxylate pathway genes; (d) PP pathway genes; (e) Respiratory chain genes.

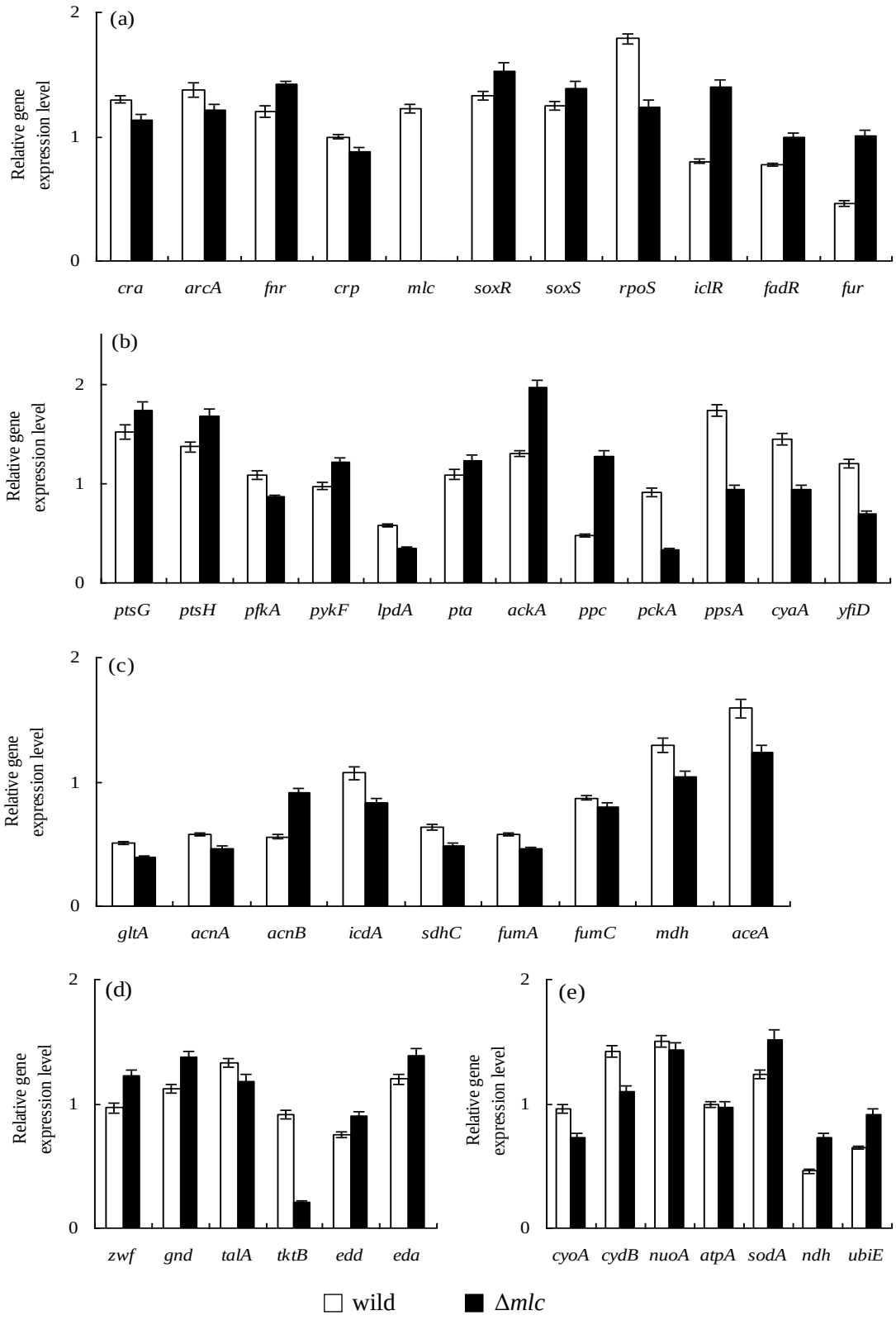

Figure 4.2 Comparison of gene transcript levels between the wild type and Δ*mlc* mutant. (a) Global regulator genes; (b) PTS, glycolysis, anaplerotic pathway, gluconeogenesis, *cyaA* and *yfiD* genes; (c) TCA cycle and glyoxylate pathway genes; (d) PP pathway genes; (e) Respiratory chain genes.

(P<0.01 for both), and upregulation of *acnB* (P<0.01) corresponded to the increase in *cra* (P<0.01). The downregulation of glyoxylate pathway gene *aceA* (P<0.01) may be caused by decrease in *cra* (P<0.01), which may also be ascribed to increase in *iclR* (P<0.01). The transcript level of *rpoS* decreased (P<0.01), thus, *tktB* and *fumC* were downregulated (P<0.01 and P<0.05, respectively) accordingly (Appendix B). The transcript levels of *soxR/S* increased (P<0.01 and P<0.05, respectively), and *sodA* increased (P<0.01) as compared to the wild type.

(c) Δ*mgsA* mutant

Figure 4.3 shows the transcript levels of Δ*mgsA* mutant as compared to wild type. The transcript levels of *crp* and *cra* as well as *mlc* were increased (P<0.01 for all genes). The increase in *crp* (P<0.01) was also coincident with the increase in *cyaA* (P<0.05). The transcript levels of glucose *pts* genes, *ptsG* and *ptsH* were decreased (P<0.01 for both), which is consistent with the decreased glucose uptake rate. For glycolytic genes, the transcript level of *pfkA* was decreased (P<0.01), while *pykF* was increased (P<0.01). The gluconeogenic genes *pckA* and *ppsA* were upregulated (P<0.01 and P<0.05, respectively). TCA cycle genes *gltA, acnA, sdhC, fumA* and *mdh* were all downregulated (P<0.01 for all genes) due to increase in *crp* (P<0.01). In addition, the upregulation of *acnA* and *icdA* (P<0.01 for both) might be due to the increase in *cra* (P<0.01). The upregulation of glyoxylate pathway gene *aceA* (P<0.05) may be caused by increase in *cra* (P<0.01), which may also be coincident to the decrease in *iclR* (P<0.01). For respiratory chain gene, the increase in *cydB* (P<0.01) may be due to the increased transcript levels of *cra* and *arcA* (P<0.01 and P<0.01, respectively). The transcript level of *rpoS* is also increased (P<0.01) for Δ*mgsA* mutant, which might be due to stress imposed on catabolism.

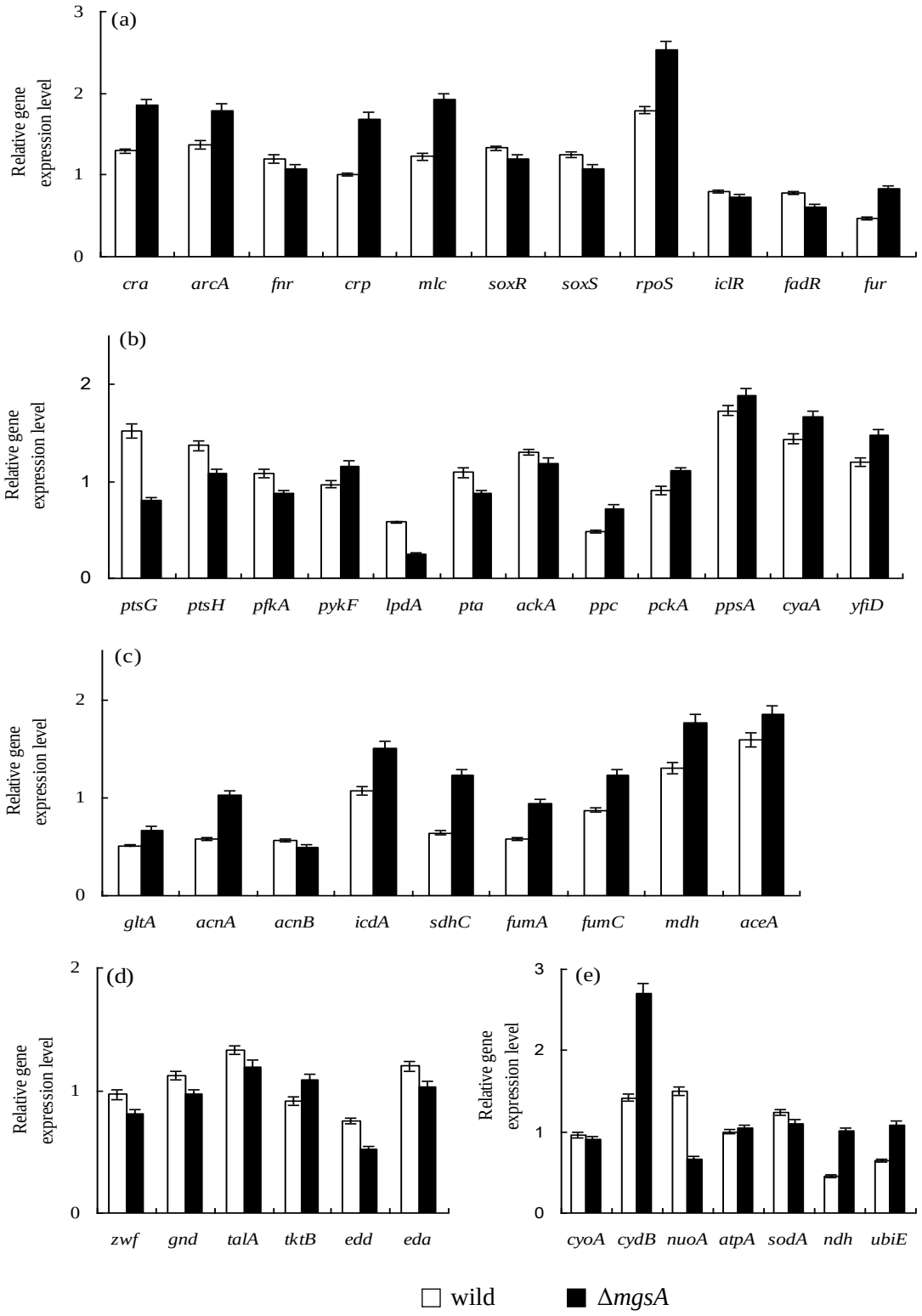

Figure 4.3 Comparison of gene transcript levels among the wild type and Δ*mgsA* mutant. (a) Global regulator genes; (b) PTS, glycolysis, anaplerotic pathway, gluconeogenesis, *cyaA* and *yfiD* genes; (c) TCA cycle and glyoxylate pathway genes; (d) PP pathway genes; (e) Respiratory chain genes.

4.3 Discussion

The overall regulation of Δ*crp* mutant is illustrated in Fig. 4.4. Due to *crp* knockout, *mlc* was also repressed (P<0.01). The decrease in glucose *pts* genes, *ptsG* and *ptsH* (P<0.01 for both) were subject to the control of Crp, while Mlc might not be dominant under this condition. Crp and Cra co-regulates glycolysis, TCA cycle and glyoxylate pathway. As a consequence, the increase in glycolysis, decrease in TCA cycle and glyoxyalte pathway caused acetate to be accumulated, where this is also reflected by the upregulation of *pta* and *ackA* transcript levels (P<0.01 and P<0.05, respectively). The batch culture of Δ*crp* mutant indicates that the acetate formed during cell growth phase, and could not be consumed during stationary phase (Appendix E).

Fig. 4.5 depicts the overall regulation of crp^+ mutant. The enhancement of *crp* (P<0.01) caused an elevated *mlc* gene transcript level (P<0.01). Note that Mlc might have repressed *ptsG* and *ptsH*, however, the *ptsG* and *ptsH* transcript levels were increased (P<0.05 and P<0.01, respectively), which indicates that Mlc regulation is dependent on the culture condition. Although glucose PTS was activated, the glucose uptake rate was not improved as compared to the wild type. It is not clear at this time why the glucose uptake rate was decreased even if *ptsG* gene was upregulated. Different from the case of Δ*crp* mutant, glycolysis was repressed, TCA cycle and glyoxyalte pathway were activated. This resulted in less acetate accumulation as reflected by the downregulation of *pta* and *ackA* transcript levels (P<0.01 for both).

Fig. 4.6 shows the overall regulation of Δ*mlc* mutant. The decrease of mlc (P<0.01) caused glucose *pts* genes to be upregulated. The decreases of *crp* (P<0.05) and *cra* (P<0.01) caused glycolytic genes (except *pfkA*) to be upregulated, while TCA cycle and glyoxylate pathway genes were downregulated. Although glucose *pts* genes *ptsG* and *ptsH* were upregulated (P<0.05 and P<0.01, respectively), this did not improve

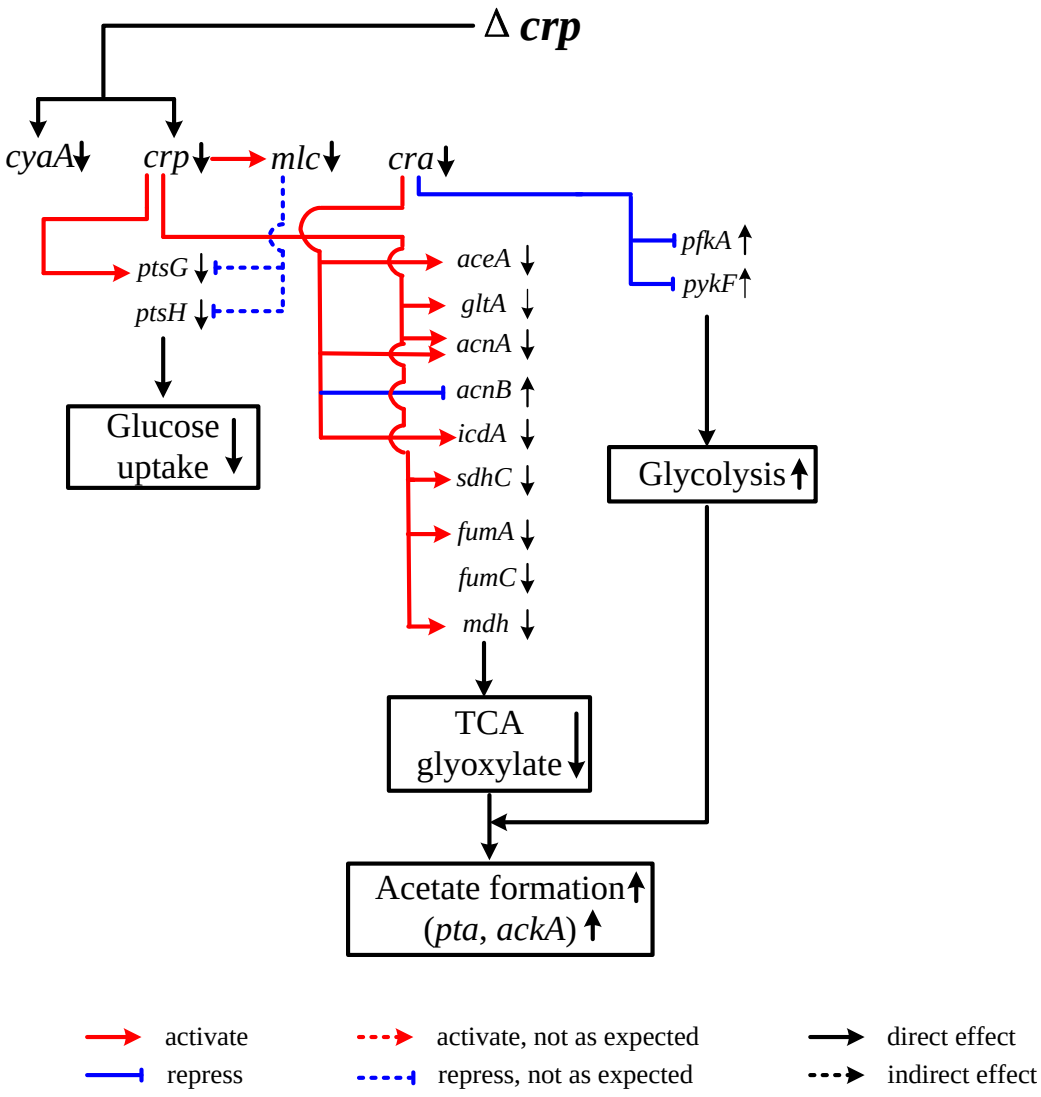

Fig. 4.4 The overall regulation of Δ*crp* mutant.

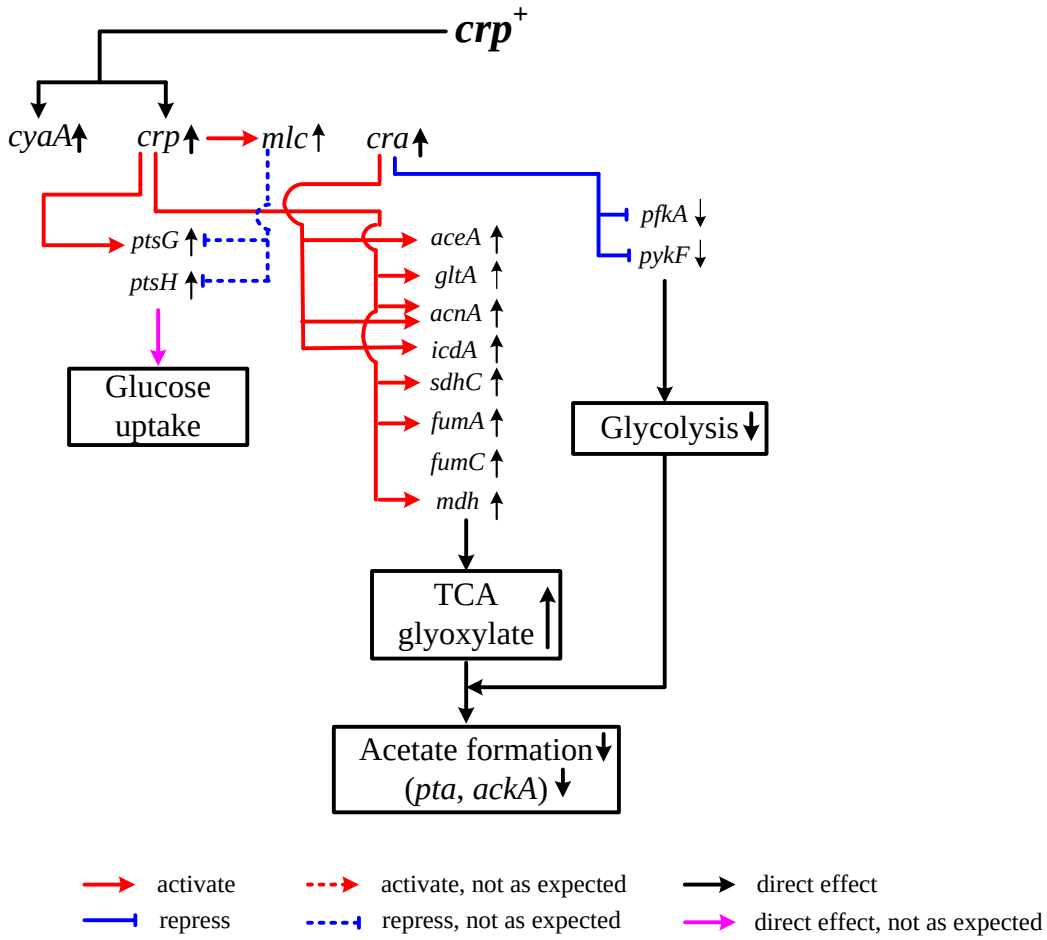

Fig. 4.5 The overall regulation of *crp*$^+$ mutant.

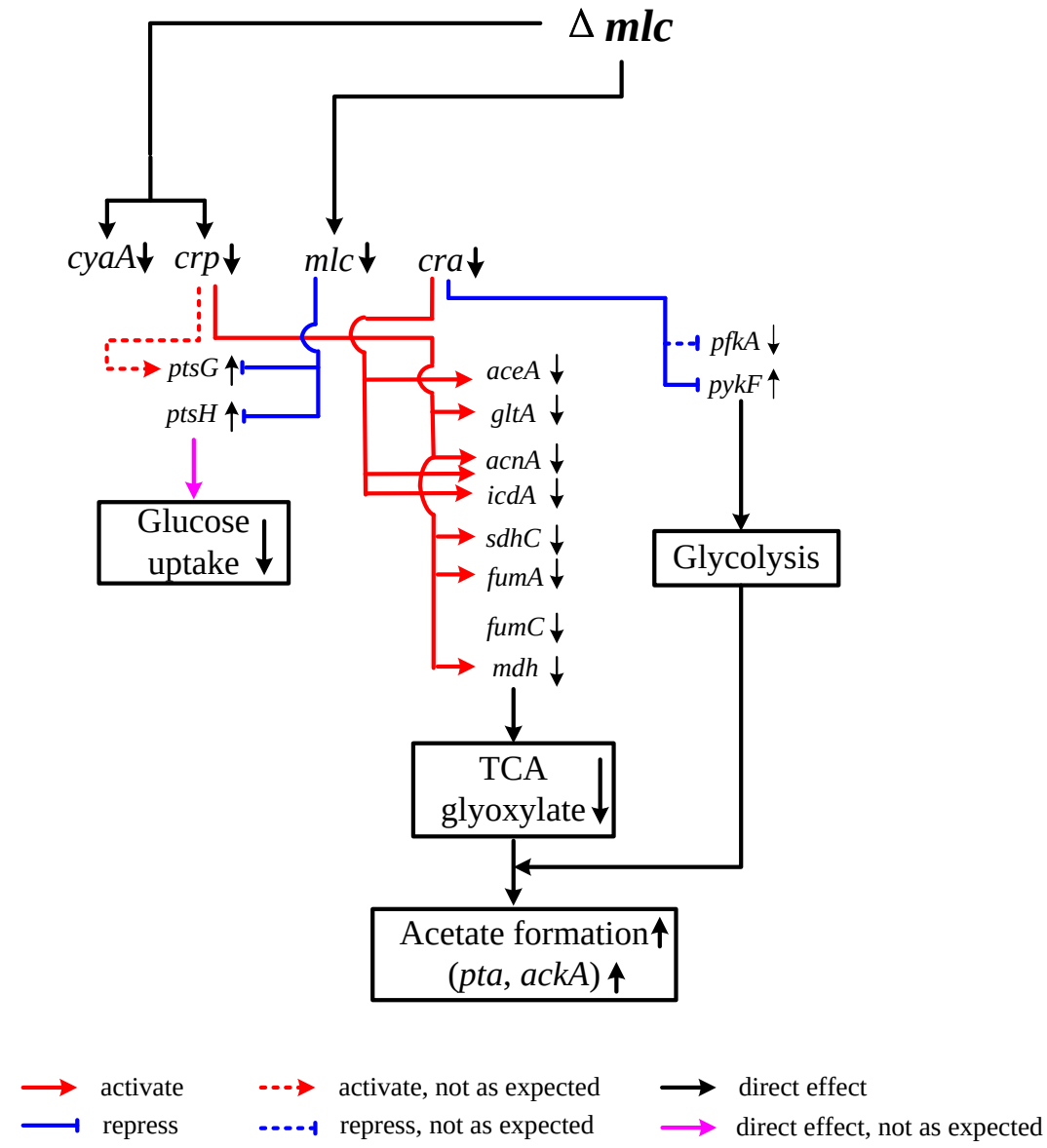

Fig. 4.6 The overall regulation of Δ*mlc* mutant.

the specific glucose uptake rate. The changes in glycolysis, TCA cycle and glyxoylate pathway were similar as the case of Δ*crp* mutant, and in turn upregulated acetate formation pathway genes, *pta* and *ackA* ($P<0.05$ and $P<0.01$, respectively). Although the higher acetate formation rate was not reflected in the continuous culture (Table 4.1), this happened indeed in the batch culture, where the acetate formed during the cell growth phase, and could not be consumed during the stationary phase (Appendix F).

Fig. 4.7 elucidates the overall regulation of Δ*mgsA* mutant. Since the terminal of MG pathway is PYR, deletion of *mgsA* would be expected to reduce PYR level. Furthermore, the absence of MG pathway increased the metabolic flux through the lower part of glycolysis by elevating GAP and PEP. Moreover, the concentration ratio between PEP and PYR (PEP/PYR) is the key factor controlling the phosphorylation of $EIIA^{Glc}$ (Hogema et al., 1998; Bettenbrock et al., 2007). In Δ*mgsA* mutant, the value of this ratio was elevated, and then $EIIA^{Glc}$ was predominantly phosphorylated. The higher $EIIA^{Glc}$-P in turn activated Cya, and thus *crp* level was increased. As stated above, Crp and Mlc co-regulated glucose PTS, the decreased levels of *ptsG* and *ptsH* were subject to the control of Mlc in Δ*mgsA* mutant. Furthermore, under the co-regulation of Crp and Cra, TCA cycle and glyoxyalte pathway were activated. This resulted in less acetate accumulation as reflected by the downregulation of *pta* and *ackA* transcript levels ($P<0.01$ and $P<0.05$, respectively).

4.4 Conclusion

The transcriptional catabolite regulation mechanism was clarified for wild type *E. coli*, and its Δ*crp*, crp^+, Δ*mlc*, Δ*mgsA* and Δ*pgi* mutants. The results indicate that carbon catabolite repression can be relaxed by crp^+, Δ*mgsA* and Δ*pgi* mutants. These

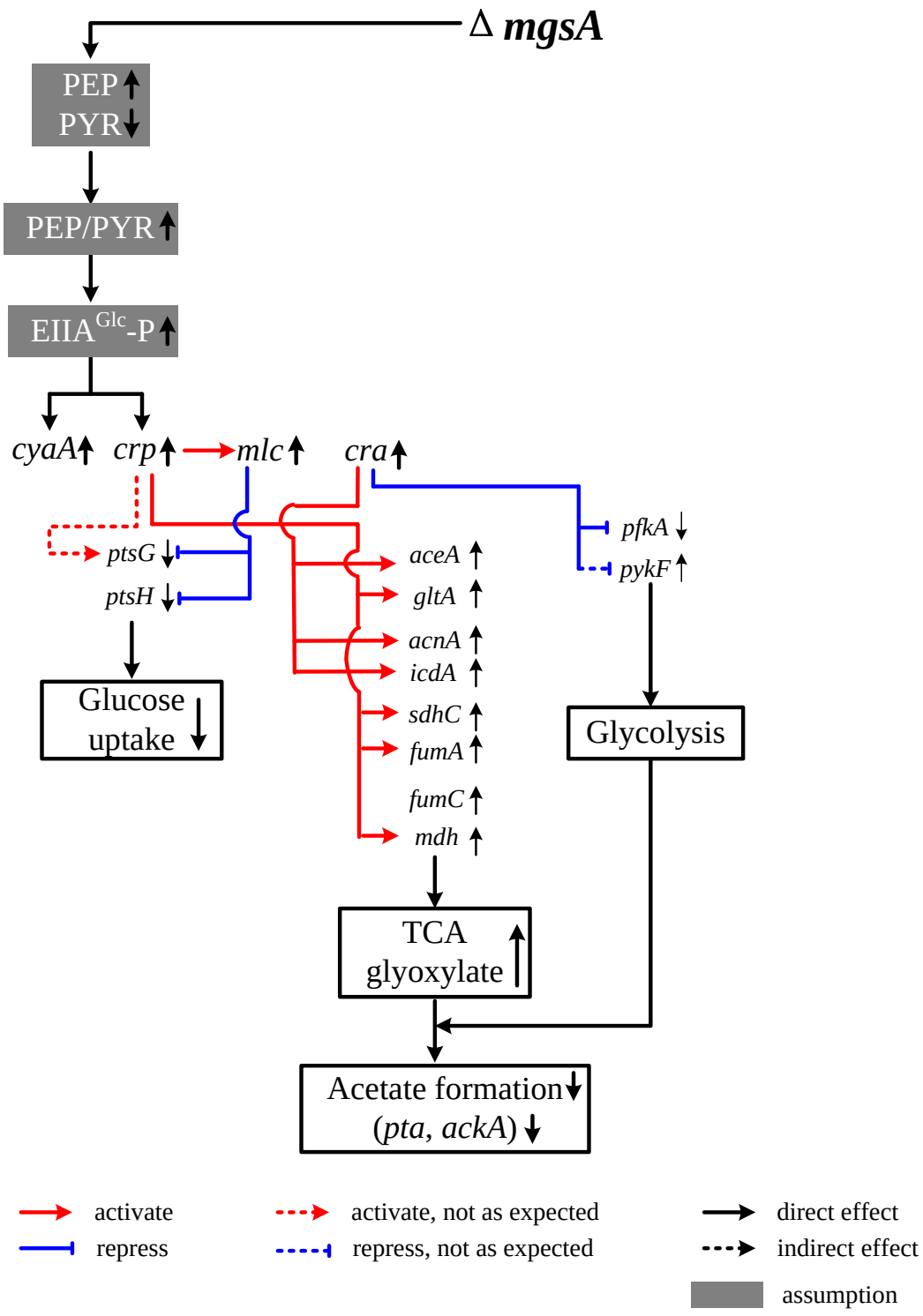

Fig. 4.7 The overall regulation of Δ*mgsA* mutant.

made the PTS activity to be decreased, resulting in increase in cAMP-Crp, which in turn activated the TCA cycle activity. Furthermore, relaxed carbon catabolite repression in these mutants may be able to attain co-consumption of multiple sugars, which will be discussed in Chapter 5. In the case of Δ*crp* and Δ*mlc* mutants, cAMP-Crp levels were decreased and TCA cycle was repressed, resulting in acetate overflow.

Chapter 5

The effects of Δ*cra*, *crp*$^{+}$ and Δ*pgi* on the co-consumption of multiple sugars

5.1 Introduction

In Chapter 3 and Chapter 4, it was clarified that the mechanism of catabolite regulation based on global regulators and their regulated metabolic pathway genes through different carbon source levels and several gene mutations. Furthermore, modulations of catabolite regulation can be applied for co-consumption of multiple sugars originated from hydrolysis of lignocellulose. In addition to glucose, another two representative sugars obtained from hydrolysis of lignocellulose, fructose and xylose (Clomburg and Gonzalez, 2010) were taken into account in this chapter. Similar as glucose, fructose is also transported by PTS. In particular, fructose PTS has its own HPr-like protein domain, FPr (Kornberg, 2001). The phosphoryl groups are transferred from PEP by successive phosphorelay reactions in turn by EI, FPr, $EIIA^{Fru}$, $EIIB'BC^{Fru}$, and subsequent transport and phosphorylation of fructose to fructose 1-phosphate (F1P). Fructose operon, *fruB* encodes diphosphoryl transfer protein (FruB), *fruK* encodes fructose 1-phosphate kinase, and *fruA* encodes the fructose-specific enzyme EIIB'BC (Saier and Ramseier, 1996). In contrast to glucose and fructose, xylose is a non-PTS sugar. Xylose uptake is made primarily through either an ATP dependent high affinity ABC transporter encoded by *xylFGH*, or an ATP independent low affinity proton symporter encoded by *xylE* (Griffth et al., 1992; Sumiya et al., 1995). Then the intracellular xylose is converted to xylulose by xylulose isomerase encoded by *xylA*, where xylulose is converted to xylulose 5-phosphate (X5P) by xylulose kinase encoded by *xylB*, and X5P finally goes into PP pathway. When xylose is present in the medium, xylose transcription factor, XylR, binds to the promoter regions of *xylAB*/*xylFGH*. In addition, XylR is activated by cAMP-Crp. Namely, the transcription in the *xylAB* and *xylFGH* operons are under positive control by XylR and cAMP-Crp (Song and Park, 1997).

Previous studies has focused on local genetic modifications of recombinant *E. coli* capable of co-utilizing of sugar mixtures (Hernández-Montalvo et al., 2001; Nichols

et al., 2001; Dien et al., 2002), whose disadvantages have been discussed in Chapter 1. Since local pathway genes are controlled by global regulators (Shimizu, 2009), the modulation of global regulators may also improve the efficiency of simultaneous consumption of multiple sugars without those disadvantages.

Chapters 1, 3 and 4 explained the role of Cra in relation to CCR, and its regulation by activating gluconeogenic genes and repressing glycolytic genes. In addition, Cra negatively controls fructose operon *fruBKA*. For the purpose of improving fructose uptake, *cra* gene knockout was considered. Moreover, the effect of Δ*cra* on the co-consumption of multiple sugars was investigated in this chapter. In addition, Chapter 4 shows that CCR can be relaxed by crp^+ and Δ*pgi* mutants. Thus, the effects of crp^+ and Δ*pgi* on the co-consumption of multiple sugars were also investigated in this chapter (Yao et al., 2013).

5.2 Results

5.2.1 Fermentation characteristics

(a) Batch fermentation characteristics under aerobic condition

Figure 5.1a shows the batch cultivation result of wild type *E. coli* under aerobic condition for the case of using a mixture of glucose and fructose as a carbon source, while Figure 5.1b shows the case of the wild type using a mixture of glucose and xylose as a carbon source. As can be seen from the figure, glucose was first consumed, while fructose or xylose was consumed after glucose was depleted. This is due to the catabolite repression caused by the low level of cAMP or cAMP-Crp when glucose was present. Figure 5.1c shows the aerobic batch cultivation result of Δ*cra* mutant for the case of using a mixture of glucose and fructose as a carbon

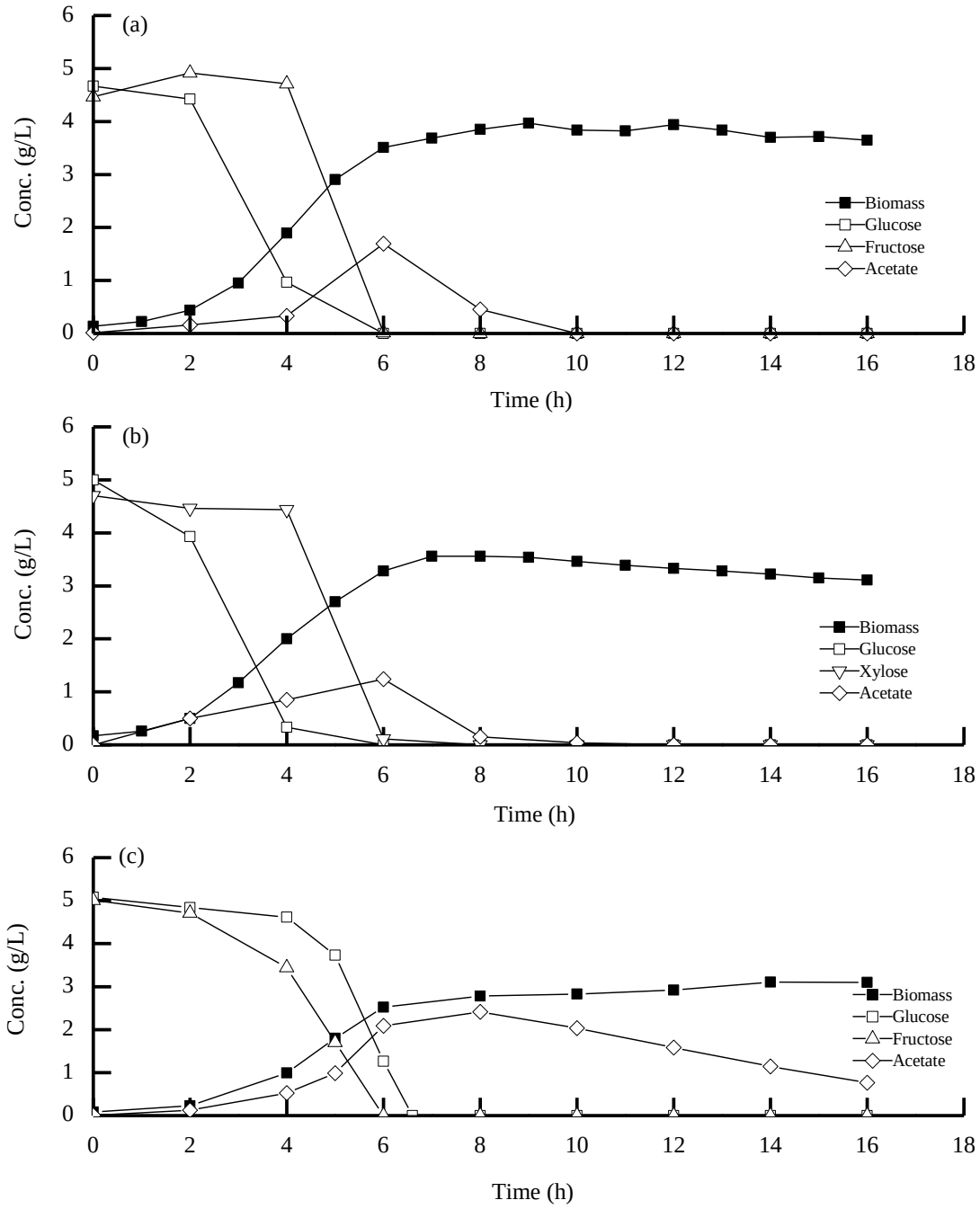

Figure 5.1 Batch aerobic cultivation result of (a) wild type using a mixture of glucose and fructose, (b) wild type using a mixture of glucose and xylose, and (c) Δ*cra* mutant using a mixture of glucose and fructose as a carbon source.

source, where it indicates an interesting phenomenon that both glucose and fructose were consumed simultaneously with fructose to be consumed a little faster as compared to glucose. However, acetate was more produced and less consumed after glucose was depleted in Δ*cra* mutant as compared to the wild type. This may be due to the repressions of *aceA* and *icdA* gene expressions caused by *cra* gene knockout, while *pfkA* and *pykF* gene expressions were activated by *cra* gene knockout (Sarkar and Shimizu 2008) (Appendix B).

Figure 5.2 shows the batch aerobic cultivation result of wild type (Fig. 5.2a), Δ*cra* mutant (Fig. 5.2b), crp^+ mutant (Fig. 5.2c), and Δ*pgi* mutant (Fig. 5.2d) for the case of using a mixture of glucose, fructose, and xylose as a carbon source. Figure 5.2a shows that fructose and xylose were both consumed after glucose was depleted due to catabolite repression in the wild type. Figure 5.2b shows that fructose and glucose were consumed simultaneously with fructose to be consumed faster than glucose, whereas xylose was consumed after glucose was depleted, where the latter phenomenon may be considered to be due to the catabolite repression by the lower level of cAMP-Crp in Δ*cra* mutant (Yao et al., 2013). It may be of practical interest to relax the catabolite repression by enhancing cAMP-Crp by crp^+ mutant. Figure 5.2c shows the similar phenomenon as observed for the case of the wild type (Fig. 5.2a). However, some differences were observed that the glucose consumption rate became a little lower, which may have caused less acetate production. Figure 5.2d shows the batch cultivation result in Δ*pgi* mutant, where all three carbon sources were consumed simultaneously, but the consumption rates were the lowest as compared to other strains.

(b) Batch fermentation characteristics under anaerobic condition

Figure 5.3 shows the batch anaerobic cultivation result of wild type (Fig. 5.3a), Δ*cra* mutant (Fig. 5.3b), crp^+ mutant (Fig. 5.3c), and Δ*pgi* mutant (Fig. 5.3d) for the case

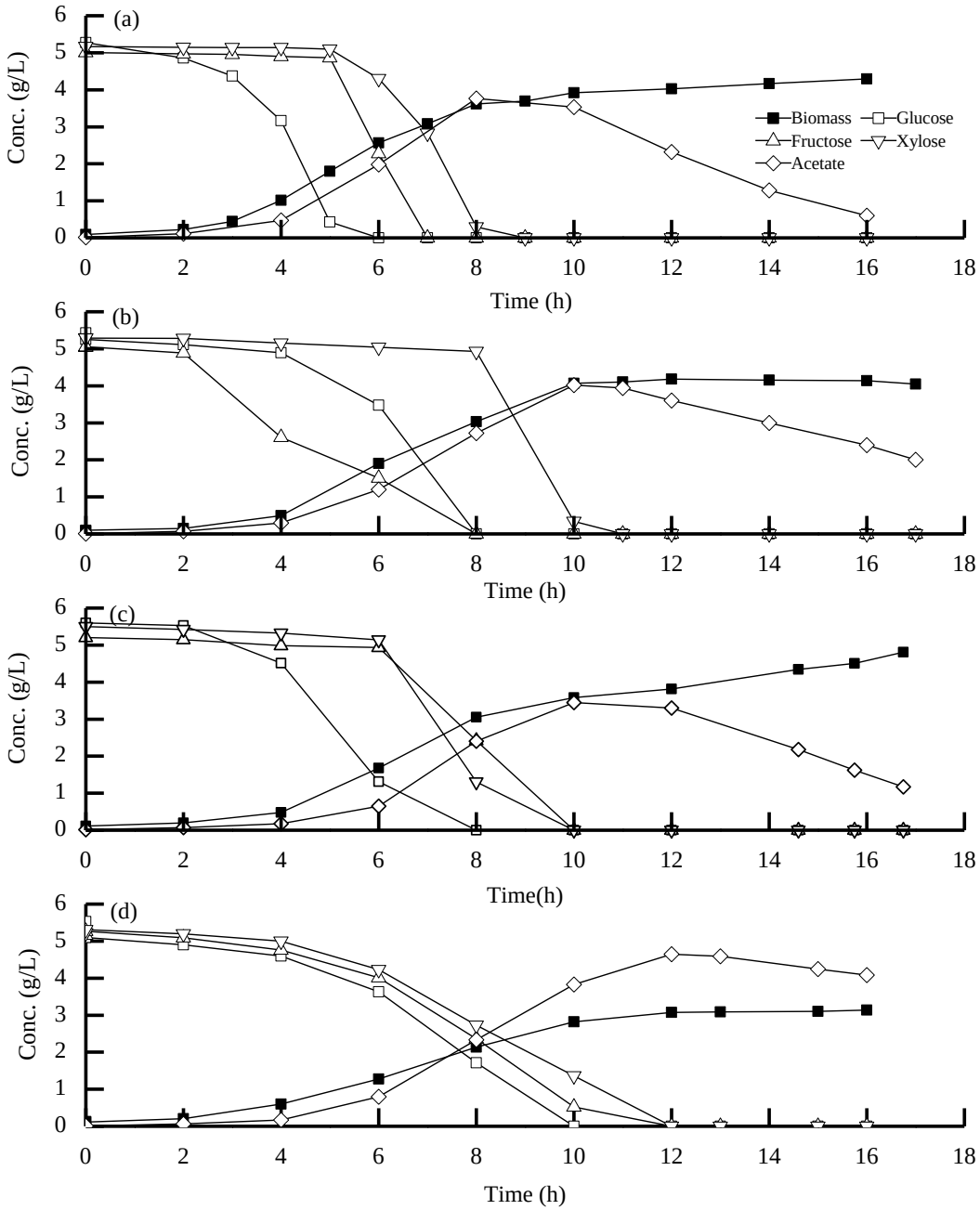

Figure 5.2 Batch aerobic cultivation result of (a) wild type, (b) Δ*cra* mutant, (c) *crp*$^{+}$ mutant, and (d) Δ*pgi* mutant using a mixture of glucose, fructose, and xylose as a carbon source.

of using a mixture of glucose, fructose, and xylose. Fig. 5.3a shows that after glucose was depleted, fructose and xylose were consumed, and that xylose was little consumed. The fermentation products were formed in the order of formate, acetate, ethanol, as well as a little lactate, where the biomass formation was mainly made during the period when glucose and fructose were used as carbon sources. In the case of Δ*cra* mutant as shown in Fig. 5.3b, fructose and glucose were consumed simultaneously where fructose was consumed faster as compared to glucose, and little xylose was consumed. The metabolite formation patterns were nearly the same as the case of wild type (Fig. 5.3a). In the case of crp^+ mutant, the glucose consumption rate became lower as compared to wild type (Fig. 5.3a) as shown in Fig. 5.3c. Notable thing is that xylose and fructose were consumed together after glucose was depleted. In addition, lactate was more produced, while other metabolites were produced in the similar pattern as observed for wild type and Δ*cra* mutant strains. In the case of Δ*pgi* mutant (Fig. 5.3d), three carbon sources were consumed together, but the consumption rates were lower as compared to the case of other strains, where the metabolite formation patterns were more or less similar to the case of other strains. In order to understand why xylose was little consumed in the wild type strain and Δ*cra* mutant, the extracellular xylitol concentration was also measured. The small windows in Fig. 5.3 depict the time courses of extracellular xylitol concentration. Little xylitol was produced in crp^+ and Δ*pgi* mutants, while some amount of xylitol was produced in the wild type and Δ*cra* mutant.

Noting that the overproduction of acetate for *cra* gene knockout is due to downregulations of *icdA* and *aceA*, thus, *pflA* gene knockout was considered to overcome acetate accumulation. The previous studies have shown that Δ*pflA* and Δ*pflB* mutants can produce higher amount of lactate from glucose (Zhu and Shimizu, 2004; Zhu and Shimizu, 2005). The genes *pflA* and *pflB* encods pyruvate formate lyase, which is used for assimilating PYR to formic acid and acetyl coenzyme A (AcCoA). The Δ*pflA* and Δ*pflB* mutants may be considered to be free from higher acetate production inherent to Δ*cra* mutant, since AcCoA production may be

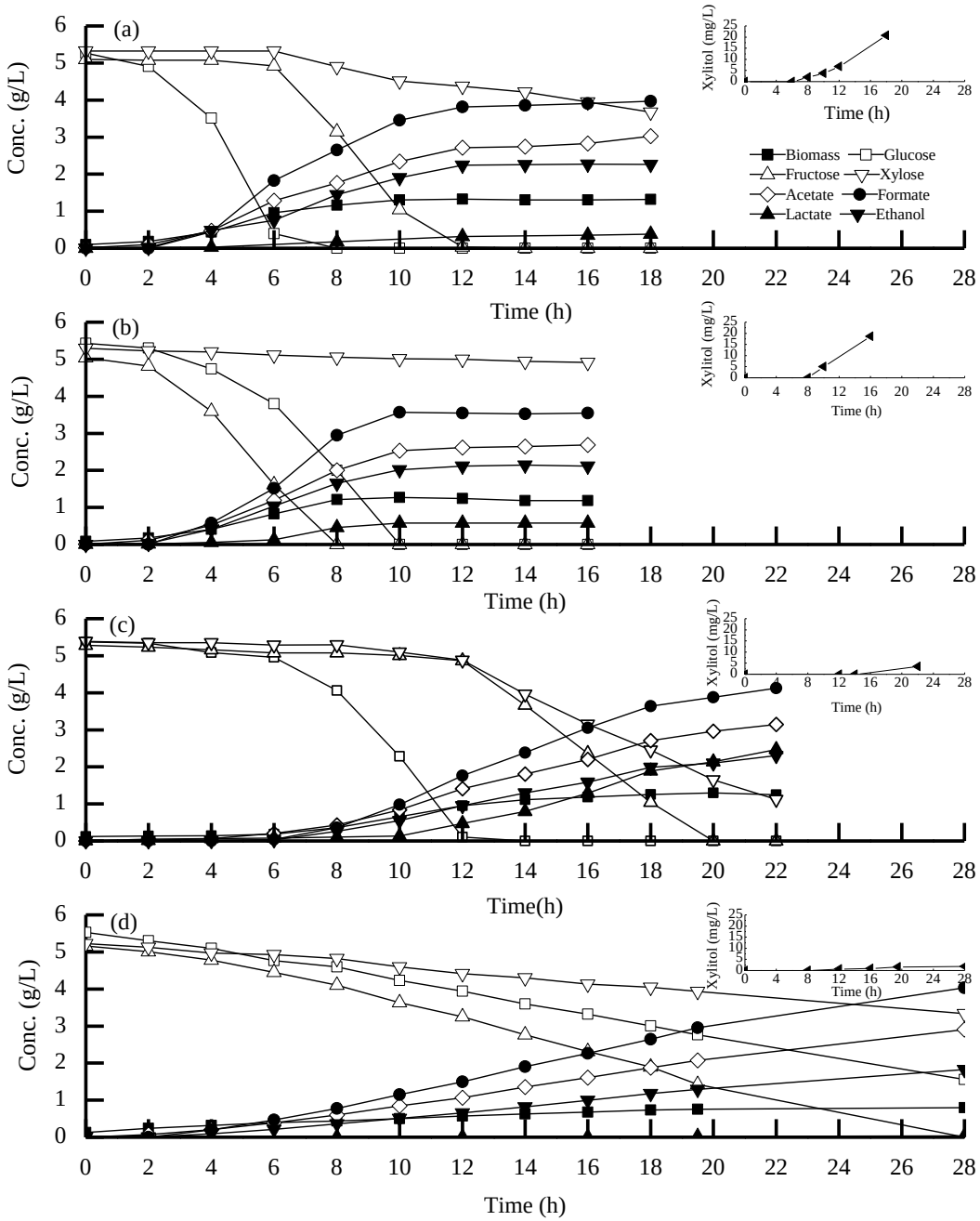

Figure 5.3 Batch anaerobic cultivation result of (a) wild type, (b) Δ*cra* mutant, (c) *crp*$^{+}$ mutant, and (d) Δ*pgi* mutant using a mixture of glucose, fructose, and xylose as a carbon source.

significantly lower for these mutants. Fig. 5.4a shows the batch anaerobic cultivation result of Δ*cra.pflA* mutant for the case of using a mixture of glucose and fructose. Both glucose and fructose were consumed simultaneously with fructose to be consumed a little faster as compared to glucose, and higher amount of lactate was produced. Note that the drawback of overproduction of acetate in Δ*cra* mutant was overcome in Δ*cra.plfA* mutant since *pflA* knockout eliminated AcCoA production. Fig. 5.4b shows the anaerobic batch cultivation result of Δ*cra.plfA* mutant for the case of using a mixture of glucose, fructose and xylose. The result indicates the similar phenomenon as observed in Fig. 5.3b, where xylose was consumed little and some amount of xylitol was produced.

(c) Continuous fermentation characteristics under anaerobic condition

In order to investigate these phenomena in particular under anaerobic condition in more detail, the anaerobic continuous cultures of wild type, Δ*cra* mutant, crp^+ mutant, and Δ*pgi* mutant were performed at the dilution rate of 0.1 h^{-1} using a mixture of glucose, fructose, and xylose as a carbon source (Table 5.1). Glucose concentration was below detectable level, and the fructose concentration was less than xylose concentration for the wild type, consistent with the batch cultivation result (Fig. 5.3a). Fructose concentration was below detectable level, while glucose concentration was lower as compared to xylose concentration for Δ*cra* mutant, consistent with the batch cultivation result (Fig. 5.3b). In the case of crp^+ mutant, glucose concentration was below detectable level, and xylose concentration was similar to fructose concentration. In the case of Δ*pgi* mutant, carbon sources were consumed in the order of fructose, glucose, and xylose, consistent with the batch culture, but the consumption rates were all relatively low, as observed in the batch cultivation (Fig. 5.3d).

5.2.2 Gene expression analysis

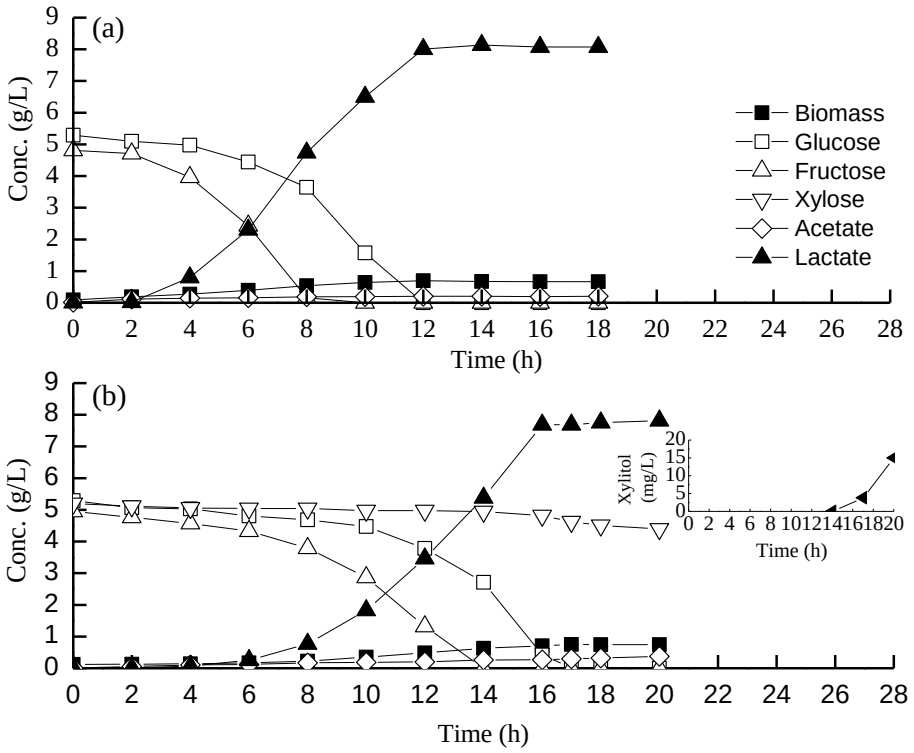

Figure 5.4 Batch anaerobic cultivation result of Δ*cra.pflA* mutant using (a) a mixture of glucose and fructose, and (b) a mixture of glucose, fructose, and xylose as a carbon source.

Table 5.1 Anaerobic continuous fermentation characteristics of *E. coli* and its Δ*cra*, *crp*$^+$ and Δ*pgi* mutant for the case of using a mixture of glucose, fructose, and xylose as a carbon source at the dilution rate of 0.1 h^{-1}.

(a) Concentrations

Strain	Biomass (g/l)	Glucose (g/l)	Fructose (g/l)	Xylose (g/l)	Acetate (g/l)	Lactate (g/l)	Formate (g/l)	Ethanol (g/l)	Xylitol (g/l)	Carbon Recovery
wild	0.58±0.02	ND[a]	3.70±0.18	4.94±0.15	1.75±0.08	0.45±0.02	2.39±0.09	1.22±0.05	ND[d]	96%
Δ*cra*	0.64±0.03	1.23±0.06	ND[b]	4.98±0.17	2.12±0.09	0.94±0.04	3.26±0.16	1.60±0.07	ND[d]	92%
crp$^+$	0.58±0.02	ND[a]	4.48±0.21	4.31±0.20	1.51±0.02	1.10±0.05	2.07±0.03	0.96±0.03	ND[d]	95%
Δ*pgi*	0.36±0.01	4.19±0.08	3.35±0.10	4.66±0.07	0.84±0.01	ND[c]	1.27±0.06	0.54±0.01	ND[d]	99%

(b) The specific rates

Strain	Glucose uptake rate (mmol/g/h)	Fructose uptake rate (mmol/g/h)	Xylose uptake rate (mmol/g/h)	Acetate production rate (mmol/g/h)	Lactate production rate (mmol/g/h)	Formate production rate (mmol/g/h)	Ethanol production rate (mmol/g/h)
wild	4.79±0.19	1.24±0.06	0	5.02±0.23	0.86±0.04	8.96±0.36	4.58±0.18
Δ*cra*	3.28±0.15	4.34±0.18	0	5.53±0.24	1.63±0.08	11.06±0.54	5.44±0.23
crp$^+$	4.79±0.19	0.50±0.02	0.79±0.03	4.34±0.17	2.11±0.10	7.76±0.36	3.60±0.14
Δ*pgi*	1.25±0.06	2.55±0.10	0.63±0.03	3.89±0.18	0	7.67±0.30	3.26±0.16

ND[a]: not detectable, where glucose detectable limit was 0.038 g/l; ND[b]: not detectable, where fructose detectable limit was 0.004 g/l.

ND[c]: not detectable, where lactate detectable limit was 0.003 g/l; ND[d]: not detectable, where xylitol detectable limit was 0.1 mg/l.

(a) Δ*cra* mutant for multiple carbon sources

Figure 5.5 compares of gene transcript levels for the case of continuous culture between wild type and Δ*cra* mutant. Global regulators *crp* and *mlc* were downregulated (P<0.01 for both). In accordance with the global regulator-metabolic pathway genes relationship (Appendix B), the transcript levels of glycolytic genes such as *pfkA*, *pykF*, PP pathway gene such as *zwf*, ED pathway genes such as *edd* and *eda* were all upregulated (P<0.01, P<0.05, P<0.01, P<0.01, and P<0.01, respectively), while gluconeogenic genes such as *pckA*, *ppsA*, *fbp*, and glyoxylate pathway gene *aceA*, as well as the TCA cycle gene *icdA* were all downregulated (P<0.01 for all genes) for the Δ*cra* mutant as compared to the wild type. The downregulation of *ptsG* transcript level (P<0.01) may be due to downregulation of *crp* (P<0.01). The fructose transport genes *fruBKA* as well as *manX* and *mtlA* genes were upreuglated in Δ*cra* mutant as compared to the wild type (P<0.01 for all genes). Due to the decreased transcript level in *crp* (P<0.01), TCA cycle genes *gltA*, *acnA*, *sdhC*, *fumA* and *mdh* were downregulated (P<0.01 for all genes). The downregulation of *aceA* transcript level (P<0.01) is also consistent with upregulation of *iclR* (P<0.01). For fermentation pathway genes, in accordance with higher production rate of acetate (Table 5.1), *pta* and *ackA* genes were upregulated (P<0.01 for both genes), and in accordance with higher ethanol production rate, *adhE* gene transcript level was upregulated (P<0.01) for Δ*cra* mutant as compared to the wild type. The *pflA* gene transcript level was increased (P<0.01), which corresponds to the higher production rate of formate (Table 5.1). For xylose assimilating pathway genes, *xylR*, *xylFGH*, *xylAB*, and *xylE* were all downregulated (P<0.01 for all genes). Note that *rpoS* transcript level was decreased (P<0.01) for Δ*cra* mutant as compared to the wild type, which might be due to higher glucose concentration, and this also corresponds to the downregulations of *acnA* and *fumC*.

(b) *crp*$^{+}$ mutant for multiple carbon sources

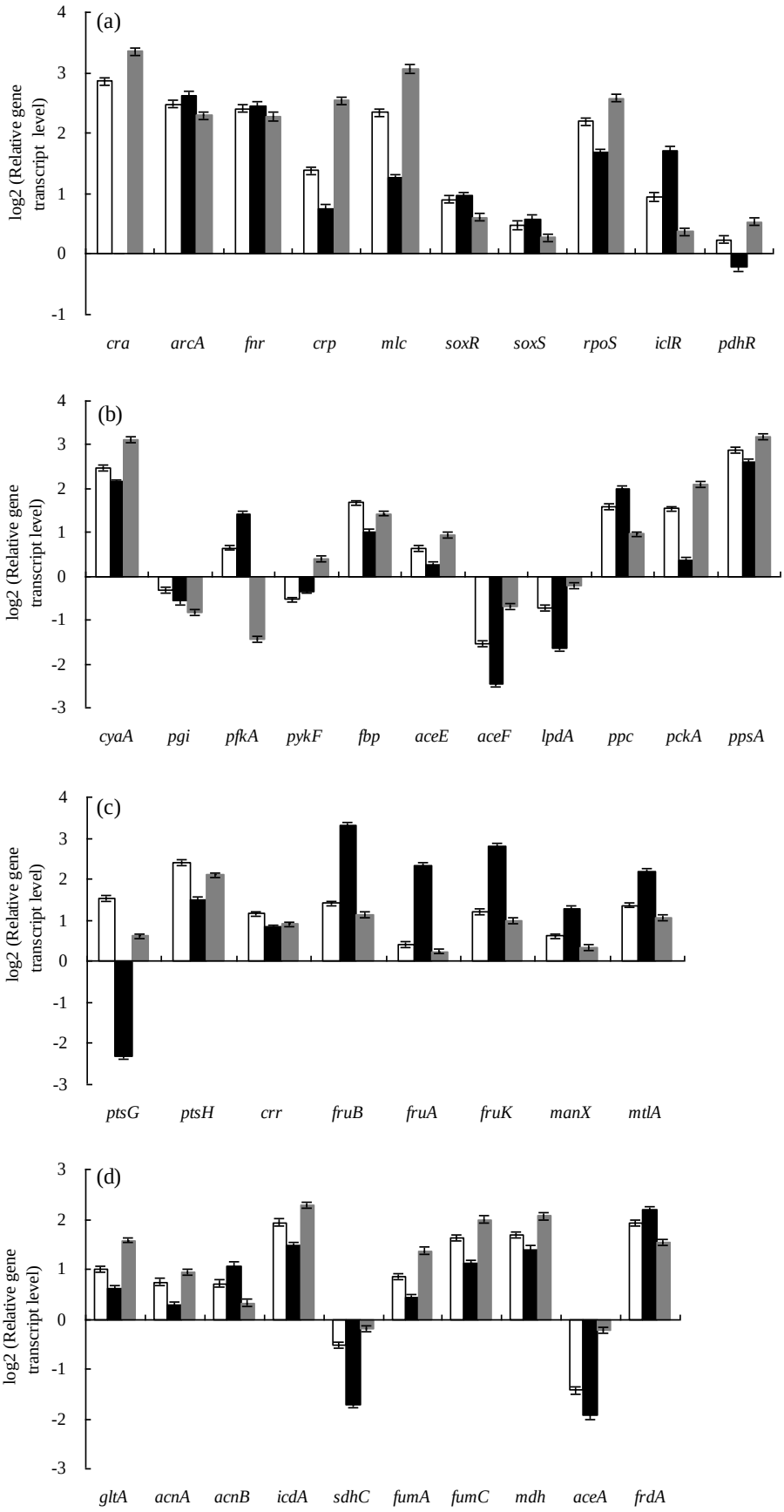
(a)
log2 (Relative gene transcript level)
4
3
2
1
0
-1
cra
arcA
fnr
crp
mlc
soxR
soxS
rpoS
iclR
pdhR
(b)
log2 (Relative gene transcript level)
4
3
2
1
0
-1
-2
-3
cyaA
pgi
pfkA
pykF
fbp
aceE
aceF
lpdA
ppc
pckA
ppsA
(c)
log2 (Relative gene transcript level)
4
3
2
1
0
-1
-2
-3
ptsG
ptsH
crr
fruB
fruA
fruK
manX
mtlA
(d)
log2 (Relative gene transcript level)
3
2
1
0
-1
-2
-3
gltA
acnA
acnB
icdA
sdhC
fumA
fumC
mdh
aceA
frdA

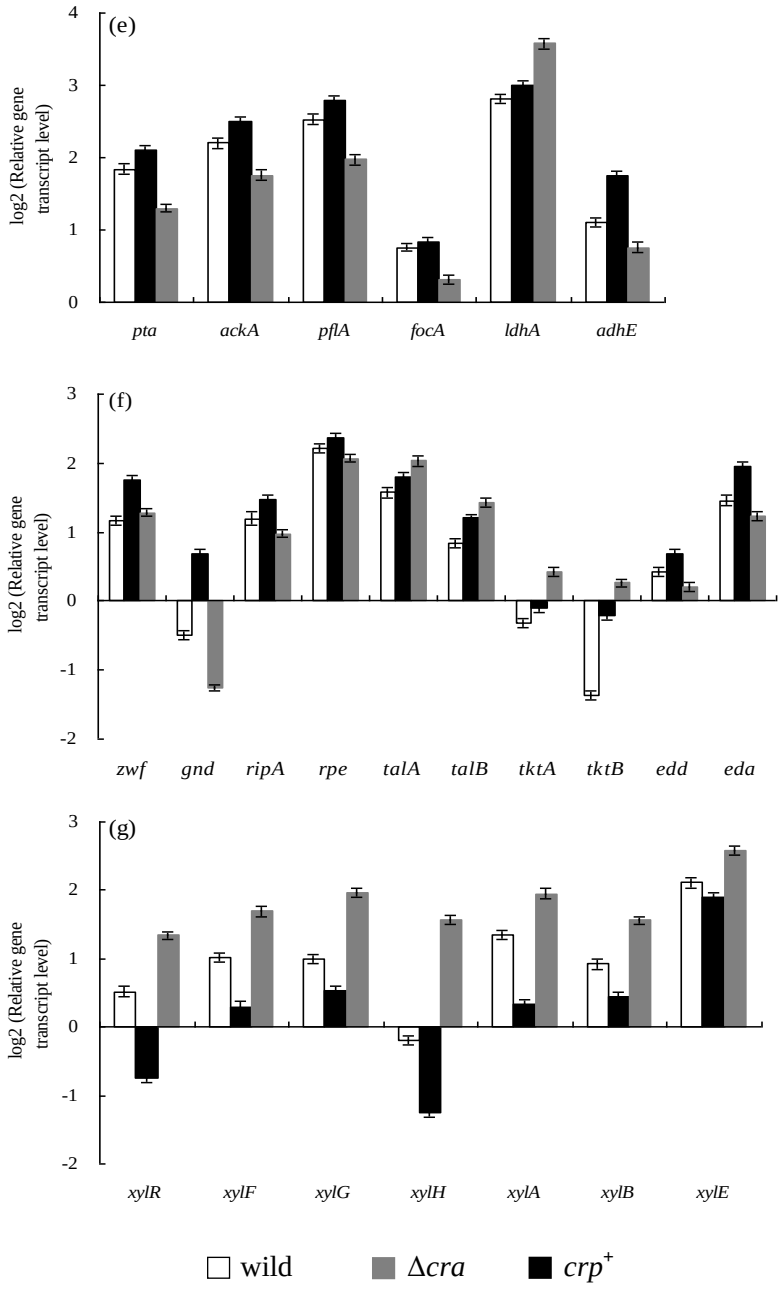

Fig. 5.5 Comparison of gene transcript levels among wild type, Δ*cra* mutant, and *crp*$^+$ mutant for the continuous cultures at the dilution rate of 0.1 h^{-1} for the case of using a mixture of glucose, fructose, and xylose as a carbon source. (a) Global regulator genes; (b) *cyaA*, glycolysis, glucoenogenesis, and anaplerotic pathway genes; (c) PTS genes; (d) TCA cycle and glyoxylate pathway genes; (e) Fermentation pathway genes; (f) PP pathway genes; (g) Xylose assimilating pathway genes.

Figure 5.5 also compares of gene transcript levels for the case of continuous culture between wild type and Δ*cra* mutant. for crp^+ mutant. The *crp* enhancement (crp^+) caused *mlc* to be increased (P<0.01). In addition, *cra* gene transcript level was also increased (P<0.01). Thus the glycolytic genes such as *pfkA*, *edd*, *eda* genes were downregulated (P<0.01, P<0.05, and P<0.05, respectively), while gluconeogenic genes such as *pckA*, *ppsA*, TCA cycle gene *icdA*, and the glyoxylate pathway gene *aceA* were upregulated (P<0.01 for all genes) for crp^+ mutant as compared to the wild type (and Δ*cra* mutant). Glucose *pts* genes *ptsG*, *ptsH* and *crr* were downregulated (P<0.01 for all genes). In addition, fructose *pts* genes *fruBKA* were also downregualted (P<0.01 for all genes), however, their changing folds were not big. The enhancement of *crp* activated TCA cycle genes *gltA*, *acnA*, *sdhC*, *fumA* and *mdh* (P<0.01 for all genes). For fermentation pathway genes, *ldhA* gene transcript level was higher (P<0.01) in accordance with higher lactate production rate, and *adhE* gene transcript level was lower for crp^+ mutant (P<0.01) in accordance with lower ethanol production rate as compared to the wild type (and Δ*cra* mutant). Xylose assimilating pathway genes *xylR*, *xylFGH*, *xylAB* and *xylE* were all significantly upregulated (P<0.01 for all genes). Note that *rpoS* transcript level was increased (P<0.01) in crp^+ mutant, and this contributes to the stress resistance.

(c) Δ*pgi* mutant for multiple carbon sources

In the case of Δ*pgi* mutant, *ptsG* gene transcript level was significantly decreased (P<0.01), while *zwf* gene transcript level significantly increased (P<0.01) as compared to the wild type (Fig. 5.6). Moreover, *cyaA* and *crp* transcript levels were increased (P<0.01 for both) for Δ*pgi* mutant as compared to the wild type (Fig. 5.6), indicating the increase of cAMP-Crp. This may have caused *xylR* transcript level to be increased for Δ*pgi* mutant (P<0.01). Furthermore, *pflA* and *ldhA* gene transcript levels were lower for Δ*pgi* mutant as compared to the wild type (P<0.01 for both) (Fig. 5.6), which corresponds to lower production of formate and lactate in Δ*pgi* mutant as compared to the wild type as shown in Table 5.1. Note that *rpoS* transcript

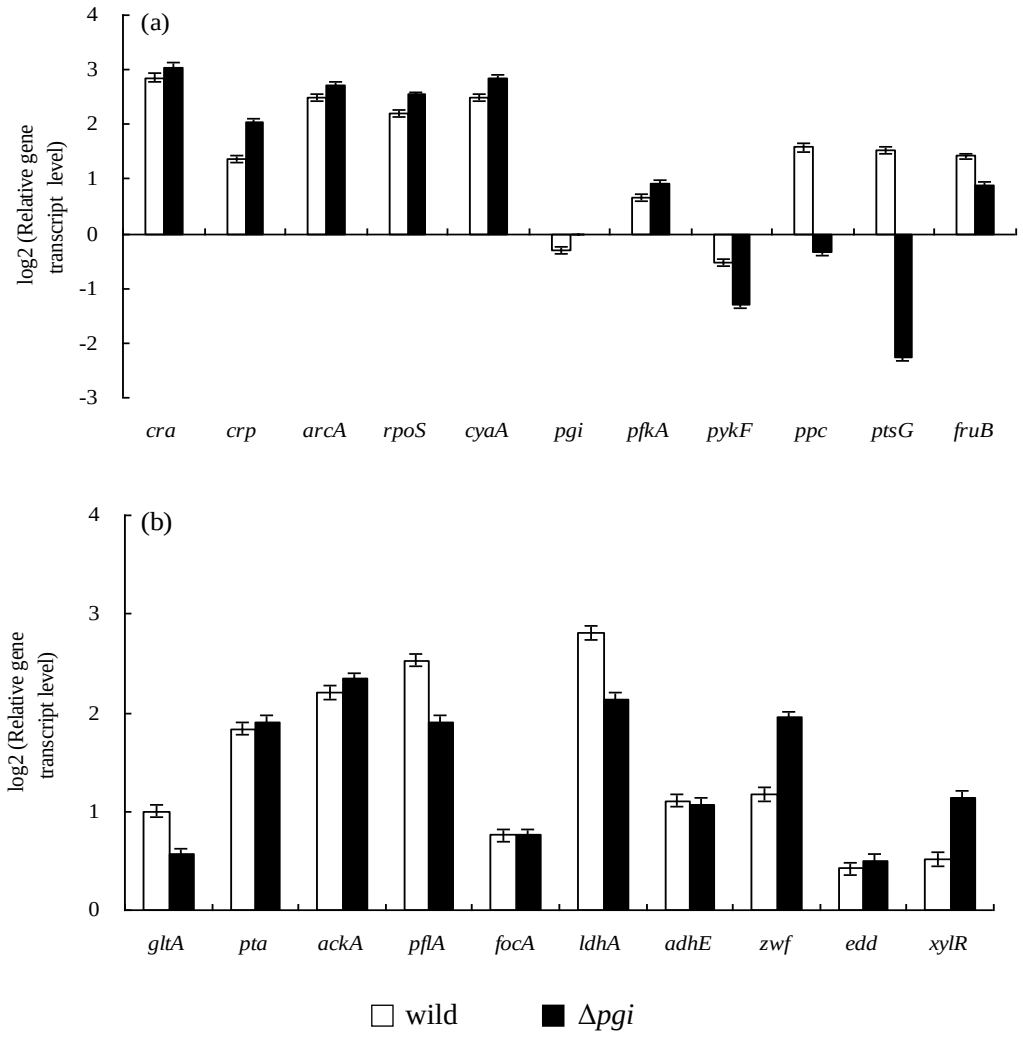

Fig. 5.6 Comparison of gene transcript levels between wild type and Δ*pgi* mutant for the continuous culture at the dilution rate of 0.1 h^{-1} for the case of using a mixture of glucose, fructose, and xylose. (a) Global regulator genes, glycolysis, anaplerotic pathway and *pts* genes; (b) TCA cycle, fermentation pathway genes and xylose transcription factor.

level was decreased ($P<0.01$) in Δ*pgi* mutant.

5.2.3 Metabolic flux analysis under anaerobic cultivation

Figure 5.7 compares the metabolic flux distribution among wild type, Δ*cra* mutant, crp^+ mutant and Δ*pgi* mutant for the continuous cultures at the dilution rate of 0.1 h^{-1} for the case of using a mixture of glucose, fructose, and xylose as a carbon source. It shows that the glycolytic flux was the highest in Δ*cra* mutant, which implies the highest substrate level phosphorylation.

Based on the flux result, the specific total carbon source consumption rate together with specific metabolites production rate can be obtained (Fig. 5.8a). It may be of practical interest that total carbon source consumption rate was the highest for Δ*cra* mutant as compared to the wild type as well as other strains. This contributes to the increase in the total metabolites production rate (Fig. 5.8a), which is attractive from the efficient metabolites production point of view. Figure 5.8b shows NADH balance based on the metabolic fluxes. Note that the NADH generation is mainly at glyceraldehyde-3-phosphate dehydrogenase (GAPDH), while the reoxidation of NADH to NAD^+ occurs mainly at lactate dehydrogenase (LDH) and alcohol dehydrogenase (ADH). Figure 5.8c compares the specific ATP production rate based on the metabolic fluxes, where this may be related to the growth rate in the batch culture or cell concentration for the continuous culture. The ATP generation by substrate level phosphorylation dominates the cell growth. As implied by Table 5.1, the cell concentration was the highest in Δ*cra* mutant, which may be implied by the highest specific ATP production rate (Fig. 5.8c).

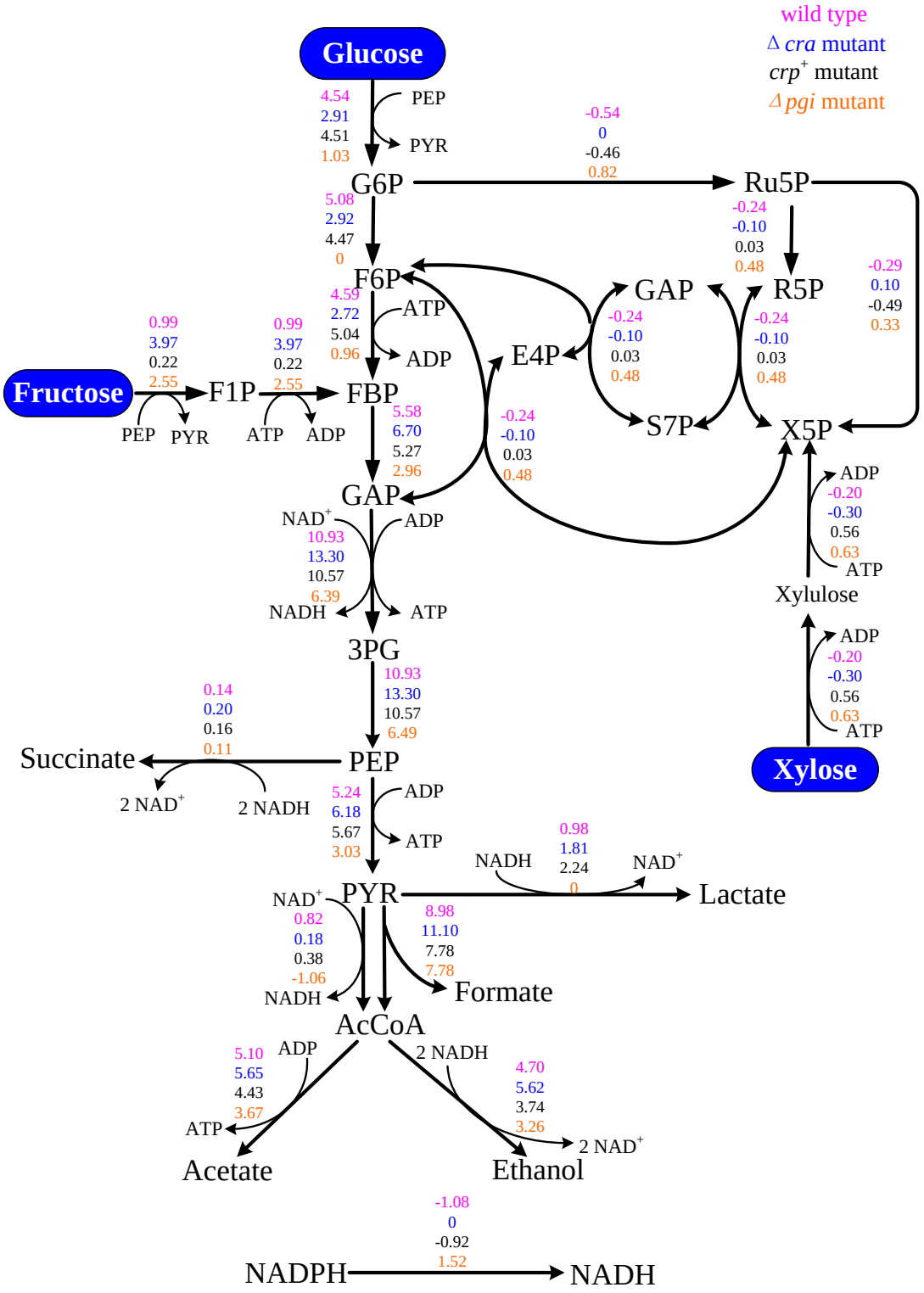

Fig. 5.7 The metabolic flux distributions of wild type, Δ*cra* mutant, *crp*$^+$ mutant and Δ*pgi* mutant for the continuous cultures at the dilution rate of 0.1 h^{-1} for the case of using a mixture of glucose, fructose, and xylose as a carbon source.

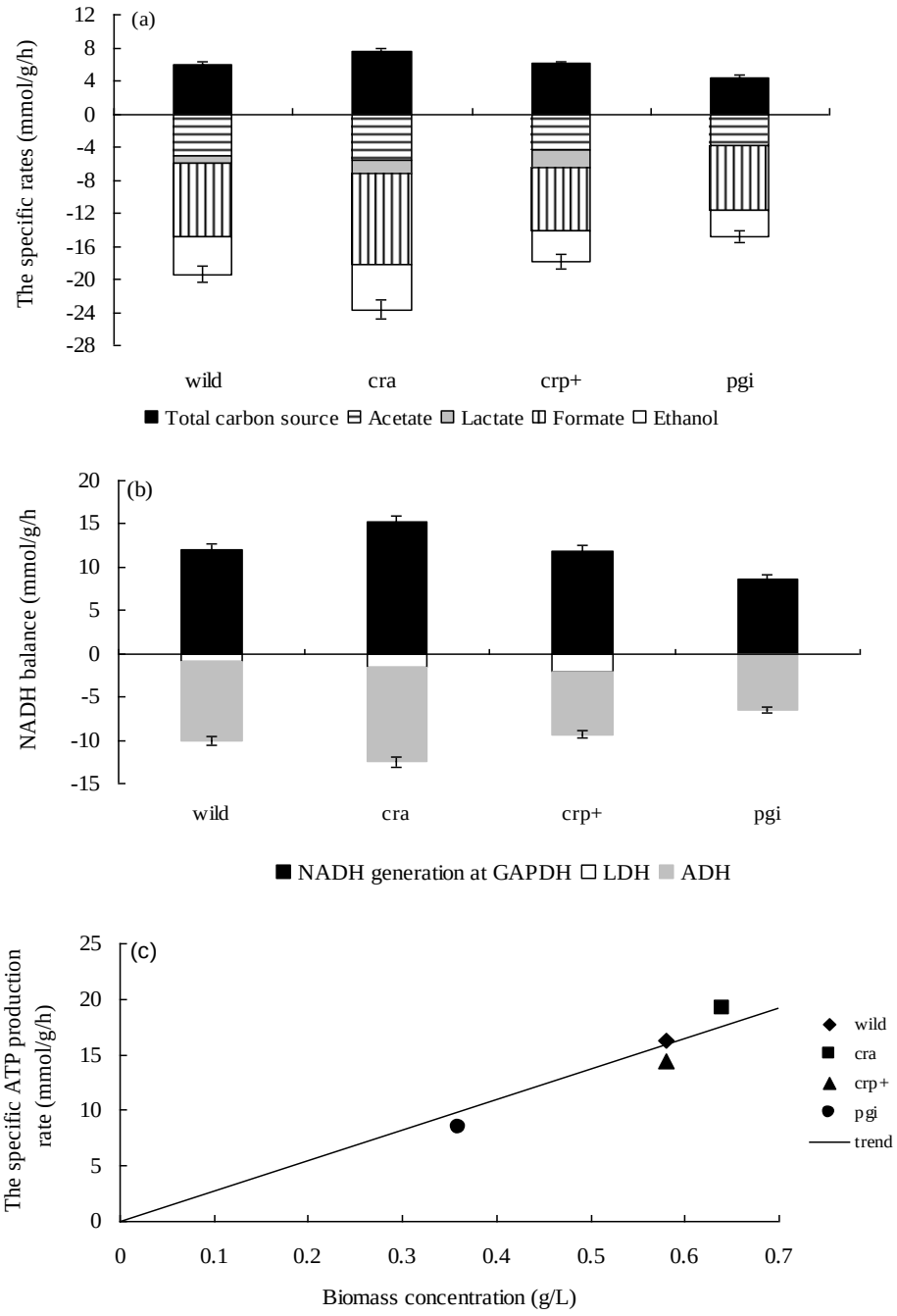

Fig. 5.8 (a) The specific total carbon source consumption rate (positive value) and specific metabolites production rate (negative value) of wild type, Δ*cra* mutant, *crp*$^{+}$ mutant and Δ*pgi* mutant for the continuous cultures at the dilution rate of 0.1 h^{-1} for the case of using a mixture of glucose, fructose, and xylose as a carbon source. (b) NADH balance. The specific NADH production rate is expressed as positive value, while the specific NADH consumption rate is shown as negative values. **(c) The specific ATP production rate vs. biomass concentration.** All the data are given on the mmol basis. ADH: Alcohol dehydrogenase; GAPDH: Glyceraldehyde-3-phosphate dehydrogenase; LDH: Lactate dehydrogenase.

5.3 Discussion

5.3.1 Overall regulation mechanism of Δ*cra* mutant for multiple carbon sources

Figure 5.9 shows the interactions between glucose PTS and fructose PTS for the phosphate transfer, and the interrelationship between fructose PTS and xylose metabolism. Figure 5.10 shows the overall regulation mechanism of Δ*cra* mutant for multiple carbon sources, where it shows how *cra* gene knockout affected the global regulatory genes and metabolic pathway genes, and in turn fermentation characteristics under anaerobic condition based on the result of Table 5.1, Fig. 5.5, as well as the global regulator-metabolic pathway gene relationship as given in Appendix B.

As stated above, fructose is transported by a fructose-specific PTS (*fruBKA*). Due to *cra* knockout, the negative control on *fruBKA* mediated by Cra was relaxed. Therefore, fructose uptake was improved. In addition, FruB was activated. FPr encoded by *fruB* and HPr encoded by *ptsH* competed for the phosphate of the phosphorylated EI, where FruB prevented $EIIA^{Glc}$ to be phosphorylated, while $EIIA^{Fru}$ was more phosphorylated in Δ*cra* mutant. As implied by the transcript levels of *cyaA* and *crp* in Fig. 5.5, Cya activity was also lower, and this caused cAMP level to be low. This suggests that $EIIA^{Fru}$ may not substitute for $EIIA^{Glc}$ as an activator of Cya. Thus, Cra mediated Cya activity indirectly by controlling the expression of fructose operon in cells growing with fructose (Crasnier-Mednansky et al., 1997). Since Δ*cra* mutant less phosphorylated $EIIA^{Glc}$ than wild type, inducer exclusion occurred in Δ*cra* mutant and prevented xylose entry by decreased cAMP-Crp, which inactivates xylose operon (Fig. 5.2b, Fig 5.5).

In addition to the own PTS of fructose, another two PTSs with primary specificity for mannose (*manXYZ)* and mannitol (*mtlA)* can also transport fructose, which are

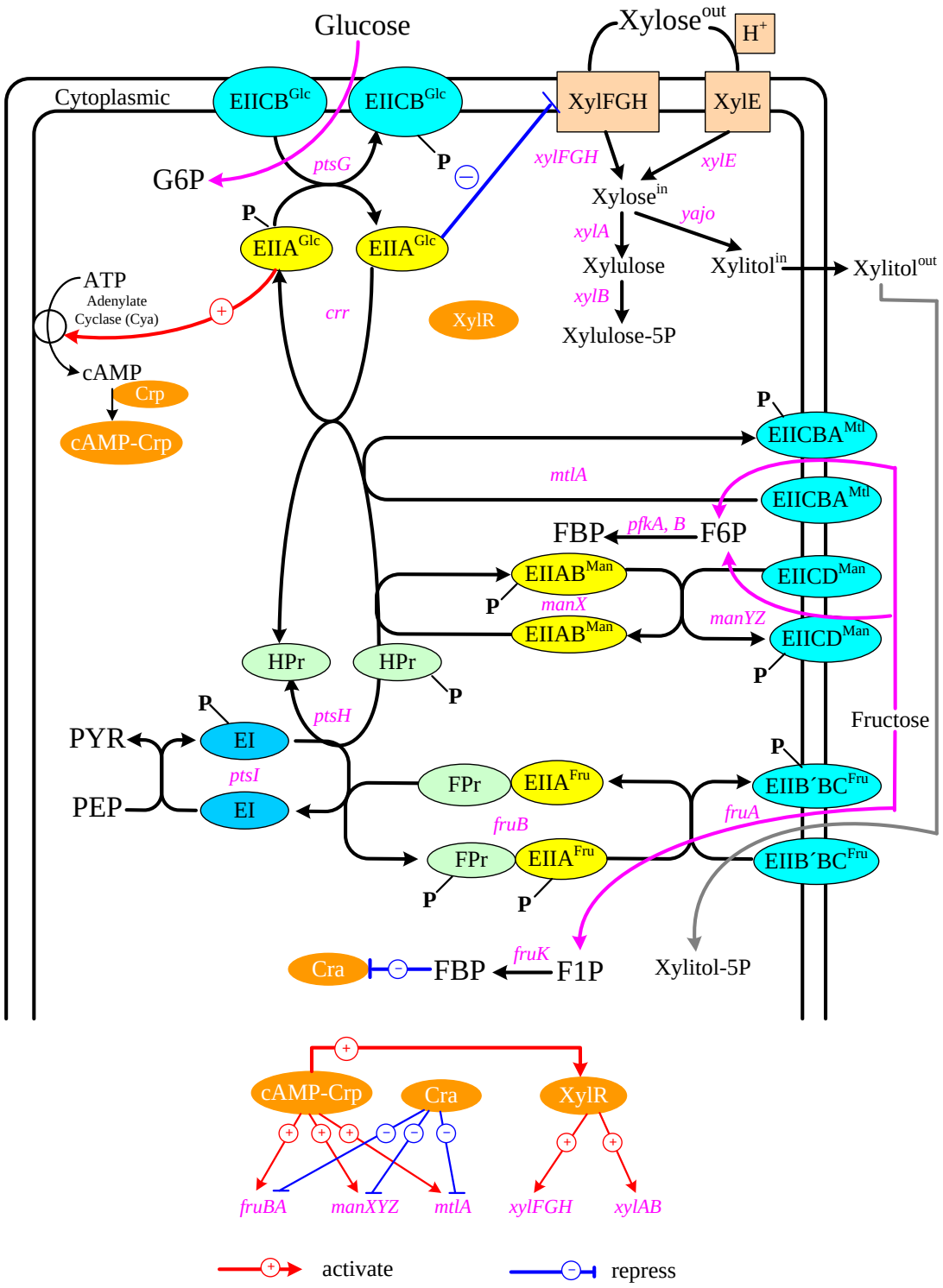

Fig. 5.9 The interactions among glucose PTS, fructose PTS and xylose metabolism.

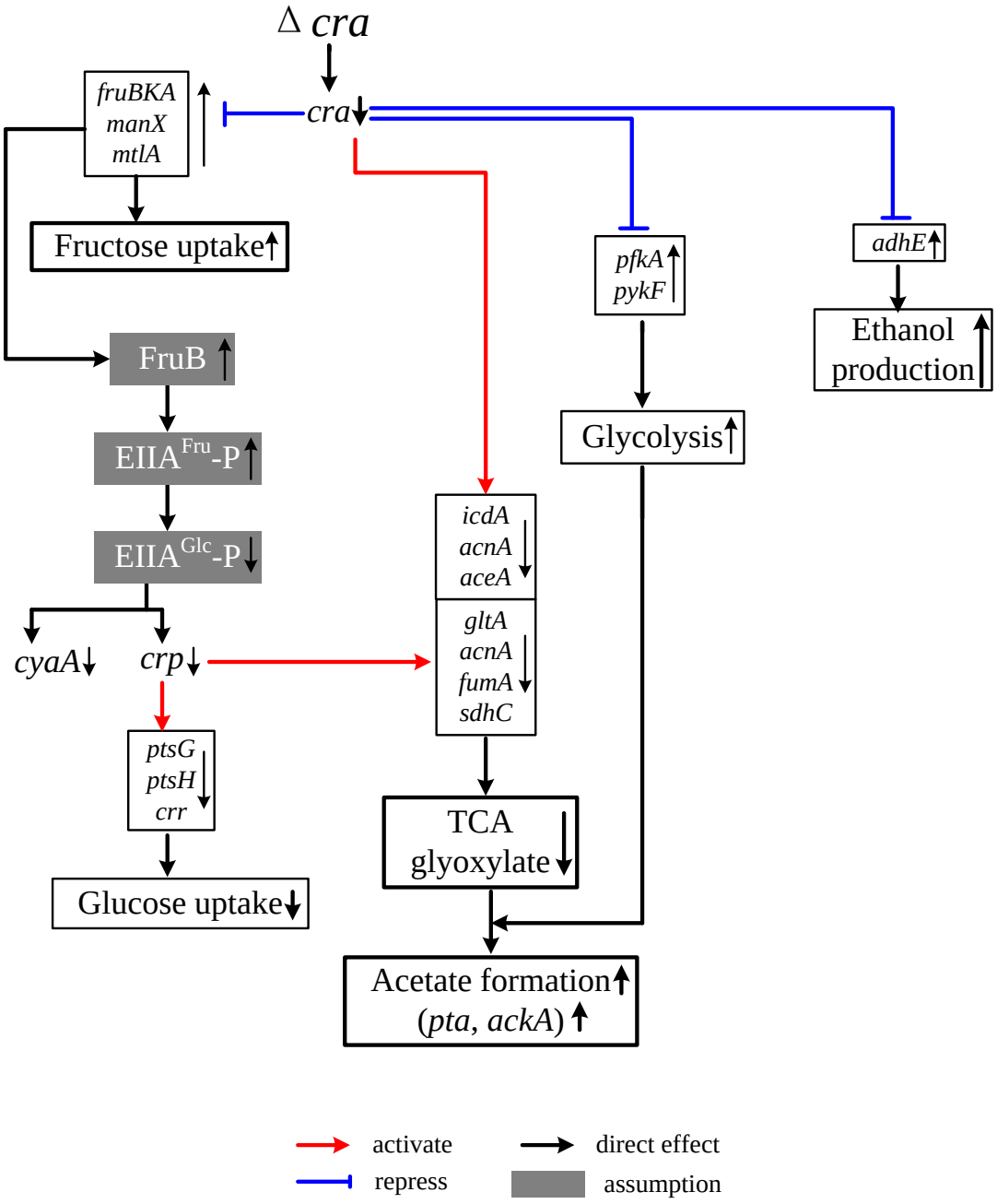

Fig. 5.10 The overall regulation of Δ*cra* mutant for multiple carbon sources.

also negatively controlled by Cra (Saier and Ramseier, 1996; Feldheim et al.,1990; Chin et al., 1989). Due to *cra* knockout, *manX* and *mtlA* gene transcript levels were higher in Δ*cra* mutant as compared to wild type and *crp*$^+$ mutant. As stated before, FPr competes with HPr for the phosphate of the phosphorylated EI, where the phosphorylated HPr not only transfers phosphoryl moiety to EIIA^{Glc} but also EIIA^{Man} and EIIA^{Mtl}, where the latter contributes to improving the fructose transport through mannose and mannitol PTSs (Kornberg, 2001).

Moreover, due to predominantly dephosphorylated EIIA^{Glc} and cAMP-Crp, glucose PTS genes such as *ptsG*, *ptsH* and *crr* were repressed (P<0.01 for all genes). In summary, the upregulation of fructose transport genes and downregulation of glucose transport genes can explain the reason why fructose consumption was faster as compared to glucose in Δ*cra* mutant as compared to wild type (Fig 5.2, Fig. 5.3, Table 5.1). In addition to mediating Cya, Cra also regulates glycolytic genes and TCA cycle genes. Under the co-regulation of Cra and Crp, TCA cycle and glyoylate pathway were repressed, and glycolysis was activated. This caused acetate overflow.

5.3.2 Overall regulation mechanism of *crp*$^+$ mutant for multiple carbon sources

The overall regulation mechanism of *crp*$^+$ mutant for multiple carbon sources is illustrated in Figure 5.11. Although it was found that CCR can be relaxed by *crp*$^+$ as shown in Chapter 4, glucose effects cannot be completely eliminated for multiple carbon sources. Nevertheless, it was shown that *crp*$^+$ mutant can achieve the simultaneous consumption of xylose and fructose. It has been reported that fructose transporter genes *fruBKA* and xylose transporter genes *xylFGH* are under positive control of cAMP-Crp (Saier and Ramseier et al., 1996; Feldheim et al., 1990; Song and Park, 1997) (Fig. 5.9). As a result, xylose uptake rate was the highest for *crp*$^+$ mutant under anaerobic cultivation (Fig. 5.3c, Table 5.1), which was reflected by the upregulation of xylose assimilating pathway genes, *xylFGH*/*xylAB* (P<0.01 for all genes). In contrast to xylose transport genes, fructose transport genes did not show a

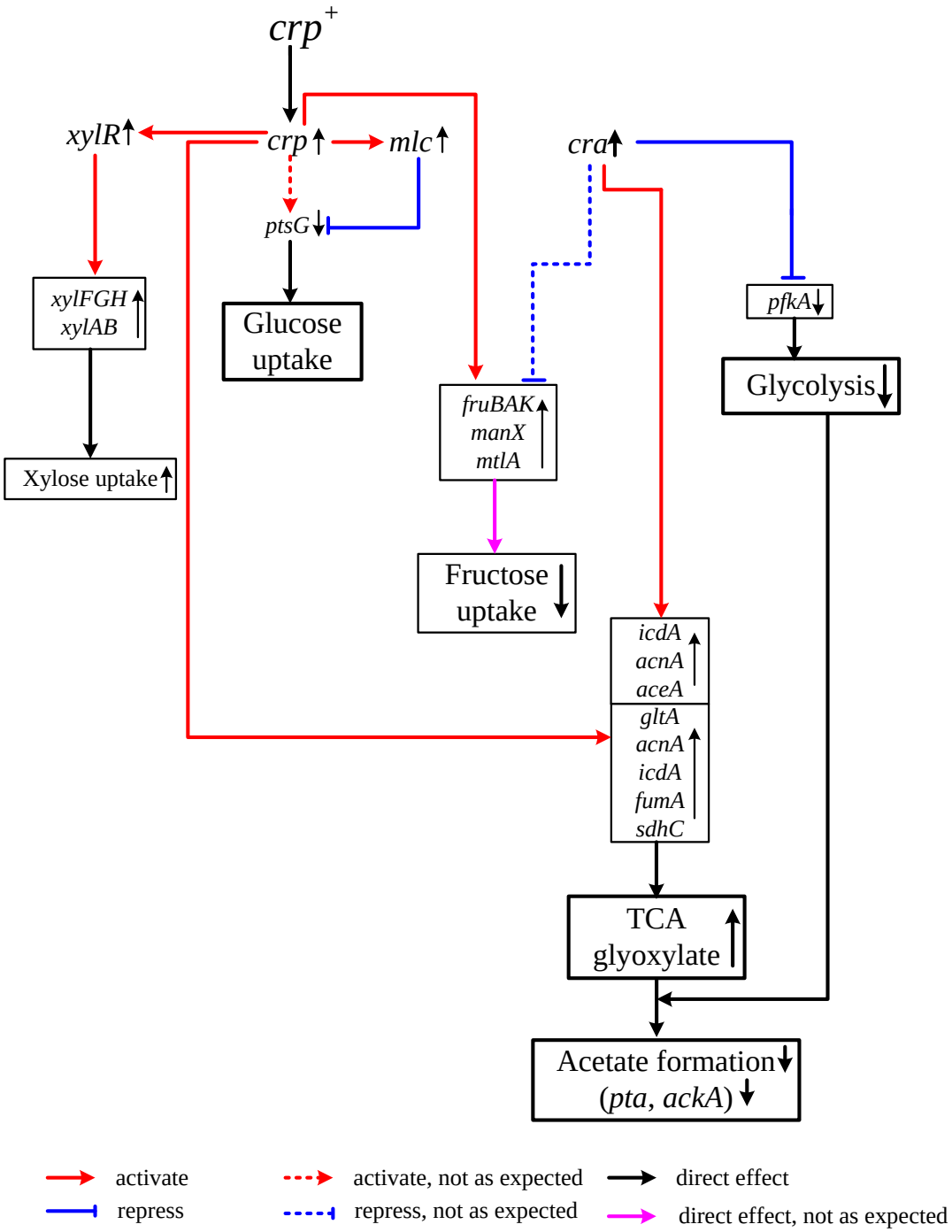

Fig. 5.11 The overall regulation of *crp*$^+$ mutant for multiple carbon sources.

drastic increase. This phenomenon indicates that *fru* operon is regulated primarily by Cra, and the cAMP-CRP complex plays a secondary role (Feldheim et al., 1990). In addition, Crp and Cra co-regulated TCA cycle, glyoxylate pathway and glycolysis. Unlike Δ*cra* mutant, the increase in TCA cycle and glyxoylate pathway, and decrease in glycolysis caused acetate to be less accumulated. Moreover, the enhancement of *crp* expression contributes to the stress resistance, which was reflected by upregulation of the stress master regulator RpoS. Gosset et al. (2004) also implied this.

5.3.3 Regulation mechanism of Δ*pgi* mutant for multiple carbon sources

In the case of Δ*pgi* mutant, three carbon sources were consumed together, where the consumption rates were lower. In our previous studies, it was also shown that the glucose consumption rate was significantly low for the case of using glucose as a sole carbon source (Kabir et al., 2003; Toya et al., 2010). The *pgi* gene knockout made glucose to be metabolized exclusively via PP pathway, which was reflected by the significant upregulation of *zwf* ($P<0.01$). Moreover, G6P accumulates and mRNA of *ptsG* degrades, and thus cAMP-Crp tends to increase. This is the reason why simultaneous consumption of multiple carbon sources could be attained, whereas the glucose consumption rate decreased. In addition, *rpoS* was increased in Δ*pgi* mutant ($P<0.01$), which might be due to the fact that the translation of *rpoS* mRNA is no longer repressed by $EIIA^{Glc}$ (Flores et al., 2008).

5.3.4 The interrelationship between fructose PTS and xylose metabolism

Consider next the interrelationship between fructose PTS and xylose metabolism. As shown in Fig. 5.2 for the case of aerobic condition, glucose was preferentially assimilated before xylose was utilized as also observed by others (Hasona et al., 2004; Hernández-Montalvo et al., 2001; Song and Park, 1997; Stülke and Hillen, 1999), where this implies that *xyl* genes are under control of cAMP-Crp (Song and

Park, 1997). However, under anaerobic condition, the substrate consumption characteristics are different from the case under aerobic condition. Figures 5.3a and 5.3b show that xylose was consumed little even after PTS sugars such as glucose and fructose were depleted, while Figures 5.2a and 5.2b show that xylose was consumed totally after glucose was depleted under aerobic condition. When PTS sugars are depleted, cAMP together with *crp* level becomes higher, and thus the possibility by catabolite repression may be excluded. One possible reason to explain the situation under microaerobic or anaerobic condition may be as follows: Under microaerobic or anaerobic condition, xylose may produce xylitol by the reduction process (Cirino et al., 2006). Xylitol inhibits the growth of many bacteria (Reiner, 1977; London and Hausman, 1982; Trahan, 1995), where xylitol toxicity was caused by the intracellular accumulation of xylitol phosphate (Hausman et al., 1984). Xylitol was phosphorylated by a constitutive fructose PTS system (Trahan et al., 1985). After the cell was induced by fructose (Fig. 5.3a), or *fru* operon was over-expressed by *cra* knockout as seen in Fig. 5.3b, cell cannot grow on xylose. Namely, xylose consumption was interrupted if the fructose induced xylitol transport pathways were activated. In Δ*cra* mutant, the gene transcript levels of *fruBKA* were the highest among all the strains, and *xyl* genes were all repressed (Fig. 5.5). In addition, the extracellular xylitol concentrations as given in the small windows in Figs. 5.3a and 5.3b show that some amount of xylitol were produced in wild type and Δ*cra* mutant, where these amounts were above the xylitol inhibition concentration, 15.2 mg/l (Reiner, 1977). Moreover, the concentration of xylitol produced in Δ*cra.pflA* mutant for three carbon sources was also higher than this threshold (Fig. 5.4b). Similar to Δ*cra* mutant, Δ*cra.pflA* mutant also consumed little xylose. In contrast to the above three strains, little xylitol was produced in crp^+ and Δ*pgi* mutants, xylose and fructose were consumed together (Fig. 5.3c and Fig. 5.3d). The xylitol concentrations were less than the threshold, which can explain for this phenomenon. It has been reported that xylitol resistant strains are defective in fructose phosphotransferase system (Gaurivaud et al., 2000), and toxic xylitol 5-phosphate was not much produced in such a strain. In crp^+ and Δ*pgi* mutants, it cost longer

time to consume the same amount of fructose as compared to wild type and Δ*cra* mutant (Fig. 5.3), suggesting that fructose induction was not enough to activate xylitol phosphorylation. On the other hand, *crp* levels were higher in *crp*$^{+}$ and Δ*pgi* mutants as compared to wild type and Δ*cra* mutant, indicating that catabolite repression was relaxed to some extent. Furthermore, *xylA* and *xylB* genes were activated in *crp*$^{+}$ mutants, *xylR* was activated in Δ*pgi* mutant, indicating that xylose was mainly assimilated through the corresponding PP pathways instead of going to xylitol production pathway (Fig. 5.9).

5.4 Conclusion

In summary, it was found for the 1st time that Δ*cra* mutant can be considered for the simultaneous consumption of multiple sugars such as glucose and fructose, where *fruBKA* operon was activated by Δ*cra*. Furthermore, it was also found that glycolytic genes were activated, and thus total substrate consumption rate as well as total metabolite production rates was increased as compared to the wild type. This is attractive from the application point of view. Moreover, it was found that *crp+* mutant may be attractive for the simultaneous consumption of xylose and fructose together with stress resistant property, whereas the catabolite repression by glucose may not be totally relaxed as expected. This indicates that multiple mechanisms are involved in mediating catabolite repression. Furthermore, Cra mediates Cya regulation indirectly by controlling expression of fructose operon. This shows that Cra also controls CCR. Thus, further modifications of *crp* and *cra* may overcome glucose repression and contribute to co-consumption of multiple sugars.

Chapter 6
Concluding summary and future perspectives

6.1 Concluding summary

In this dissertation, catabolite regulation mechanism was clarified in terms of global regulators and their regulated metabolic pathway genes based on the fermentation data, gene transcript levels and metabolic flux analysis. This regulation mechanism was investigated through different carbon source levels and gene mutations. The knowledge on catabolite regulation mechanism could be applied to co-consumption of multiple sugars obtained from lignocellulosic biomass. The overall study is summarized in Fig. 6.1. In the following, some important points are summarized:

- Carbon catabolite repression (CCR) can be reduced by limiting glucose supply in the culture environment and by the enhancement of *crp* from the point of view of genetic modifications.

- In reducing CCR, glucose PTS is inactivated, which influences glucose catabolism.

- In response to the decreased glucose uptake rate, the overloading of TCA cycle is reduced, and less acetate is accumulated.

- The *crp*+ mutant may be attractive for the simultaneous consumption of xylose and fructose, where the catabolite repression by glucose may be relaxed to some extent. This phenomenon confirms that Crp plays an important role in CCR. In addition, the residual glucose repression indicates that multiple mechanisms are involved in mediating catabolite repression.

- The Δ*cra* mutant can be considered for the simultaneous consumption of multiple sugars such as glucose and fructose, where fructose operon was activated by *cra* gene knockout. Furthermore, Cra mediates adenylate cyclase regulation indirectly by controlling expression of fructose operon. This phenomenon reveals that Cra

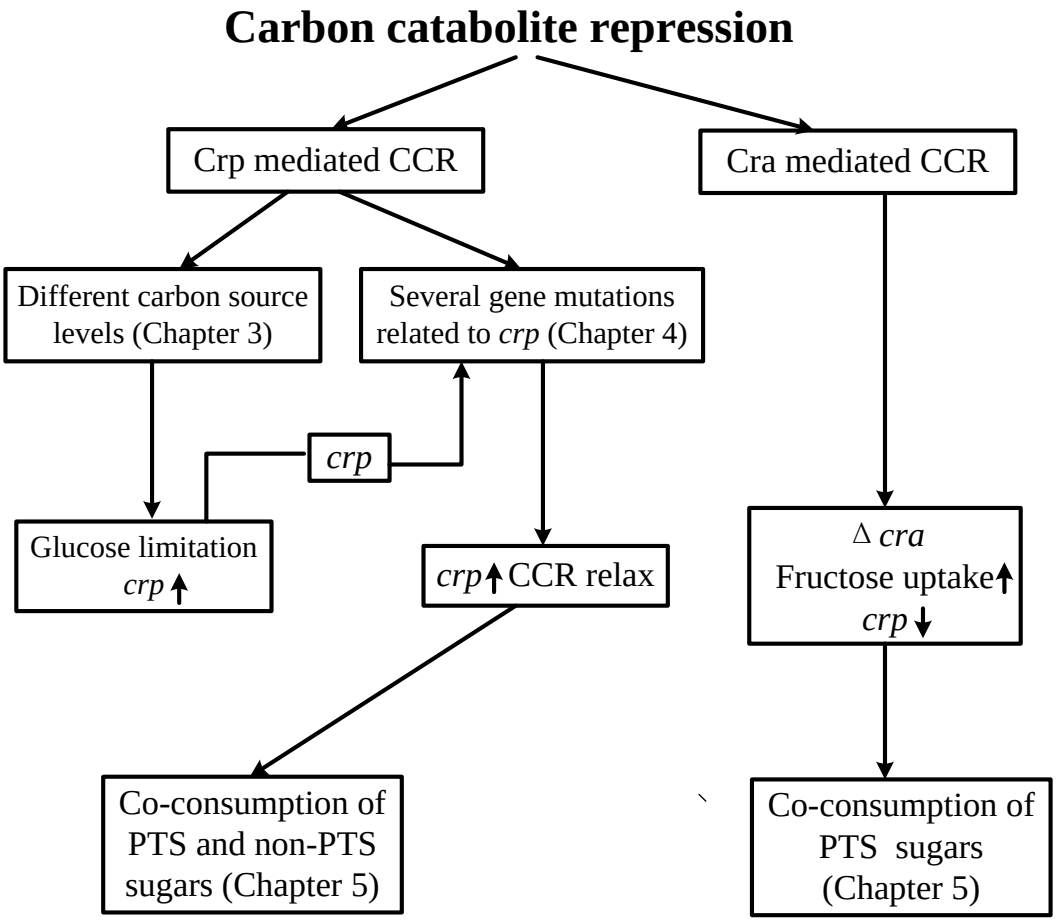

Figure 6.1 The overall structure of this thesis

controls catabolite repression in addition to Crp.

6.2 Future perspectives

Due to complex regulatory mechanism of CCR that designs metabolic pathways for optimized utilization of multiple sugars, it is very important to identify appropriate target of genetic perturbation. Furthermore, each sugar combination requires a specific engineering strategy because different sugars are regulated through different mechanisms (Kim et al., 2012). However, many previous investigations only focus

on local pathway modifications, without considering the whole regulation scheme, resulting in decreased yields and production rates. In the present study, the overall catabolite regulation mechanism was clarified, and the improved co-consumption of multiple sugars which could be attained by the global regulator mutants such as Δ*cra* and *crp*$^{+}$ mutants. From the practical application point of view, it is attractive to use these two mutants for the simultaneous consumption of multiple sugars obtained from lignocellulosic biomass. Nevertheless, this study is the first step. The above efforts combined with biofuel producing strains will enhance the productivity and yield of target biofuels and biochemicals production from lignocellulosic biomass. In addition, the developments for the effective manipulation and engineering of *E. coli* enable co-consumption of multiple sugars based on different levels of information such as genomics, transcriptomics, protemics, metabolomics and fluoxmics. Furthermore, the advancements in the fields of synthetic biology tools can help reduce the time required to make genetic constructs as well as increasing their predictability and reliability. These tools will help facilitate the design, characterization, and integration of new metabolic pathways for biofuels and biochemicals production.

References

Ackerman RS, Cozzarelli NR, Epstein W. Accumulation of toxic concentrations of methylglyoxal by wild-type *Escherichia coli* K-12. J Bacteriol 1974;119:357-362.

Aiba H, Nakamura T, Mitani H, Mori H. Mutations that alter the allosteric nature of cAMP receptor protein of *Escherichia coli*. EMBO J 1985;12:3329-3332.

Alakomi HL, Skyttä E, Saarela M, Malttila-Sandholm T, Latva-Kala K, Helander IM. Lactic acid permeabilizes gram-negative bacteria by disrupting the outer membrane. Appl Environ Microb 2000;66:2001-2005.

Aristidou A, Penttilä M. Metabolic engineering applications to renewable resource utilization. Curr Opin Biotechnol 2000;11:187-198.

Baba T, Ara T, Hasegawa M, Takai Y, Okumura Y, Baba M, Datsenko KA, Tomita M, Wanner BL, Mori H. Construction of *Escherichia coli* K-12 inframe, single gene knockout mutants: the Keio collection. Mol Syst Biol 2006;2.

Bahr T, Lüttmann D, März RB, Görke B. Insight into bacterial phosphotransferase system-mediated signaling by interspecies transplantation of a transcriptional regulator. J Bacteriol 2011;193:2013-2026.

Bettenbrock K, Fischer S, Kremling A, Jahreis K, Sauter T. A quantitative approach to catabolite repression in *Escherichia coli*. J Biol Chem 2006;281:2578-2584.

Bettenbrock K, Sauter T, Jahreis K, Kremling A, Lengeler JW, and Gilles ED. Correlation between growth rates, $EIIA^{Crr}$ phosphorylation, and intracellular cyclic AMP levels in *Escherichia coli* K-12. J Bacteriol 2007;189:6891-6900.

Blencke HM, Homuth G, Ludwi H, Mäder U, Hecker M, Stülke J. Transcriptional profiling of gene expression in response to glucose in *Bacillus subtilis*: regulation of the central metabolic pathways. Metab Eng 2003;5:133-149.

Bothast RJ, Nichols NN, Dien BS. Fermentations with new recombinant organisms. Biotechnol Progr 1999;15:867-875.

Chin AM, Feldheim DA, Saier MH Jr. Altered transcriptional patterns affecting several metabolic pathways in strains of *Salmonella typhimurium* which overexpress the fructose regulon. J Bacteriol 1989;171:2424-2434.

Cirino PC, Chin JW, Ingram LO. Engineering *Escherichia coli* for xylitol production from glucose-xylose mixtures. Biotech Bioeng 2006;95:1167-1176.

Clomburg J, Gonzalez R. Biofuel production in *Escherichia coli*: the role of metabolic engineering and synthetic biology. Appl Microbiol Biotechnol 2010;86:419-434.

Crasnier-Mednansky M, Park MC, Studley WK, Saier MH Jr. Cra-mediated regulation of Escherichia coli adenylate cyclase. Microbiology 1997;143:785-792

Cunningham L, Gruer MJ, Guest JR. Transcriptional regulation of the aconitase genes (*acnA* and *acnB*) of *Escherichia coli*. Microbiology 1997;143:3795-3805.

Datsenko KA, Wanner, BL. One-step inactivation of chromosomal genes in *Escherichia coli* K-12 using PCR products. Proc Natl Acad Sci USA 2001;97: 6640-6645.

Dauner M, Bailey JE, Sauer U. Metabolic flux analysis with a comprehensive isotopomer model in *Bacillus subtilis*. Biotechnol. Bioeng 2001;76:144-156.

de la Cruz MA, Fernänez-Mora M, Guadarrama C, Flores-Valdez MA, Bustamante VH, Vázquez A, Calva E. Leuo antagonizes H-NS and StpA-dependent repression in *Salmonella enterica* ompS1. Mol Microbiol 2007;66:727-743.

de Reuse H, Danchin A. The ptsH, ptsI, and crr genes of the *Escherichia coli* phosphoenolpyruvate-dependent phosphotransferase system: a complex operon with several modes of transcription. J Bacteriol 1988;170: 3827-3837.

DeRisi JL, Iyer VR, Brown PO. Exploring the metabolic and genetic control of gene expression on a genomic scale. Science 1997;278:680-686.

Dessein A, Schwartz M, Ullmann A. Catabolite repression in *Escherichia coli* mutants lacking cyclic AMP. Mol Gen Genet 1978;162:83-87.

Deutscher J, Francke C, Postma PW. How phosphotransferase system-related protein phosphorylation regulates carbohydrate metabolism in bacteria. Microbiol Mol Biol Rev 2006;70:939-1031.

Deutscher J. The mechanism of carbon catabolite repression in bacteria. Curr Opin Microbiol 2008;11:87-93.

Dien BS, Nichols NN, Bothast RJ. Fermentation of sugar mixtures using *Escherichia coli* catabolite repression mutants engineered for production of L-lactic acid. J Ind Microbiol Biotechnol 2002;29:221-227.

Escalante A, Cervantes AS, Gosset G, Bolívar F. Current knowledge of the *Escherichia coli* phosphoenolpyruvate-carbohydrate phosphotransferase system: peculiarities of regulation and impact on growth and product formation. Appl Microbiol Biotechnol 2012;94:1483-1494.

Feldheim DA, Chin AM, Nierva CT, Feucht BU, Cao YW, Xu YF, Sutrina SL, Saier MH Jr. Physiological consequences of the complete loss of phosphoryl-transfer proteins HPr and FPr of the phosphoenolpyruvate:sugar phosphotransferase system and analysis of fructose (*fru*) operon expression in *Salmonella typhimurium*. J Bacteriol 1990;172:5459-5469

Ferenci T. Hungry bacteria - definition and properties of a nutritional state. Environ Microbiol 2001;3:605-611.

Flores N, Leal L, Sigala JC, de Anda R, Escalante A, Martínez A, Ramírez OT, Gosset G, Bolivar F. Growth recovery on glucose under aerobic conditions of an *Escherichia coli* strain carrying a phosphoenolpyruvate:carbohydrate phosphotransferase system deletion by inactivating *arcA* and overexpressing the genes coding for glucokinase and galactose permease. J Mol Microbiol Biotechnol 2007;13:105-116.

Flores N, Escalante A, de Anda R, Báez-Viveros JL, Merino E, Franco B, Georgellis D, Gosset G, Bolívar F. New insights into the role of sigma factor RpoS as revealed in *Escherichia coli* strains lacking the phosphoenolpyruvate:carbohydrate phosphotransferase system. J Mol Microbiol Biotechnol 2008;14:176-192.

Galbe M, Zacchi G. Pretreatment of lignocellulosic materials for efficient bioethanol production. Adv Biochem Eng Biotechnol 2007;108:41-65.

Gaurivaud P, Laigret F, Verdin E, Garnier M, Bové JM. Fructose operon mutants of *Spiroplasma citri*. Microbiology 2000;146:2229-2236.

Goldie H. Regulation of transcription of the Escherichia coli phosphoenolpyruvate carboxykinase locus: studies with *pck-lacZ* operon fusions. J Bacteriol 1984;159:832-836.

Görke B, Stülke J. Carbon catabolite repression in bacteria: many ways to make the most out of nutrients. Nat Rev Microbiol 2008;6:613-624.

Gosset G, Zhang Z, Nayyar S, Cuevas WA, Saier MH Jr. Transcriptome analysis of Crp-dependent catabolite control of gene expression in *Escherichia coli*. J Bacteriol 2004;186:3516-3524.

Gosset G. Improvement of *Escherichia coli* production stains by modification of the phosphoenolpyruvate:sugar phosphotransferase system. Microb Cell Fact 2005;4:14.

Griffith JK, Baker ME, Rouch DA, Page MG, Skurray RA, Paulsen IT, Chater KF, Baldwin SA, Henderson, PJ. Membrane transport proteins: implications of sequence comparisons. Curr Opin Cell Biol 1992;4:684-695.

Gui L, Sunnarborg A, Laporte DC. Regulated expression of a repressor protein: FadR activates *iclR*. J Bacteriol 1996;178:4704-4709.

Guidi-Rotani C, Danchin A, Ullmann A. Catabolite repression in *Escherichia coli* mutants lacking cyclic AMP receptor protein. Proc Natl Acad Sci USA 1980;77:5799-5801

Hasona A, Kim Y, Healy FG, Ingram LO, Shanmugam KT. Pyruvate formate lyase and acetate kinase are essential for anaerobic growth of *Escherichia coli* on xylose. J Bacteriol 2004;186:7593-7600.

Hausman SZ, Thompson J, London J. Futile xylitol cycle in *Lactobacillus casei*. J Bacteriol 1984;160:211-215.

Hernández-Montalvo V, Valle F, Bolivar F, Gosset G. Characterization of sugar mixtures by an *Escherichia coli* mutant devoid of the phosphotransferase system.

Appl Microbiol Biotechnol 2001;57:186-191.

Hogema BM, Arents JC, Bader R, Eijkemans K, Yoshida H, Takahashi H, Aiba H, Postma PW. Inducer exclusion in *Escherichia coli* by non-PTS substrates: the role of the PEP to pyruvate ratio in determining the phosphorylation state of enzyme IIA^{Glc}. Mol Mcriobiol 1998;30:487-498.

Hogema BM, Arents JC, Bader R, Postma PW. Autoregulation of lactose uptake through the LacY permease by enzyme IIA^{Glc} of the PTS in *Escherichia coli* K-12. Mol Microbiol 1999;31:1825-1833

Hopper DJ, Cooper RA. The regulation of *Escherichia coli* methylglyoxal synthase: a new control site in glycolysis? FEBS Lett 1971;13:213-216.

Hoskisson PA, Hobbs G. Continuous culture – making a comeback? Microbiology 2005;151:3153.

Huffer S, Roche CM, Blanch HW, Clark DS. *Escherichia coli* for biofuel production: bridging the gap from promise to practice. Trends Biotechnol 2012;30:538-545.

Ingram LO, Vreeland NS. Differential effects of ethanol and hexanol on the *Escherichia coli* cell envelope. J Bacteriol 1980;144:481-488.

Ishii N, Nakahigashi K, Baba T, Robert M, Soga T, Kanai A, Hirasawa T, Naba M, Hirai K, Hoque A, Ho PY, Kakazu Y, Sugawara K, Igarashi S, Harada S, Masuda T, Sugiyama N, Togashi T, Hasegawa M, Takai Y, Yugi K, Arakawa K, Iwata N, Toya Y, Nakayama Y, Nishioka T, Shimizu K, Mori H, Tomita M. Multiple high-throughput analyses monitor the response of *E. coli* to perturbations. Science 2007;316:593-597.

Jackson DW, Simecka JW, Romeo T. Catabolite repression of *Escherichia coli*

biofilm formation. J Bacteriol 2002;184:3406-3410.

Jiang P, Ninfa AJ. *Escherichia coli* PII signal transduction protein controlling nitrogen assimilation acts as a sensor of adenylate energy charge in vitro. Biochemistry 2007;46:12979-12996.

Johansson J, Balsalobre C, Wang SY, Urbonaviciene J, Jin DJ, Sondén B, Uhlin BE Nucleoid proteins stimulate stringently controlled bacterial promoters: a link between the cAMP–CRP and the (p)ppGpp regulons in *Escherichia coli*. Cell 2000;102:475-485.

Jung IL, Phyo KH, Kim IG. RpoS-mediated growth-dependent expression of the *Escherichia coli tkt* genes encoding transketolases isoenzymes. Curr Micobiol 2005; 50:314-318.

Kabir MD, Shimizu K. Gene expression patterns for metabolic pathway in *pgi* knockout *Escherichia coli* with and without *phb* genes based on RT-PCR. J Biotechnol 2003;105:11-31.

Kang Y, Weber KD, Qin Y, Kiley PJ, Blattner FR. Genome-wide expression analysis indicates that FNR of *Escherichia coli* K-12 regulates a large number of genes of unknown function, J Bacteriol 2005;187:1135-1160.

Kerr RA. Global warming is changing the world. Science 2007;316:188-190.

Kim JH, Block DE, Mills DA. Simultaneous consumption of pentose and hexose sugars: an optimal microbial phenotype for efficient fermentation of lignocellulosic biomass. Appl Microbiol Biotechnol 2010; 88:1077-1085.

Kim SR, Ha SJ, Wei N, Oh EJ, Jin YS. Simultaneous co-fermentation of mixed

sugars: a promising strategy for producing cellulosic ethanol. Trends Biotechnol 2012;30: 274-282.

Kimata K, Inada T, Tagami H, Aiba H. A global repressor (Mlc) is involved in glucose induction of the ptsG gene encoding majorglucose transporter in *Escherichia coli*. Mol Microbiol 1998;29:1509-1519.

Kornberg HL. Routes for fructose utilization by *Escherichia coli*. J Mol Microbiol Biotechnol 2001;3:355-359.

Kremling A, Fischer S, Sauter T, Bettenbrock K, Gilles ED. Time hierarchies in the *Eshcerichia coli* carbohydrate uptake and metabolism. Biosystems 2004;73:57-71.

Liochev SI, Hausladen A, Fridovich I. Nitroreductase A is regulated as amember of the *soxRS* regulon of *Escherichia coli*. Proc Natl Acad Sci USA 1999;96:3537-3539.

Liu M, Durfee T, Cabrera JE, Zhao K, Jin DJ, Blatner FR. Global transcriptional programs reveal a carbon source foraging strategy by *Escherichia coli*. J Biol Chem 2005;280:15921-15927.

Liu X, Wulf PD. Probing the ArcA-P modulon of *Escherichia coli* by whole genome transcriptional analysis and sequence recognition profiling. J Biol Chem 2004; 279:12588-12597.

London J, Hausman S. Xylitol-mediated transient inhibition of ribitol utilization by *Lactobacillus casei*. J Bacteriol 1982;150:657-661.

Lu J, Tang J, Liu Y, Zhu X, Zhang T, Zhang X. Combinatorial modulation of *galP* and *glk* gene expression for improved alternative glucose utilization. Appl Micriobol Biotechnol 2012;93:2455-2462.

Lynd LR, Weimer PJ, van Zyl WH, Pretorius IS. Microbial cellulose utilization: fundamentals and biotechnology. Microbiol Mol Biol Rev 2002;66:506-577.

Malpica R, Franco B, Rodriguez C, Kwon O, Georgellis D. Identification of a quinone-sensitive redox switch in the ArcB sensor kinase. Proc Natl Acad Sci USA 2004;101:13318-13323.

Mao XJ, Huo YX, Buck M, Kolb A, Wang YP. Interplay between CRP–cAMP and PII–Ntr systems forms novel regulatory network between carbon metabolism and nitrogen assimilation in *Escherichia coli*. Nucl Acids Res 2007;35:1432-1440.

Mazzoli R, Lamberti C, Pessione E. Engineering new metabolic capabilities in bacteria: lessons from recombinant cellulolytic strategies. Trends Biotechnol 2012;30:111-119.

Moat AG, Foster JW, Spector MP. Microbial Physiology, fourth ed. John Wiley & Sons Press, New York;2002.

Morita T, El-Kazzaz W, Tanaka Y, Inada T, Aiba H. Accumulation of glucose 6-phosphate or fructose 6-phosphate is responsible for destabilization of glucose transporter mRNA in *Escherichia coli*. J Biol Chem 2003;278:15608-15614.

Nanchen A, Schicker A, Revelles O, Sauer U. Cyclic AMP-dependent catabolite repression is the dominant control mechanism of metabolic fluxes under glucose limitation in *Escherichia coli*. J Bacteriol 2008;190:2323-2330.

Nichols NN, Dien BS, Bothast RJ. Use of catabolite repression mutants for fermentation of sugar mixtures to ethanol. Appl Microbiol Biotechnol 2001;56:3751-3756

Park YH, Lee BR, Seok YJ, Peterkofsky A. In vitro reconstitution of catabolite repression in *Escherichia coli*. J Biol Chem 2006;281:6448-6454.

Perrenoud A, Sauer U. Impact of global transcriptional regulation by ArcA, ArcB,Cra, Crp, Cya, Fnr, and Mlc on glucose catabolism in *Escherichia coli*. J Bacteriol 2005;187:31711-3179

Plumbridge J. Regulation of gene expression in the PTS in *Escherichia coli*: the role and interactions of Mlc. Curr Opin Microbiol 2002;5:187-193.

Pomposiello PJ, Demple B. Redox-operated genetic switches: the soxR and OxyR transcription factors. Trends Biotechnol 2001;19:109-114.

Pósfai G, Kolisnychenko V, Bereczki Z, Blattner F. Markerless gene replacement in *Escherichia coli* stimulated by a double-strand break in the chromosome. Nucleic Acid Res 1999;27:4409-4415.

Postma PW, Lengeler JW, Jacobson GR. Phosphoenolpyruvate:Carbohydrate phosphotransferase systems. In: Neidhart FC (ed) *Escherichia coli* and *Salmonella*. Cellular and molecular biology. ASM Press, Washington, DC;1996, pp 1149-1174.

Rahman M, Hassan MR, Shimizu K. Growth phase-dependent changes in the expression of global regulatory genes and associated metabolic pathways in *Escherichia coli*. Biotechnol Lett 2008;30:853-860.

Rahman M, Shimizu K. Altered acetate metabolism and biomass production in several *Escherichia coli* mutants lacking rpoS-dependent metabolic pathway genes. Mol Biosyst 2008;4:160-169.

Reiner AM. Xylitol and D-arabitol toxicites due to derepressed fructose, galactitol,

and sorbitol phosphotransferases of *Escherichia coli*. J Bacteriol 1977; 132:166-173.

Saha BC. Hemicellulose bioconversion. J Ind Microbiol Biotechnol 2003;30:279-291.

Saier MH Jr, Ramseier TM. The catabolite repressor/activator (Cra) protein of enteric bacteria. J Bacteriol 1996;178:3411-3417.

Saier MH Jr, Ramseier TM, Reizer J. Regulation of carbon utilization, In F. C. Neidhardt FC, Curtiss III R , Ingraham JL, E. Lin ECC, Low KB, Magasanik B, Reznikoff WS, Riley M, Schaechter M, and Umbarger HE (ed.), *Escherichia coli* and *Salmonella:* cellular and molecular biology, 2nd ed. ASM Press, Washington, DC;1996. pp 1325-1343.

Sambrook J, Russell DW. Molecular Cloning: A Laboratory Manual, 3rd ed. Cold Spring Harbor Laboratory Press, Cold Spring Harbor, NY;2001.

Sarkar D, Shimizu K. Effect of *cra* gene knockout together with other genes knockouts on the improvement of substrate consumption rate in *Escherichia coli* under microaerobic condition. Biochem Eng J 2008;42:224-228.

Schmidt LD, Dauenhauer PJ. Chemical engineering: hybrid routes to biofuels. Nature 2007;447:914-915.

Shimizu K. Metabolic flux analysis based on ^{13}C-labeling experiments and integration of the information with gene and protein expression patterns. Adv Biochem Eng Biotechnol. 2004;91:1-49.

Shimizu K. Toward systematic metabolic engineering based on the analysis of

metabolic regulation by the integration of different levels of information. Biochem Eng J 2009;46:235-251.

Shimizu K. Metabolic regulation of a bacterial cell system with emphasis on *Escherichia coli* metabolism. ISRN Biochemistry; 2013.

Song S, Park C. Organization and regulation of the D-xylose operons in *Escherichia coli* K-12: XylR acts as a transcriptional activator. J Bacteriol 1997;179:7025-7032.

Stülke J, Hillen W. Carbon catabolite repression in bacteria. Curr Opin Microbiol 1999;2:195-201.

Sumiya M, Davis EO, Packman LC, McDonald TP, Henderson PJ. Molecular genetics of a receptor protein for D-xylose, encoded by the gene *xylF*, in *Escherichia coli*. Receptors Channels 1995;3:117-128.

Szyperski T. Biosynthetically directed fractional ^{13}C-labeling of proteinogenic amino acids-an efficient analytical tool to investigate intermediary metabolism. Eur J Biochem 1995;232:433-448.

Tanaka Y, Kimata K, Aiba H. A novel regulatory role of glucose transporter of *Escherichia coli*: membrane sequestration of a global repressor Mlc. EMBO J 2000;19:5344-5352.

Tötemeyer S, Booth NA, Nichols WW, Dunbar B, Booth IR. From famine to feast: the role of methylglyoxal production in *Escherichia coli*. Mol Microbiol 1998;27:553-562.

Toya Y, Ishii N, Nakahigashi K, Hirasawa T, Soga T, Tomita M, Shimizu K: ^{13}C-metabolic flux analysis for batch culture of *Escherichia coli* and its *pyk* and *pgi* gene knockout mutants based on mass isotopomer distribution of intracellular metabolites. Biotechnol Prog 2010;26:975-992.

Trahan L, Bareil M, Gauthier L, Vadeboncoeur C. Transport and phosphorylation by a fructose phosphotransferase system in Streptococcus mutants. Caries Res 1985;19:53-63.

Trahan L. Xylitol: a review of its action on mutants streptococci and dental plaque-its clinical significance. Int Dent J 1995;45:77-92.

Tsai SP, Lee YH. Application of metabolic pathway stoichiometry to statistical analysis of bioreactor measurement data. Biotechnol Bioeng 1988;32:713-715.

Van Winden WA, Wittmann C, Heinzle E, Heijnen JJ. Correcting mass isotopomer distributions for naturally occurring isotopes. Biotechnol Bioeng 2002;80:477-479.

Vogel RF, Entian KD, Mecke D. Cloning and sequence of the *mdh* structural gene of *Escherichia coli* coding for malate dehydrogenase. Arch Microbiol 1987;149:36-42.

Wiechert W. ^{13}C metabolic flux analysis. Metab Eng 2001;3:195-206.

Wittman C. Fluxome analysis using GC–MS. Microb Cell Fact 2007;6:1-17.

Yamamoto K, Ishihama A. Two different modes of transcription repression of the *Escherichia coli* acetate operon by IclR. Mol Microbiol 2003;47:183-194.

Yang C, Hua Q, Baba T, Mori H, Shimizu K. Analysis of *Escherichia coli* anaplerotic metabolism and its regulation mechanisms from the metabolic responses to altered dilution rates and phosphoenolpyruvate carboxykinase knockout. Biotechnol Bioeng 2003;84:129-144.

Yao R, Hirose Y, Sarkar D, Nakahigashi K, Ye Q, Shimizu K. Catabolic regulation analysis of *Escherichia coli* and its *crp, mlc, mgsA, pgi* and *ptsG* mutants. Microb Cell Fact 2011;10:67.

Yao R, Kurata H, Shimizu K. Effect of *cra* gene mutation on the metabolism of *Escherichia coli* for a mixture of multiple carbon sources. Adv. Biosci. Biotechnol., 2013;4:477-486.

Yao R, Shimizu K. Recent progress in metabolic engineering for the production of biofuels and biochemicals from renewable sources with particular emphasis on catabolite regulation and its modulation. Process Biochem, accepted.

Yomano LP, York SW, Shanmugam KT, Ingram LO. Deletion of methylglyoxal synthase gene (*mgsA*) increased sugar co-metabolism in ethanol-producing *Escherichia coli*. Biotechnol Lett 2009;31:1389-1398.

Zaldivar J, Nielsen J, Olsson L. Fuel ethanol production from lignocellulose: a challenge for metabolic engineering and process integration. Appl Microbiol Biotechnol 2001;56:17-34.

Zhang Z, Gosset G, Barabote R, Gonzalez CS, Cuevas WA, Saier MH Jr. Functional interactions between the carbon and iron utilization regulators, Crp and Fur, in *Escherichia coli*. J Bacteriol 2005;187:980-990.

Zhao J, Shimizu K. Metabolic flux analysis of *Escherichia coli* K12 grown on ^{13}C-labeled acetate and glucose using GC-MS and powerful flux calculation method. J Biotechnol 2003;101:101-117.

Zhao J, Baba T, Mori H, Shimizu K. Effect of *zwf* gene knockout on the metabolism of *Escherichia coli* grown on glucose or acetate. Metab Eng 2004;6:164-174.

Zhu J, Shimizu, K. The effect of *pfl* gene knockout on the metabolism for optically pure D-lactate production by *Escherichia coli*. Appl Microbiol Biotechnol 2004;64: 367-375.

Zhu J, Shimizu K. Effect of a single-gene knockout on the metabolic regulation in *Escherichia coli* for D-lactate production under microaerobic condition. Metab Eng 2005;7:104-115.

Appendix

Appendix A: Abbreviations

Metabolites

3PG: 3-Phosphoglyceric acid; 6PG: 6-Phosphogluconolactone; AKG: 2-Keto-D-gluconate; AcCoA: Acetyl-CoA; ADP: Adenosine diphosphate; ATP: Adenosine-5'-triphosphate; cAMP: Cyclic AMP; CIT: Citrate; DHAP: Dihydroxyacetone phosphate; E4P: Erythrose 4-phosphate; F1P: Fructose 1-phosphate; F6P: Fructose 6-phosphate; FBP: Fructose 1,6-bisphosphate; FUM: Fumarate; G6P: Glucose-6-phosphate; GAP: Glyceraldehyde 3-phosphate; GLX: Glyoxylate; ICIT: Isocitrate; MAL: Malate; MG: methylglyoxal; OAA: Oxaloacetate; P: Phosphate; PEP: Phosphoenolpyruvate; PYR: Pyruvate; R5P: Ribulose 5-phosphate; Ru5P: Ribose 5-phosphate; S7P: Sedoheptulose 7-phosphate; SUCCoA: Succinyl-CoA; SUC: Succinate; X5P: Xylulose 5-phosphate;

Protiens (enzymes)

ADH: Alcohol dehydrogenase; G6PDH: Glucose-6-phosphate dehydrogenase; GAPDH: Glyceraldehyde-3-phosphate dehydrogenase; LDH: Lactate dehydrogenase.

Appendix B: Global regulators and their regulated genes

Global Regulators	Regulation	Metabolic Pathway Genes
Crp/Cya	+	*aceEF, acnAB, acs, focA, fumA, fur, gltA, malT, manXYZ, mdh, mlc, pckA, pflB, pgk, ptsG, sdhCDAB, sucABCD, fruBKA, manXYZ, mtlA*
	–	*cyaA, lpdA, rpoS*
Cra	+	*aceBAK, acnA, cydB, icdA, pckA, pgk, ppsA, fbp*
	–	*acnB, adhE, eda, edd, pfkA, pykF, zwf, fruBKA, manXYZ, mtlA*
ArcA/B	+	*cydAB, focA, pflB*
	–	*aceBAK, aceEF, acnAB, cyoABCDE, fumAC, gltA, icdA, lpdA, mdh, nuoABCEFGHIJKLMN, pdhR, sodA, sdhCDAB, sucABCD*
Fnr	+	*acs, focA, frdABCD, pflB, yfiD*
	–	*acnA, cyoABCDE, cydAB, fumA, fnr, icdA, ndh, nuoABCEFGHIJKLMN, sdhCDAB, sucABCD*
Mlc	–	*crr, ptsG, ptsHI, manXYZ, malT*
FadR	+	*iclR*
	–	
IclR	–	*aceBAK, acs*
SoxR/S	+	*acnA, sodA, zwf, fumC, fur*
	–	
RpoS	+	*acnA, acs, adhE, fumC, gadAB, talA, tktB, poxB, osmC*
	–	*ompF*
XylR	+	*xylFGH, xylAB*

	–	
PdhR	+	
	–	*aceEF, lpdA*

Appendix C: Metabolic reaction model for ^{13}C-MFA (Chapter 3)

	Enzyme	Reaction
v_1	Glucose:PTS enzymes; Enzyme I, HPr, $EIIA^{Glc}$, $EIICB^{Glc}$	Glucose + PEP -> G6P + PYR
v_2	Phosphoglucose isomerase	G6P <-> F6P
v_3	Phosphofructokinase, fructose bisphosphate aldolase, triose phosphate isomerase	F6P + ATP -> 2 GAP + ADP
v_4	Glyceraldehyde 3-phosphate dehydrogenase, phosphoglycerate kinase	GAP + NAD^+ + ADP -> 3PG + NADH + ATP
v_5	Enolase	3PG -> PEP
v_6	Pyruvate kinase	PEP + ADP -> PYR + ATP
v_7	Pyruvate dehydrogenase	PYR + HSCoA + NAD^+ -> AcCoA + NADH + CO_2
v_8	Phosphotransacetylase, acetate kinase A	AcCoA + ADP -> Acetate + ATP + HSCoA
v_9	Glucose 6-phosphate-1-dehydrogenase	G6P + $NADP^+$ -> 6PG + NADPH
v_{10}	6-Phosphogluconate dehydrogenase	6PG + $NADP^+$ -> Ru5P + NADPH + CO_2
v_{11}	Ribulose phosphate 3-epimerase	Ru5P -> X5P
v_{12}	Ribose-5-phosphate isomerase	Ru5P -> R5P
v_{13}	Transketolase	R5P + X5P <-> GAP + S7P
v_{14}	Transketolase	X5P + E4P <-> F6P + GAP
v_{15}	Transaldolase B	S7P + GAP <-> E4P +F6P
v_{16}	Citrate synthase	AcCoA + OAA -> CIT + OAA
v_{17}	Aconitase	CIT -> ICIT
v_{18}	Isocitrate dehydrogenase	ICIT + $NADP^+$ -> AKG + NADPH + CO_2
v_{19}	2-Ketoglutarate dehyrogenase	AKG + NAD^+ + CoA -> SUCCoA + NADH + CO_2
v_{20}	Succinyl-CoA synthetase	SUCCoA + ADP -> SUC + ATP
v_{21}	Succinate dehydrogenase	SUC + FAD^+ -> FUM + $FADH_2$
v_{22}	Fumarase	FUM <-> MAL
v_{23}	Malate dehydrogenase	MAL + NAD^+ -> OAA + NADH
v_{24}	Phosphoenolpyruvate carboxylase/ phosphoenolpyruvate carboxykinase	PEP + CO2 <-> OAA
v_{25}	Malic enzyme	MAL + $NADP^+$ -> PYR + NADPH + CO_2
v_{26}	Isocitrate lyase, malate synthase	ICIT + AcCoA -> MAL + HSCoA
v_{27}	NADH-Q reductase, succinate-Q reductase, cytochrome reductase, cytochrome oxidase	NADH + O_2 -> P/O ATP
v_{28}	Pyridine nucleotide transhydrogenase	NAD^+ + NADPH -> NADH + $NADP^+$

Appendix D: Metabolic reaction model for overdetermined system (Chapter 5)

	Enzyme	Reaction
v_1	Glucose:PTS enzymes; Enzyme I, HPr, $EIIA^{Glc}$, $EIICB^{Glc}$	Glucose + PEP -> G6P + PYR
v_2	Fructose:PTS enzymes; Enzyme I, FPr, $EIIA^{Fru}$, $EIIB'BC^{Fru}$	Fructose + PEP -> F1P + PYR
v_3	Xylose ABC transporter	Xylose + ATP -> Xylulose + ADP
v_4	Lactate dehydrogenase	PYR + NADH -> Lactate + NAD^+
v_5	Pyruvate formate-lyase	PYR + CoA -> AcCoA + Formate
v_6	Aldehyde dehydrogenase, Alcohol dehydrogenase	AcCoA + 2 NADH -> Ethanol + HSCoA + 2 NAD
v_7	Malate dehydrogenase, fumarase C, fumarate reductase	PEP + CO_2 + 2 NADH + ADP -> Succinate + 2 NAD + ATP
v_8	Glucose 6-phosphate-1-dehydrogenase, 6-phosphogluconate dehydrogenase	G6P + 2 $NADP^+$ -> Ru5P + 2 NADPH
v_9	Acetate phosphotransferase, acetate kinase	AcCoA + ADP -> Acetate + ATP + HSCoA
v_{10}	Ribose-5-phosphate isomerase	Ru5P -> R5P
v_{11}	Ribulose phosphate 3-epimerase	Ru5P -> X5P
v_{12}	Xylulose kinase	Xylulose + ATP -> X5P + ADP
v_{13}	Transketolase	R5P + X5P <-> GAP + S7P
v_{14}	Transaldolase B	S7P + GAP <-> E4P +F6P
v_{15}	Transketolase	X5P + E4P <-> F6P + GAP
v_{16}	Phosphoglucose isomerase	G6P <-> F6P
v_{17}	Phosphofructokinase	F6P + ATP -> FBP + ADP
v_{18}	Fructose-1-phosphate kinase	F1P + ATP -> FBP + ADP
v_{19}	Fructose bisphosphate aldolase, triose phosphate isomerase	FBP -> 2 GAP
v_{20}	Glyceraldehyde 3-phosphate dehydrogenase, phosphoglycerate kinase	GAP + NAD^+ + ADP -> 3PG + NADH + ATP
v_{21}	Enolase	3PG -> PEP
v_{22}	Pyruvate kinase	PEP + ADP -> PYR + ATP
v_{23}	Pyruvate dehydrogenase	PYR + HSCoA + NAD^+ -> AcCoA + NADH + CO_2
v_{24}	Pyridine nucleotide transhydrogenase	NAD^+ + NADPH -> NADH + $NADP^+$

Appendix E: Batch fermentation result of using glucose as a carbon source for Δ*crp* mutant

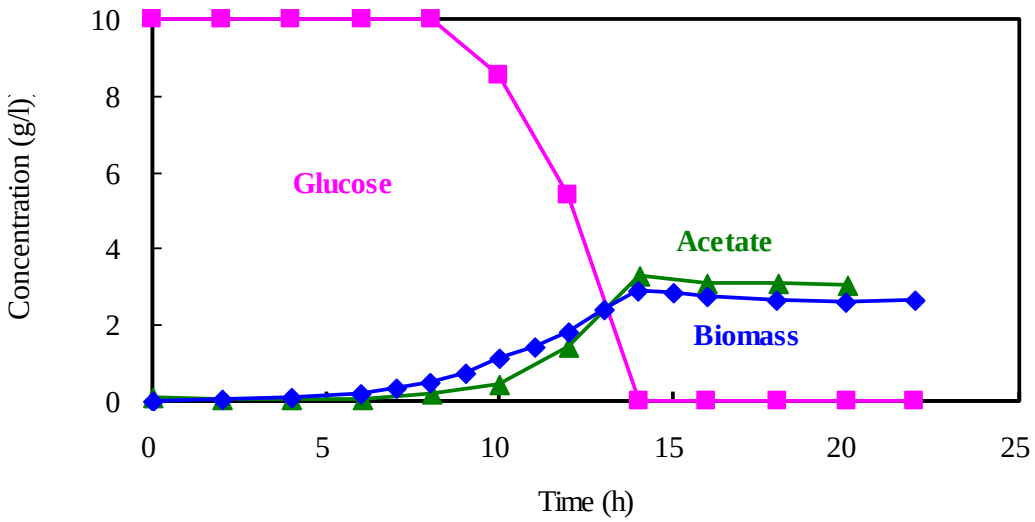

Appendix F: Batch fermentation result of using glucose as a carbon source for Δ*mlc* mutant

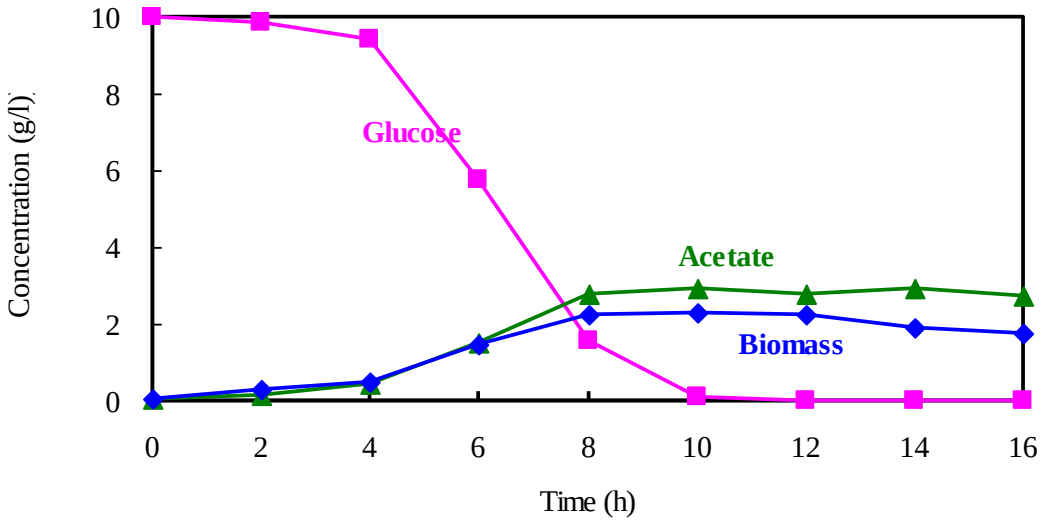

List of publications and international conference presentations

List of publications

1. Yao R, Hirose Y, Sarkar D, Nakahigashi K, Ye Q, Shimizu K. Catabolic regulation analysis of *Escherichia coli* and its *crp*, *mlc*, *mgsA*, *pgi* and *ptsG* mutants. Microb Cell Fact 2011;10:67.

2. Yao R, Kurata H, Shimizu K. Effect of *cra* gene mutation on the metabolism of *Escherichia coli* for a mixture of multiple carbon sources. Adv. Biosci. Biotechnol., 2013;4:477-486.

3. Yao R, Shimizu K. Recent progress in metabolic engineering for the production of biofuels and biochemicals from renewable sources with particular emphasis on catabolite regulation and its modulation. Process Biochem, accepted.

List of international conference presentations

1. Catabolic regulation analysis of *Escherichia coli* and its *crp*, *mlc*, *mgsA* and *pgi* mutants. Yao R, Sarkar D, Hirose Y, Nakahigashi K, Ye Q, Shimizu K. Asian Congress on Biotechnology, China, 2011.

2. Catabolite regulation of *Escherichia col*i by modulation of *cra* and *crp* genes for the case of using a mixture of PTS and non-PTS sugars as a carbon source. Yao R, Shimizu K. The 15th International Biotechnology Symposium and Exhibition, Korea,

2012.

3. Catabolic regulation and its modulation by the specific gene mutations in *Escherichia coli* for the case of multiple carbon sources. Yao R, Shimizu K, Kurata H. The First BMIRC International Symposium on Frontiers in Computational Systems Biology and Bioengineering, Japan, 2013.

Acknowledgements

I take profound privilege to express my sincere thanks and heartfelt gratitudes to esteemed teachers, supervisors and guides, Professor Kazuyuki Shimizu and Professor Hiroyuki Kurata, Department of Bioscience and Bioinformatics, Kyushu Institute of Technology, for their keen interests, inspirations, enthusiatstics through guidances, criticisms, helps and all-round supports throughout this study and in preparing this dissertation. I learnt a lot from them.

I am grateful to Professor Aoki, Professor Sakamoto and Professor Nagayama, Kyushu Institute of Technology, for their continuous inspirations, supports and valuable criticisms.

I thank to my reverend teachers of the Department of Bioscience and Bioinformatics, Kyushu Institute of Technology, for their co-operations, inspirations and good wishes during the course of this Ph. D. work.

I also thank all the Professor Shimizu's and Professor Kurata's laboratory members, past and present, for a wonderful co-operative working environment and atmosphere, especially Dr. Matsuoka and Dr. Maeda who always helped me with a smile.

Financial support from the Strategic International Cooperative Program, Japan Science and Technology Agency (JST) is gratefully acknowledged.

I am also grateful to my beloved parents, friends for their tremendous supports, inspirations and encouragements extend to me.